Longitudinal in vitro assessment of mechanical and compositional changes in cartilage under mechanical trauma, inflammation and cyclic loading

Ruwandi I. Abeysekara[1], Ari Saastamoinen[1,2], Katja Honkapää[2], Jaqueline Lourdes Rios[3], Petri Tanska[2,4], Mikko A. J. Finnilä[1]

[1]Faculty of medicine, University of Oulu, Finland [2]Department of Technical Physics, University of Eastern Finland [3]Department of orthopaedics, University Medical Centre, Utrecht, Netherlands [4]Department of Oncology, Kuopio University Hospital, Wellbeing Services County of North-Savo, Finland

INTRODUCTION: Physiological cyclic loading maintains matrix homeostasis while mechanical trauma and inflammation drive catabolic remodeling leading to matrix loss, tissue softening, and disruption of mechanotransduction and mechanical integrity of cartilage (Dwivedi et al., 2022) (Moo et al., 2022)(Li et al., 2021). This study aimed to determine how mechanical injury, inflammation and cyclic loading modify the mechanical properties of cartilage over five days and whether physiological cyclic loading can alleviate degenerative changes.

METHODS: Bovine osteochondral plugs were harvested from two femoral condyles of two bovine donors and equilibrated for 3 days. Samples were subjected to four treatments: 1) free swelling control, 2) cyclic loading, 3) injured and inflamed and 4) injured, inflamed and cyclically loaded samples. Injury was done using drop tower for an energy density of 3mJ/mm^3 and inflammation was induced by 10 ng/ml IL-1β in culture media. Samples were subjected to unconfined compression with 20kPa preload, three consecutive 3% linear compression steps followed by 10% sinusoidal loading for one hour per day for 5 days (from day 3 to day 7) (Eskelinen et al., 2022). Instantaneous, equilibrium, and dynamic moduli of same samples were calculated on day 3 and day 7.

RESULTS: Inflammation and mechanical trauma have significantly reduced the equilibrium and dynamic moduli of cartilage over time (figure 1). In addition, cyclic loading showed trend of increase in the instantaneous, equilibrium and dynamic moduli of both healthy and degenerated samples.

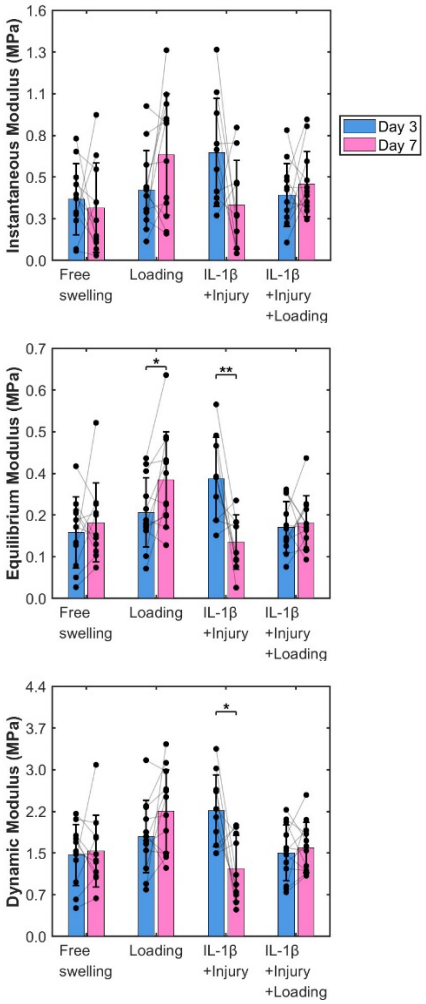

Figure 1: Changes in instantaneous, equilibrium and dynamic moduli of bovine osteochondral plugs from day 3 to day 7 (Paired t-test between day 3 and day 7: $p < 0.05$ (*), $p < 0.01$ (**))

DISCUSSION & CONCLUSIONS: We quantified the effect of inflammation and mechanical trauma on cartilage mechanical properties longitudinally. Our results suggest that mechanical trauma and inflammation reduce the equilibrium and dynamic modulus of cartilage at day 7 while physiological cyclic loading appeared to mitigate loss of moduli indicating a protective role. Future studies are needed to investigate whether this protective effect is related to stimulation of matrix synthesis or prevention of catabolic activity.

References:

Dwivedi, G., Flaman, L., Alaybeyoglu, B., Struglics, A., Frank, E. H., Chubinskya, S., Trippel, S. B., Rosen, V., Cirit, M., & Grodzinsky, A. J. (2022). Inflammatory cytokines and mechanical injury induce post-traumatic osteoarthritis-like changes in a human cartilage-bone-synovium microphysiological system. *Arthritis Research and Therapy*, *24*(1). https://doi.org/10.1186/s13075-022-02881-z

Eskelinen, A. S. A., Florea, C., Tanska, P., Hung, H. H. K., Frank, E. H., Mikkonen, S., Nieminen, P., Julkunen, P., Grodzinsky, A. J., & Korhonen, R. K. (2022). Cyclic loading regime considered beneficial does not protect injured and interleukin-1-inflamed cartilage from post-traumatic osteoarthritis. *Journal of Biomechanics*, *141*. https://doi.org/10.1016/j.jbiomech.2022.111181

Li, K., Zhang, P., Zhu, Y., Alini, M., Grad, S., & Li, Z. (2021). Establishment of an Ex Vivo Inflammatory Osteoarthritis Model With Human Osteochondral Explants. *Frontiers in Bioengineering and Biotechnology*, *9*. https://doi.org/10.3389/fbioe.2021.787020

Moo, E. K., Ebrahimi, M., Sibole, S. C., Tanska, P., & Korhonen, R. K. (2022). The intrinsic quality of proteoglycans, but not collagen fibres, degrades in osteoarthritic cartilage. *Acta Biomaterialia*, *153*, 178–189. https://doi.org/10.1016/j.actbio.2022.09.002

IDENTIFICATION OF REPURPOSING DRUGS THAT PROTECT CHONDROCYTES FROM BCP CRYSTALS IN OSTEOARTHRITIS

Joël E.J. Beaumont[1], Marjolein M.J. Caron[1], Andy Cremers[1], Marjolein de Vries[1], Guus G.H. van den Akker[1], Tim J.M. Welting[1,2]

[1] *Laboratory for Experimental Orthopedics, Department of Orthopedic Surgery, Caphri School for Public Health and Primary Care, Maastricht University, Maastricht, the Netherlands*

[2] *Laboratory for Experimental Orthopedics, Department of Orthopedic Surgery, Maastricht University Medical Center, Maastricht, the Netherlands*

INTRODUCTION: Pathological calcification of articular cartilage is a key feature of osteoarthritis (OA). Basic calcium-phosphate (BCP) crystals are detected in 100% of the articular cartilage samples at the time of joint replacement[1], correlate with pain[2] and play a critical role in OA disease progression[3,4]. BCP crystals are a major contributor to the inflammatory and catabolic OA joint environment and induce the secretion of IL-6, VEGF, MMP1 and MMP13 by chondrocytes[5]. Despite the critical role of BCP crystals in OA pathobiology, there are currently no disease-modifying OA drugs (DMOADs) targeting chondrocyte calcification and their pathological responses to BCP crystals. Drug repurposing could provide an expedited strategy to fill this gap. We aimed to identify drug compounds tackling pathological calcification in OA by high-throughput screening of a drug-repurposing library for compounds protecting chondrocytes from BCP crystal-induced pathological responses.

METHODS: A library composed of 3152 FDA/EMA-approved compounds was screened for their ability to protect chondrocytes from BCP crystal-induced pathological responses. Primary human OA articular chondrocytes (OA-HACs) were isolated from cartilage acquired from total knee arthroplasty (METC permit 2022-3235). OA-HACs from 32 patients (50% male/female) were pooled, cryo-preserved and used at passage 3 for all experiments. OA-HACs were exposed to BCP crystals (50 µg/ml) in the presence or absence of the individual drug compounds (10 µM). Secretion of IL-6, VEGF, MMP1 and MMP13 was determined by ELISA. Cell viability was assessed by total ATP measurements using CellTiter-Glo. The effects of 40 selected candidate compounds reducing BCP-induced secretion of IL-6, VEGF, MMP1 and MMP13 (>60%), without causing cytotoxicity (viability >90%), were validated in an independent OA-HAC cohort.

RESULTS: Upon exposure to BCP crystals, OA-HAC viability decreased by 50% (±8.30%) and secretion of IL-6, VEGF, MMP1 and MMP13 increased to 1.15 ng/ml, 0.56 ng/ml, 2.03 ng/ml and 1.43 ng/ml, respectively. Average Z′ scores of 0.7 (±0.2), 0.6 (±0.2), 0.7 (±0.05) and 0.8 (±0.05) for IL-6, VEGF, MMP1 and MMP13, respectively, indicated excellent high-throughput assay performance. Out of 3152 compounds in the repurposing library, 1279 reduced BCP-induced IL-6 secretion, 814 of which did not cause cytotoxicity in OA-HACs. Additionally, 635 compounds suppressed BCP-induced VEGF secretion, 375 of which maintained OA-HAC viability >90% vs BCP-only. Of the compounds suppressing both BCP-induced IL-6 and VEGF secretion, 110 compounds and 162 compounds suppressed BCP-induced secretion of MMP1 and MMP13, respectively. The effect of the top-40 most potent inhibitors of BCP-induced IL-6, VEGF, MMP1 and MMP13 secretion was subsequently validated in an independent pool of OA-HACs. In the validation, 19 compounds were found to successfully suppress BCP-induced IL-6 and VEGF without causing cytotoxicity.

DISCUSSION & CONCLUSIONS: Screening of a repurposing drug library resulted in the identification of 19 drug candidates that suppressed BCP crystal-induced IL-6 and VEGF secretion by OA-HACs. Next, we aim to validate the effect of these compounds on BCP-induced secretion of MMP1 and MMP13. Furthermore, we will test their effectiveness in the presence of OA synovial fluid *in vitro*, as well as in 3D culture models. Identification of repurposing-class drugs that tackle the largely unaddressed crystal pathobiology in OA could lead to the development of a promising novel class of DMOADs.

REFERENCES:

[1][Hubert et al., 2020]
[2][Liew et al., 2023]
[3][Ea et al., 2013]
[4][Stücker et al., 2025]
[5][Stassen et al., 2023]

DECELLULARIZED ANNULUS FIBROSUS SCAFFOLDS FOR *IN VITRO* DISEASE MODELLING

Ana Luísa Castro[1,2], Mariana Macedo[1,2,3], João B. Costa[4] , Raquel M. Gonçalves[1,2,3]

1- i3S – Instituto de Investigação e Inovação em Saúde, Universidade do Porto, Porto, Portugal

2- INEB – Instituto de Engenharia Biomédica, Universidade do Porto, Porto, Portugal

3- ICBAS – Instituto de Ciências Biomédicas Abel Salazar, Universidade do Porto, Porto, Portugal

4- CBQF-Centro de Biotecnologia e Química Fina–Laboratório Associado, Universidade Católica Portuguesa, Escola Superior de Biotecnologia, Rua Diogo Botelho 1327, Porto, 4169-005 Portugal

INTRODUCTION: Annulus Fibrosus (AF) failure involves biochemical and mechanical alterations, often driven by inflammation, leading to intervertebral disc (IVD) degeneration/herniation, through unclear mechanisms [1, 2, 3]. Current research lacks relevant and biomimetic in vitro disease models to disclose AF pathology, as previously reviewed by our team [3]. This work aims to develop a decellularized-based AF in vitro model to better understand AF physiology and establish diseased microenvironments.

METHODS: Bovine AF tissue was decellularized using SDS-based protocols adapted from [4], with confirmation of cell removal by DNA quantification and H&E/DAPI staining. Extracellular matrix (ECM) preservation in decellularized AF (dAF) was assessed by components quantification, immunostainings and proteomic analysis. Structural and mechanical integrity were evaluated through rheometer, texturometer and SEM analysis. Human AF cells, previously isolated as optimized [5], were cultured on dAF. AF cell metabolic activity, viability and distribution were evaluated throughout 14 days, together with the production of collagen I and TGF-B1.

RESULTS: AF tissue was successfully decellularized, with reduced DNA content, while retaining GAGs, collagen and elastin (Fig 1A). Proteomic analysis dissecting other ECM components and growth factors preservation is currently being performed. Both lamellar structure (SEM analysis) and rheological properties (Fig 1B) were preserved. Human AF cells remained viable and metabolic active within dAF for 14 days, interacting and aligning along ECM structure. Gene expression analysis for AF ECM production is currently being evaluated, together with the production of TGF-B1.

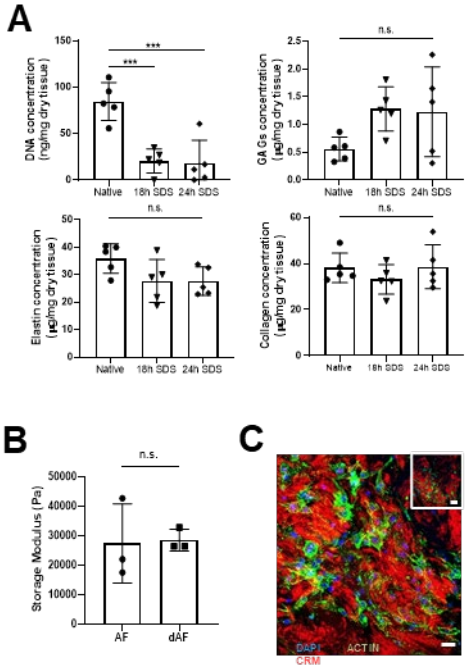

Fig1: A: DNA and ECM components quantification; B: Rheological evaluation of native and decellularized AF tissue; C: Human AF cell evaluation on dAF, using DAPI and F-actin staining, and visualizing dAF ECM under confocal reflection microscopy (CRM). 10x: scale bar=100 µm; 40x: scale bar = 100 µm.

DISCUSSION & CONCLUSIONS: This work establishes a dAF matrix that preserves the native ECM composition, architecture and mechanical properties, providing a promising platform to study human AF cell behavior in a physiologically relevant environment. Further studies establishing diseased microenvironments will support the future use of these matrices as advanced in vitro AF pre-clinical models.

REFERENCES:

[1] Castro, A.L., et al., Arthritis Research & Therapy, 2022. [2] Gonçalves, R.M., et al., Front Bioeng Biotechnol, 2021. [3] Castro AL, Gonçalves RM. Acta Biomater. 2025. [4]: Fiordialisi, MF., et al., Biomaterial Advances, 2022; [5]: Castro AL, et al., Acta Biomater. 2025.

Mechanical environment drives acetylation-mediated epigenetic remodeling in C28/I2 chondrocytes.

Rocío Castro-Viñuelas[1], **Dennis M Minton[1]**, and Ilse Jonkers[1]
[1]*Department of Movement Science, KU-Leuven, Leuven, Belgium*

Introduction: Articular chondrocytes are highly specialized cells that continuously integrate biochemical and mechanical cues to remodel and maintain the extracellular matrix (ECM), preserving cartilage function. Their behavior is tightly regulated by the mechanical properties of their microenvironment. During osteoarthritis (OA), degenerative changes in the ECM composition and stiffness disrupts this finely tuned mechanobiological balance, leading to aberrant and catabolic cellular responses. Emerging evidence suggests that the mechanical environment of a cell can induce persistent epigenetic modifications, thereby influencing cellular responses to subsequent environmental changes[1,2]. However, it remains unclear whether such "mechanical memory" exists in chondrocytes. Therefore, the objective of this study was to investigate whether distinct mechanical environments modulate epigenetic regulatory mechanisms in chondrocytes, providing evidence for the existence of mechanical memory.

Methods: C28/I2 chondrocytes were seeded on polyacrylamide substrates of 4.5 or 30 kPa, representing "soft" and "stiff" conditions, respectively, and cultured for 72 hours. Cells were subsequently fixed for immunofluorescence analysis of YAP localization and lysine residue acetylation, or harvested for RNA extraction and qPCR to assess the expression of genes associated with mechanoresponse (AGRN, HIF1a, HIF2a) and epigenetic regulation (HDAC1, 2, 3, 8, HAT1, EZH2, WDR5). Data represent 3 independent experiments and were analyzed using 2-tailed unpaired t-tests to compare between soft and stiff conditions.

Results: To confirm the sensitivity of C28/I2 chondrocytes to substrate stiffness, we evaluated nuclear translocation of YAP. Immunofluorescence demonstrated increased nuclear YAP localization under stiff compared to soft conditions, confirming responsiveness to substrate stiffness (**Fig 1a**). Gene expression analysis revealed that stiff substrates decreased HDAC1 and HDAC2 expression while increasing HDAC3, with no significant changes observed in histone methylation–related genes (EZH2, WDR5) or mechanoresponsive transcription factors (AGRN, HIF1α, HIF2α) (**Fig 1b**). Because acetylation-related genes showed the most potent response to mechanical environment, we next evaluated lysine acetylation by immunofluorescence, which was increased under stiff conditions compared to soft (**Fig 1c**).

Discussion and Conclusions: The mechanical environment influences YAP nuclear localization, the expression of acetylation-related epigenetic regulators, and total lysine acetylation levels in chondrocytes. These findings suggest that the mechanical environment may imprint a form of mechanical memory in chondrocytes through histone acetylation. Future work will assess protein-level changes, determine whether these epigenetic alterations translate to chondrogenic gene expression, and validate these finding in primary human chondrocytes.

References

1.Killaars, A.R., Walker, C.J., and Anseth, K.S. (2020). Nuclear mechanosensing controls MSC osteogenic potential through HDAC epigenetic remodeling. Proc. Natl. Acad. Sci.

2.Scott, A.K., Casas, E., … Foster, K.J. (2023). Mechanical memory stored through epigenetic remodeling reduces cell therapeutic potential. Biophys. J.

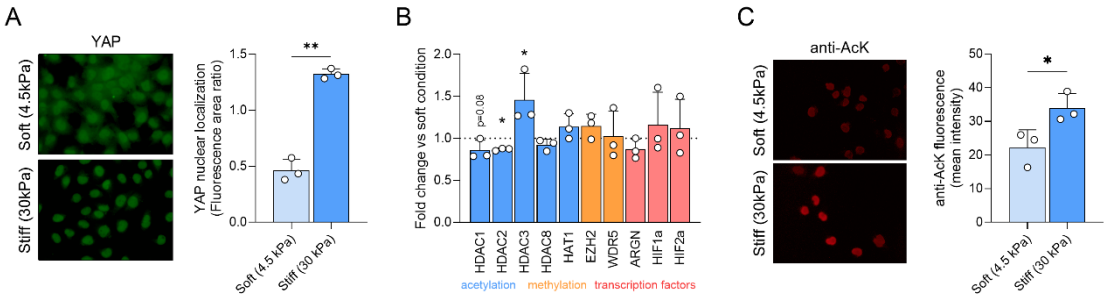

Biomimetic and injectable aminated collagen-hyaluronic acid-glycosaminoglycan (aCol-HA-GAG) biomaterial scaffold for cell-based intervertebral disc regeneration

Mansoor Chaaban[1], Tosmi Goel[1], Xingxing Yang[2], Du-Hao Cher[1], Jerome Guicheux[1], Marion Fusellier[1], Barbara P. Chan[2], Catherine Le Visage[1]

1. Nantes Université, Oniris, INSERM, CHU Nantes, Regenerative Medicine and Skeleton, RMeS, UMR 1229, F-44000 Nantes France
2. Tissue Engineering Lab, School of Biomedical Science, Institute of Tissue Engineering and Regenerative Medicine, Department of Biomedical Engineering, The Chinese University of Hong Kong, Hong Kong Special Administrative Region, China

INTRODUCTION: Intervertebral disc (IVD) degeneration is a leading cause of chronic back pain, yet current treatments fail to restore its function. Here, we focused on a biomimetic scaffold that replicates the native disc matrix. This aminated collagen-hyaluronic acid (HA)- glycosaminoglycan (GAG) biomaterial was engineered to mimic the native NP tissue ratio. [1] We investigated whether this biomaterial scaffold can support cell viability, proliferation, and differentiation. In a separate experiment, a method for evaluating scaffold localization within a disc was developed using an ex vivo bovine tissue.

METHODS: Human adipose stromal stem cells (ADSCs) were mixed with the material and cultured for 28 days in hypoxic conditions. [2] The projected surface area of the seeded scaffold was imaged every 3 days for 28 days using a Leica microscope. The cells were cultured with transforming growth factor β-3 (TGF-β3) and growth differentiation factor-5 (GDF-5) to induce nucleopulpogenic differentiation. Cell viability, proliferation, metabolic activity, morphology, and differentiation were evaluated using CCK8, EdU, PicoGreen, and histological and imaging techniques at various time points, respectively. A micro-CT analysis was performed to visualize the material in ex vivo bovine discs. Samples were incubated in 3% phosphotungstic acid for 3 minutes before being injected into the IVD defect.

RESULTS: Cell association with the collagen-HA-GAG biomaterial scaffold was successful. The CCK-8 assay showed increased metabolic activity, while EdU staining and Picogreen assay provided inconclusive results on proliferation due to interference from the biomaterial with the absorbance signal. The projected surface area initially decreased gradually, indicating a contraction of the seeded material, as expected. Histological analysis with Alcian Blue staining revealed the presence of cells associated with the scaffold at all time points. The faint staining did not provide information regarding cell differentiation. Finally, Micro-CT imaging enabled a clear distinction between the scaffold and the surrounding bovine NP tissue.

DISCUSSION & CONCLUSIONS: The aminated collagen-HA-GAG scaffold supported cell viability during an in vitro differentiation protocol. Future work will focus on assessing specific markers of nucleopulpogenic differentiation and on conducting long-term studies in an ex vivo model.

REFERENCES:

[1] A. T. H. Choy, K. W. Leong, and B. P. Chan, "Chemical modification of collagen improves glycosaminoglycan retention of their co-precipitates," *Acta Biomater.*, vol. 9, no. 1, pp. 4661–4672, Jan. 2013, doi: 10.1016/j.actbio.2012.09.016.

[2] P. Colombier *et al.*, "TGF-β1 and GDF5 Act Synergistically to Drive the Differentiation of Human Adipose Stromal Cells toward Nucleus Pulposus-like Cells," *Stem Cells*, vol. 34, no. 3, pp. 653–667, Mar. 2016, doi: 10.1002/stem.2249.

ACKNOWLEDGEMENTS:

This study was supported by the International Research Projects from Inserm (IRP Glycodisc 1R22040NTENTE) and Fondation pour la Recherche Médicale (FRM, REP202110014192).

Using Mesendoderm Progenitor Cells Seeded in Hydrogel Biomaterial as a strategy to Regenerate the Intervertebral disc

C. Cicione[1], RJ. Williams[2], J Snuggs[2], J Warin[3], C Sammon[4], B Gatenbein[5], D Noel[6], JM LeMaitre[6], A Camus[3], MA. Tryfonidou[7], G Vadalà[1] Christine Le Maitre[2]

1: Campus Bio-Medico University of Rome, 2: University of Sheffield, 3: Nantes University, 4: Sheffield Hallam University, 5: University of Bern; 6: INSERM, 7: Utrecht University

INTRODUCTION: Low back pain, the leading cause of disability worldwide, is strongly associated with degeneration of the intervertebral disc (IVD). We have previously demonstrated that an injectable biomaterial 'NPgel' can induce regeneration within organ culture systems of goat and human cadaveric IVDs. The combination of this biomaterial with embryonic precursors for the nucleus pulposus (NP) cells, could be an attractive regeneration strategy. This study investigates the ability of NPgel to drive differentiation of mesendoderm progenitor cells (MEPCs) generated from human induced pluripotent stem cells (hiPSC) into matrix producing cells under conditions which mimic the IVD. An ovine nuclectomy model of disc degeneration was then utilized to investigate the safety and short-term efficacy of NPgel either alone or in combination with iPSC-MEPCs.

METHODS: HiPSC were differentiated into MEPCs seeded into NPgel and cultured for 4 weeks at 5% O_2. MEPCs viability, phenotype, and extracellular matrix synthesis investigated. Disc degeneration was induced in sheep through nucleotomy, 5 wks post degeneration sheep were treated in 3 alternating lumbar discs with NPgel or NPgel+iPSC-MEPC injection. Remaining discs remained as untreated degeneration only controls. MRI determination of disc height and Pfirmann grading was performed. Peripheral blood collected for haematological, biochemical, metabolic and immunological evaluation. Three months following treatment sheep were sacrificed and spines processed for: macroscopic Thompson grading, Histological grading, immunohistochemical assessment, and Alu-sequence-PCR.

RESULTS: MEPCs cultured within NPgel survived and were immunopositive for brachyury, and Sox 9, and Aggrecan and Collagen type II indicating matrix synthesis (Figure 1A). Ovine *in vivo* treatment with NPgel+MEPCs showed a slight increase in disc height index (108% increase compared to degeneration only). No local adverse reactions were seen nor systemically. Histological grading showed similar degeneration all discs regardless of treatment group, including evidence of degeneration in untreated controls (Figure 1B). PKH-26 labelled iPSC-MEPCs were visible within discs 3 months following injection with NPgel+MEPC, and Alu sequences were identified in discs injected with NPgel+MEPC but no discs where MEPCs were not injected. The number of immunopositive cells for TBXT, Sox-9, aggrecan and collagen type II were similar across all groups (Figure 2A&B), whilst the number of cells positive for IL-1, and ADAMTs4 within the NP was increased in nucleotomy discs and decreased following NPgel injection, which reached significance following NPgel+MEPC injection compared to nucleotomy alone ($P<0.05$)(Figure 1C).

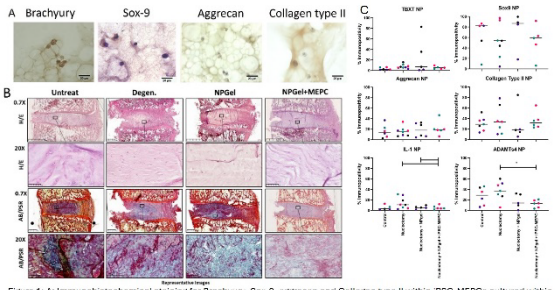

Figure 1: A: Immunohistochemical staining for Brachyury, Sox-9, aggrecan and Collagen type II within iPSC-MEPCs cultured within NPgel in low glucose DMEM under 5% O_2 conditions for 4 weeks. B: Histological staining of sheep discs following in vivo investigation of nucleotomy induced degeneration and treatment with NPgel alone or in combination with iPSC-MEPCs. Haematoxylin and Eosin (H&E), Alcian Blue / Picrosirius red (AB/PSR) staining show regions of injected NPgel within injected discs showing excellent integration. C: Immunopositivity for TBXT, Sox-9, aggrecan, collagen type II, IL-1 and ADMATs 4 in sheep NP. Individual sheep spines shown in individual colors. Discs were either left untreated (control), degeneration induced with nucleotomy and either left to degenerate or treated with Npgel alone or in combination with iPSC-MEPCs.

DISCUSSION & CONCLUSIONS: NPgel was shown to support the differentiation of MEPCs towards notochordal/nucleus pulposus cells. Human MEPCs were delivered safely to an animal model of disc degeneration. MEPCs were found in sheep discs 3 months following injection, and whilst matrix staining for aggrecan and collagen type II were similar across all treatment groups a decrease in IL-1 immunopositivity was seen in discs injected with NPgel+MEPCs compared to nucleotomy alone.The injectable gel system described here shows promise to deliver induced pluripotent stem cells in a safe manner to the disc to induce regeneration.

ACKNOWLEDGEMENTS: This project has received funding from the European Union's Horizon 2020 research and innovation program under grant agreement No 825925.

CONFLICT OF INTEREST: CLM and CS are inventors on the patent for NPgel which has been licensed to Orthoson Ltd.

Why does animal health matter - Correlation of postoperative welfare with clinical parameters in a rabbit model of knee osteoarthritis

RZ. Coeti[1], M. Carretero-Hernández[1], Y. Zhang[1], F. Li[1], JK. Venkatesan[1], A. Acheli[1], G. Schmitt[1], M. Cucchiarini[1], H. Madry[1]

[1]Center of Experimental Orthopaedics, Saarland University, 66421 Homburg, Germany

INTRODUCTION: Anterior cruciate ligament transection (ACLT) is an established model to induce osteoarthritis (OA) in rabbits. This study evaluates how the rabbit welfare score obtained postoperatively [individual behaviour; food intake; facial pain expression via Grimace scale (Keating et al., *PloS one* 2012, 7, e44437) for orbital tightening, cheek flattening, nose shape, whisker position, ear position, and surgical wound] correlates with clinical parameters obtained at 3 weeks postoperatively [range of motion for flexion/extension; joint swelling; percentage of weight change].

METHODS: Healthy female New Zealand white rabbits [n = 24, mean body weight (BW), 2.18 ± 0.28 kg] underwent transection of both ACL. Immediately postoperatively, they were monitored for 10 consecutive days, to monitor (1) facial expression using data from the Grimace scale indicating pain, (2) individual animal behaviour, (3) food intake and (4) surgical wound to compound a welfare score. After 3 weeks, animals were euthanized. Clinical evaluation comprised (1) maximum range of knee flexion and extension, (2) amount of knee joint swelling and (3) weight change (as percent of change from day 0 to 21). All data were submitted to statistical analyses of normality, lognormality, and parametric or nonparametric tests. Covariance (ANOVA) and correlation tests were used according the nature of the data.

RESULTS: The surgical procedure was performed bilaterally in 44 joints (n = 22 rabbits; two animals died at anaesthesia) without intra- or postoperative surgical complications. The rabbits recovered quickly, as indicated by the full weightbearing on both operated hindlimbs 24 h postoperatively. At day 2 postoperatively, individual animal behaviour (r = -0.62; P < 0.05), food intake (r = -0.66; P < 0.05), and welfare score sum (r = -0.50; P < 0.05, correlated negatively, significantly with swelling of the knee joint at 3 weeks. At day 2, the Grimace scale positively correlated with the knee extension at 3 weeks (r = 0.51; P = 0.01). At 4 days postoperatively, the Grimace scale positively correlated with the knee extension (r = 0.60; P < 0.05) and swelling of the knee joint (r = 0.53; P = 0.01) at 3 weeks. The Grimace scale at 4 days negatively correlated with the percentage of weight change over the 3 weeks period (r = -0.44; P = 0.04). Similar observations were noted at day 4, with the sum of the welfare score that positively correlated with knee extension (r = 0.61; P < 0.05) and swelling (r = 0.52; P = 0.01), whereas it negatively correlated with the percentage of weight change (r = -0.44; P = 0.04). At day 6, the welfare score negatively correlated with the percentage of weight change (r = -0.43; P = 0.04). No correlations were identified beyond 8 days.

DISCUSSION & CONCLUSIONS: Individual parameters and the overall animal welfare score in the first days after surgery were linked to clinical parameters obtained 3 weeks postoperatively, suggesting that these parameters may immediately indicate short-term clinical outcomes in this model of early OA after ACLT. They also highlight that postoperative pain and welfare monitoring are essential for a worthy health of animals after surgery.

ACKNOWLEDGEMENTS: Funded in part by the collaborative research network "SINPAIN" (EU Horizon - Grant Agreement no. 10105777).

SHH- and *TBXT*-mRNA-loaded lipid nanoparticles as a promising regenerative therapy for degenerated intervertebral disc

D. Corraini[1], A. Varela-Moreira[1], M. Buiter[1], A. Eversdijk[1], C. Voskamp[1], Q. Yang[2], Z. Lei[2], R. M. Schiffelers[2], M. A. Tryfonidou[1]

[1] *Utrecht University, Utrecht, NL;* [2] *University Medical Centre Utrecht, Utrecht, NL.*

INTRODUCTION: The intervertebral disc (IVD) degenerates with ageing and may lead to low back pain. Being the largest avascular organ in the body, it represents a unique target for local drug administration, reducing the off-target and adverse effects of systemic administration. Lipid nanoparticles (LNPs) represent a promising therapeutic nucleic acid delivery platform for regenerative therapies. The present study investigates the administration efficiency and therapeutical efficacy of potential regenerative targets (SHH and TBXT) delivered as mRNA payloads in LNPs to nucleus pulposus cells (NPCs) cultured in a degenerated IVD-mimicking environment (1).

METHODS: *SHH*- and *TBXT*-mRNA-loaded LNPs were prepared using a clinically approved lipid formulation via Impinged Jet Mixing technology (Nova™ IJM, Helix Biotech). The average diameter, polydispersity and surface charge were measured by Dynamic and Electrophoretic Light Scattering. LNPs were Cy5.5-labelled to determine via flow cytometry cellular association after 24 hrs to dog NPCs monolayer cultured in degenerate IVD medium (350 mOsm/L, pH 6.8 - forward transfection with 1 µg mRNA/35.000 cells). 24 hrs post-treatment, transfection efficiency was determined assessing mRNA translation via immunofluorescence for TBXT and SHH, and functionality was determined by measuring gene expression of respective downstream targets (*ACAN* and *PTCH1*) via qPCR. Transfection efficiency of mRNA-LNPs in a 3D *in vitro* dog NPC model (pellet culture) was tested using *eGFP* mRNA-loaded LNPs (reversed transfection with 1.2 µg mRNA/pellet; 24hrs) and evaluating eGFP expression via immunohistochemistry and flow cytometry.

RESULTS: Therapeutical *SHH* or *TBXT* mRNA-loaded LNPs presented commonly accepted characteristics in regard to diameter (141, 105 nm, respectively), polydispersity (0.24, 0.19 PDI), surface charge (-14.5, 0 mV) and mRNA encapsulation efficiency (69, 81%). They both showed 100% association to monolayer NPCs, however with higher Cy5.5 mean fluorescence intensity for *SHH*-LNPs compared to *TBXT*-LNPs, possibly due to the relatively lower mRNA encapsulation efficiency of *SHH*-mRNA. Upon 24 hrs of *SHH*-LNP treatment, SHH protein expression in monolayer NPCs was comparable to untreated condition, while TBXT expression appeared upon *TBXT*-LNPs transfection. SHH downstream *PTHC1* and TBXT downstream *ACAN* expression in monolayer NPC were upregulated at 24 hrs from *SHH*-LNP and *TBXT*-LNP treatment. NPCs pellet transfected with 1.2 µg *eGFP* mRNA-loaded LNPs maintained 100% cell viability, with 19% NPCs expressing eGFP after 24 hrs.

DISCUSSION & CONCLUSIONS: This work shows that the clinically approved LNP formulation can be effectively employed to deliver functional therapeutical mRNAs coding for rejuvenating molecules to NPCs residing in a degenerate disc environment. Moreover, it indicates that SHH and TBXT delivery as mRNA to NPCs potentially exerts beneficial effects. Ongoing functional studies *in vitro* on dog NPC pellets cultured in degenerative conditions (1 week) and e*x vivo* on bovine NP explant culture (14 days) intend to assess the regenerative effects of therapeutical *SHH*- or *TBXT*-LNPs via histological and biochemical analysis for cell phenotype and extracellular matrix characteristics.

REFERENCES:

(1) Snuggs J, et al. JOR Spine. 2025: 8:e70153.

Degenerate intervertebral disc environment impairs the regenerative potential of notochordal cell-derived extracellular vesicles

D. Corraini[1], C. Voskamp[1], A. Eversdijk[1], F. M. Riemers[1], H. R. Vos[2], P. Vader[2], G. G. H. van den Akker[3], T. J. M.Welting[3], K. Ito[4], M. H. M. Wauben[1], M. A. Tryfonidou[1]

[1] Utrecht University, Utrecht, NL; [2] University Medical Centre Utrecht, Utrecht, NL; [3] Maastricht University Medical Centre, Maastricht, NL; [4] Eindhoven University of Technology, Eindhoven, NL.

INTRODUCTION: During IVD degeneration, the tissue environment changes with reducing pH and osmolarity, while the residing large vacuolated notochordal cells (NCs) are replaced by the smaller non-vacuolated nucleus pulposus cells (NPCs). NCs maintain disc health and homeostasis via their secretome which is rich in extracellular vesicles (EVs). However, it is unknown how the changing IVD environment affects the regenerative potential of NC-derived EVs. Therefore, this study investigates the impact of healthy and degenerate IVD environment (1) on the characteristics and the regenerative potential of NC-derived EVs.

METHODS: NC-rich tissue was isolated from porcine spines (N=5) and cultured for 4 days either in healthy (7.1 pH, 450 mOsm - H-EVs) or degenerate (6.8 pH, 350 mOsm - D-EVs) medium, generating donor matched conditioned media. The extracellular matrix and cell phenotype of the cultured tissues were characterized via biochemical analysis and (immuno-)stainings. The levels of inflammatory regulators upon tissue culture in respective media were determined via multiplex ELISA. NC-EVs were isolated from these tissue conditioned media via differential centrifugation, followed by size exclusion chromatography. Isolated NC-EV size and concentration were determined via nanoparticle tracking analysis (NTA), while EV morphology was investigated via transmission electron microscopy. EV markers presence was determined via proteomics analysis. The regenerative potential of H-EV and D-EV was tested on NPC pellets (from degenerated dog discs) via (immuno)histological and biochemical analysis for extracellular matrix and cell phenotype. The mode of action of NC-EVs was determined via bulk RNA sequencing of EV-treated NPCs, as well as, functional studies on chondrosarcoma reporter cell lines.

RESULTS: After 4 days of tissue culture, NC phenotype and matrix characteristics were preserved and comparable between the two conditions. Also, the levels of inflammatory factors in the conditioned media (PGE2, CCL2, IL10, IL6, ILRA, CXCL8, TNF, IFNG, IL1B, MMP1) were comparable between healthy and degenerate conditions. Measured by NTA, released D-EV were half as abundant as H-EV, while having a comparable average particle size (200 nm) and morphology. At the protein level, they presented common EV markers which were drastically decreased in the respective EV-depleted controls. Functional studies showed that H-EVs significantly increased GAG production in NPC pellets compared to EV-depleted controls, while there was no significant difference between D-EV and respective EV-depleted controls. This indicates that H-EVs could modulate matrix deposition of NPCs in an EV-specific manner, while these effects are lost for D-EVs. Interestingly, H-EVs upregulated the expression of genes involved in matrix metabolism in NPCs, while D-EVs upregulated the expression of genes involved in cell proliferation, regulation of inflammation and the WNT pathway. Complementary functional analysis using reporter cell lines, showed activation of SMAD3/4 and STAT3 signalling, while both NC-EV groups did not activate TCF/LEF-mediated signalling.

DISCUSSION & CONCLUSIONS: This study highlights the negating effects of the degenerated IVD environment on the release of NC-derived EVs and their matrix anabolic effects on NPCs. Moreover, it elucidates that the mildly degenerated IVD environment shifts the mode of action of NC-EVs towards their involvement in cellular replication and inflammation regulation. All together these results demonstrate that the degenerated IVD environment in the short-term negatively affects the NC-derived EVs.

REFERENCES:

(1) Snuggs J, et al. JOR Spine. 2025: 8:e70153.

Extracellular Matrix Depletion Underlies Mechanical Dysfunction in the Aging Intervertebral Disc of Mouse

Dahia C.L.[1,2], Hallmark A.P.[1], Bogdan S.[1], Ali A.M.[3]
[1]Hospital for Special Surgery, New York City, NY, USA. [2]Weill Cornell Medical College, New York City, NY, USA. [3]Columbia University, New York City, NY, USA.

INTRODUCTION: Intervertebral disc (IVD) degeneration is a major contributor to chronic back pain and mechanical instability, particularly in older adults worldwide. The IVD forms a cartilaginous joint within the spine that provides flexibility while resisting compressive forces under healthy conditions. Proper IVD function depends on a highly specialized extracellular matrix (ECM) that maintains tissue hydration, structure, and mechanical integrity. This ECM is organized into a proteoglycan-rich nucleus pulposus (NP) core and collagen-rich lamellae of the annulus fibrosus (AF), which together sustain disc function. However, injury and natural aging drive progressive molecular and structural changes within the IVD, resulting in ECM loss and pathological disc degeneration—a leading cause of chronic back pain.

Mice are widely used as pre-clinical models for IVD research, and, like humans, degeneration commonly affects their lumbosacral discs [1,2,3]. Despite this, age-associated molecular, structural, and mechanical changes in mouse lumbar IVDs remain poorly defined. Addressing this gap is essential for improving translational understanding of disc degeneration. Here, using RNA sequencing, proteomics, histochemical analyses, and atomic force microscopy (AFM) we systematically characterized structural, biochemical, and mechanical changes in lumbar IVDs from early postnatal life through advanced aging in mice.

METHODS: Lumbosacral IVDs were collected from newborn, 3-month-old, 12-month-old, and >24-month-old male and female mice under institutionally approved IACUC protocols. NP and AF tissues from L6/S1 discs were microdissected and subjected to bulk RNA sequencing for deep transcriptomic profiling, and label-free proteomic analysis using LC-MS/MS. Additional age-matched L6/S1 discs were fixed, cryosectioned for histochemical staining, immunostaining, and AFM-based mechanical testing.

RESULTS: Integrated transcriptomic and proteomic analyses revealed a pronounced, age-dependent decline in ECM synthesis and turnover in both NP and AF cells of mouse lumbosacral IVDs. Histochemical staining with Safranin-O/fast green and picrosirius red demonstrated progressive structural alterations and region-specific changes in biochemical composition across the lifespan and were used to define regions of AFM analysis. AFM measurements showed significant age-related alterations in the viscoelastic properties indicating loss of stiffness in all components with age, which was associated with decline in ECM.

DISCUSSION & CONCLUSIONS: Disc degeneration is commonly thought to involve fibrotic stiffening of the NP; however, our multi-modal biochemical and mechanical analyses reveal that aging is instead associated with a decline in collagens and other matrisome-associated proteins in both NP and AF, accompanied by tissue softening. These findings suggest that impaired mechanical performance of the aging or degenerating IVDs arises primarily from loss of essential structural ECM components rather than excessive fibrosis.

ACKNOWLEDGEMENTS: We thank NIA/NIH R01AG070079, NIAMS/NIH R01AR077145, and OD/NIH S10OD026763 for funding support.

REFERENCES:

1. *Vincent K. et al., Bone 2019*
2. *Mohanty S. et al., Aging Cell 2019*
3. *Mehta R. et al., JOR Spine 2026*

In Search of a Disease-modifying Osteoarthritis Drug Using Aptamer Technology

Lotte J.M. Deneer[1], Mickey R. Schlüter[1], Kelly Warmink[1], Harrie H. Weinans[1,2] and Jaqueline L. Rios[1].

[1] *Department of Orthopaedics, University Medical Centre Utrecht, Utrecht, Netherlands*
[2] *Department of Biomechanical Engineering, Delft University of Technology, Delft, The Netherlands*

INTRODUCTION: Osteoarthritis (OA) is one of the most disabling musculoskeletal diseases, and one for which no disease-modifying drugs are currently available [1]. Thus highlighting a pressing need for novel effective therapeutic strategies. A promising group of molecules that has recently gained traction as potential therapeutics is that of aptamers which are short single-stranded oligonucleotides (ssDNA and RNA), which can be used to selectively bind target moieties [2]. Emerging evidence implicates the Akt-mediated phosphorylation of forkhead box O (FoxO) transcription factors in OA pathogenesis, making the FoxO-Akt axis an attractive target [3,4]. In this study, we aim to select aptamers targeting the FoxO3 phosphorylation sites and thereby modulate Akt-FoxO signalling in osteoarthritic tissue.

METHODS: ssDNA aptamers were selected via *in-vitro* Systematic Evolution of Ligands by EXponential enrichment (SELEX). Synthetic peptides corresponding to key FoxO3 phosphorylation motifs were used as targets. After 14 rounds of SELEX for each individual peptide, the enriched aptamer pools were subjected to high-throughput sequencing in order to evaluate the top aptamer candidates. Lastly, the secondary structures of the most abundant aptamers in the final pools were predicted using the RNAfold WebServer (http://rna.tbi.univie.ac.at/cgi-bin/RNA WebSuite/RNAfold.cgi).

RESULTS: High-throughput sequencing of the first SELEX targeting peptide Ser315 (selection rounds R0, R3, R6, R9, R12 and R14) showed a moderate decrease, of 26%, in the number of unique sequences found across the SELEX process (Figure 1.A). Enrichment of the aptamer pool was further confirmed from the shift in nucleotide distribution (Figure 1.B). Secondary structure predictions of the three most abundant aptamers present in the last selection round showed inclusion of a stable stem-loop in all three structures (Figure 1.C).

DISCUSSION & CONCLUSIONS: Preliminary data obtained for the first FoxO phosphorylation target site shows enrichment of the aptamer pool after 14 rounds of SELEX. This resulted in a narrowed down selection of promising aptamer candidates for targeting FoxO phosphorylation. These will be further characterised in terms of binding affinities and cellular uptake using an inducible FoxO-GFP reporter cell line. Further development of these aptamers could pave the way for the first targeted, disease-modifying therapy for OA.

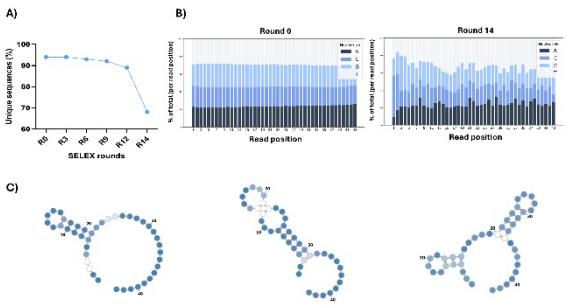

Figure 1. (**A**) Decrease in the number of unique sequences found across each selection round. (**B**) Shift in nucleotide distribution found in the aptamer's random region (43 nt) from an equal distribution in the starting pool to position-dependent changes in nucleotide contribution after the last round of selection. (**C**) **S**econdary structure prediction of the top three aptamer candidates.

REFERENCES:

[1] Rodriguez-Merchan. The Current Role of Disease-modifying Osteoarthritis Drugs. 2023.
[2] Nimjee et al. Aptamers as Therapeutics. 2017
[3] Ohzono et al. Targeting FoxO transcription factors with HDAC inhibitors for the treatment of osteoarthritis. 2022.
[4] Matsuzaki et al. FoxO transcription factors modulate autophagy and proteoglycan 4 in cartilage homeostasis and osteoarthritis. 2018.

HLA-A*26:01 is associated with vertebral endplate bone marrow lesions (Modic changes): evidence for an immunogenetic component in spinal degeneration

J. Devan[1,2], C.J. Smith[3], J. Määttä[4], J. Zhou[5], P. Leary[6], P-H. Wu[7], T. Link[7], O. Distler[1], J. Karppinen[4], F.M.K. Williams[3], A. Fields[5], S. Dudli[1,2]

[1]Center of Experimental Rheumatology, University Hospital Zurich, University of Zurich, CH. [2]Department of Physical Medicine and Rheumatology, Balgrist University Hospital, Balgrist Campus, University of Zurich, CH. [3]School of Life Course and Population Sciences, King's College London, UK. [4]Research Unit of Health Sciences and Technology, University of Oulu, Finland. [5]Department of Orthopaedic Surgery, University of California San Francisco, USA. [6]Institute of Molecular Cancer Research, University of Zurich, CH. [7]Department of Radiology and Biomedical Imaging, University of California San Francisco, USA.

INTRODUCTION: Modic changes (MC) are vertebral endplate bone marrow lesions associated with chronic low back pain. Although mechanical degeneration is considered the primary driver of MC, increasing evidence indicates an important inflammatory and immune component. The human leukocyte antigen (HLA) system is a major genetic determinant of immune-mediated diseases, but its role in MC remains unknown. We therefore investigated whether specific HLA alleles are associated with susceptibility to MC.

METHODS: HLA allele associations with MC were analysed across three independent cohorts: the REACH cohort from UCSF (n=326), the UK Twins registry (n=657), and the Northern Finland Birth Cohort 1966 (n=1092). Multivariable logistic regression models adjusted for age, sex, body mass index, smoking, and population background were used to estimate cohort-specific effects. Alleles with concordant direction of effect were combined using inverse-variance weighted random-effects meta-analysis with false discovery rate (FDR) correction. Age–allele interaction effects were evaluated in the UCSF cohort using Firth-penalised logistic regression**.**

RESULTS: Meta-analysis identified HLA-A*26:01 as a significant risk allele for MC (OR = 2.15, 95% CI 1.22–4.13; FDR = 0.026). Conversely, HLA-A*11:01 showed a protective association (OR = 0.60, 95% CI 0.40–0.89; FDR = 0.030). In the UCSF cohort, HLA-A26:01 significantly modified the age–MC relationship, with carriers showing a steeper age-related increase in MC risk (interaction OR per 10 years = 2.89, p = 0.047).

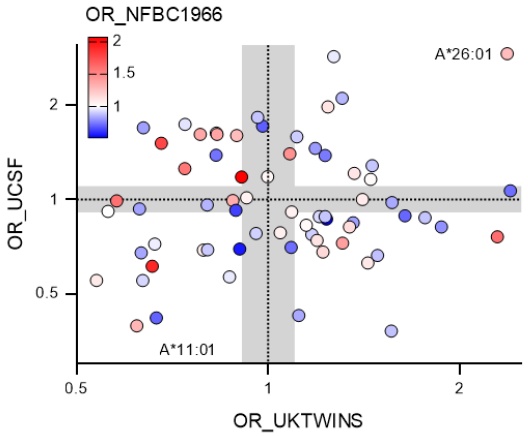

Figure 1. *Scatter plot of ORs for individual HLA alleles across three independent cohorts.*

DISCUSSION & CONCLUSIONS: This study identifies HLA-A*26:01 as the first immunogenetic risk factor for MC. The involvement of an MHC class I allele suggests a potential role for $CD8^+$ T-cell–mediated immune mechanisms in vertebral endplate pathology. The age-dependent effect of HLA-A*26:01 further indicates that genetic susceptibility may interact with degenerative processes during ageing. These findings indicate that HLA typing may support precision medicine, including risk stratification and treatment strategies in chronic low back pain patients with MC.

Modeling Neutrophil Responses to Annulus Fibrosus Secretomes Under Physiological and Inflammatory Conditions

Jun Dong[1, 2], Ezgi Bektas[1], Esther Bovay[1], Luca Buonarrivo[1], Marcia Mürner[1], Wen Chen[1], Junxuan Ma[1], Elena Della Bella[1], Zhen Li[1], Sybille Grad[1], Matteo D'Este[1,*]

*1.AO Research Institute, AO Foundation, Davos, Switzerland. 2.Department of orthopedics, Second Affiliated Hospital of Xi'an Jiaotong University, Xi'an 710004, China. * Corresponding Author: Matteo D'Este, Email: matteo.deste@aofoundation.org*

INTRODUCTION:

While the intervertebral disc (IVD) maintains a state of immune privilege under physiological conditions, in case of tissue damage the immune compartment gains access to the IVD. Neutrophils are the first responders recruited to sites of tissue damage, and as such they orchestrate the inflammatory response[1]. However, their role in IVD degeneration and discogenic pain remains unclear. The objective of this study is to establish a model to study the effect of annulus fibrosus (AF) secretome under physiological and inflammatory conditions on human neutrophils response.

METHODS: Human AF cells from three donors were cultured under hypoxia with or without cytokine priming (IL 1β + TNF α, 10 ng/mL) and with or without washing, generating four conditioned medium groups: washed non-primed (WNP), washed cytokine primed (WCP), unwashed non-primed (UWNP) and unwashed primed (UWCP). $3*10^5$ human neutrophils co-cultured in each well with conditioned medium diluted by equal volume of RPMI in 48-well plate for 5 hours. Cell viability and cytotoxicity of neutrophil were tested by Celltiter-Blue (CTB) and lactate dehydrogenase (LDH) detecting, respectively. RPMI medium was used in negative control. Triton X100 was used in dead control in cytotoxicity detection. Neutrophil elastase (NE) and myeloperoxidase (MPO) from the medium were detected by ELISA. PMA served as inflammatory control. One-way Anova was used for data analysis.

RESULTS: $2.32*10^7$ neutrophils were isolated from one donor's peripheral blood. Cell viability of neutrophils in the four conditioned media s was comparable but significantly lower compared to pristine RPMI medium. Neutrophils cultured in the conditioned medium, except WCP group, had even lower viability when compared to the inflammatory stimulus PMA. LDH release in four conditioned media was comparable within groups and with negative control. Neutrophils cultured in the unwashed conditioned medium showed higher LDH release, especially for AF cultured under inflammatory conditions, demonstrating how this model is suitable to detect neutrophils inflammation. Similar results were observed for NE, and to a lesser extent for MPO as detected by ELISA.

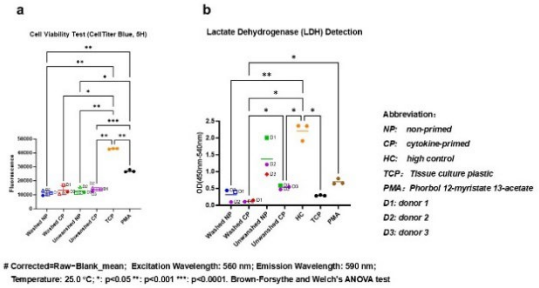

Fig. 1 Cell viability test and LDH release detection. a, the cell viability of neutrophils in four conditioned mediums. b, the LDH release detection of neutrophils in four conditioned mediums. *: p<0.05, **: p<0.01, ***: p<0.001.

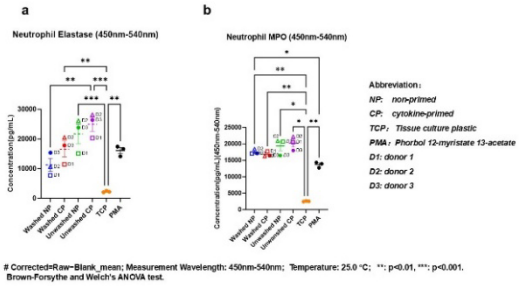

Fig. 2 ELISA results of NE and MPO. a. NE concentration of different groups. b. MPO concentration of different groups. NE and MPO in WCP, UWNP and UWCP groups were significantly higher than the RPMI group. *: p<0.05, **: p<0.01, ***: p<0.001.

DISCUSSION & CONCLUSIONS: Conditioned medium derived from AF cell decreased the metabolic activity of neutrophil but had low cytotoxicity. All the four conditioned mediums could promote neutrophil releasing NE and MPO.

REFERENCES:

1. Wesdorp, M. A., A. Schwab, E. I. Bektas, R. Narcisi, D. Eglin, M. J. Stoddart, Gjvm Van Osch, and M. D'Este. "A Culture Model to Analyze the Acute Biomaterial-Dependent Reaction of Human Primary Neutrophils in Vitro." Bioact Mater 20 (Feb 2023): 627-37.

Molecular Patterns in Early Osteoarthritis: The Role of Cellular Senescence

E. Duman[1], G. Pattappa[1], P. Pann[2], S. Reppenhagen[1], M. Rudert[1], P. Angele[2], D. Docheva[1]

[1] Department of Musculoskeletal Tissue Regeneration and Department of Orthopaedics, Orthopaedic Hospital König-Ludwig-Haus, Germany, [2] Laboratory of Experimental Trauma Surgery, Department of Trauma Surgery, University Hospital Regensburg, Germany

INTRODUCTION: Cellular senescence (CS) is an irreversible state characterized by permanent cell-cycle arrest, dysfunctional mitochondria, impaired autophagy and resistance to programmed cell death. Senescent cells release a specific secretome marked by the secretion of inflammatory cytokines such as interferons (IFN), and extracellular matrix (ECM)-degrading enzymes that can trigger CS in neighboring cells. The contribution of CS to late-stage osteoarthritis has been established; however, its role in focal early OA (FEOA) development remains unexplored. Therefore, this study seeks to identify for the first time, differentially expressed genes (DEG) between FEOA and focal cartilage trauma (FCT) using bulk RNA-sequencing (RNA-seq) and to assess the involvement of CS pathways in FEOA pathogenesis with the overall aim of improving autologous chondrocyte-based therapies.

METHODS: Primary chondrocytes were isolated from cartilage chips derived from defect cleaning during autologous chondrocyte implantation procedures, and clinically classified as either FEOA or FCT. The RNA was extracted using RNeasy Plus Micro Kit (Qiagen, Hilden, Germany). RNA-seq was performed by NovoGene GmBH (Munich, Germany), with nine donors per group (n=9) included in the final analysis following quality control with FastQC software. DEG assessment was conducted using DESeq2 within NovoMagic platform, whilst gene ontology (GO) enrichment analysis, pathway analysis (PA) and gene network predictions were performed using gProfiler, Reactome and GeneMANIA respectively.

RESULTS: In total there were 431 significantly DEGs in FEOA ($log_2FC \geq 1$, $padj < 0.05$) compared to FCT samples (180 upregulated, 251 downregulated). Principal component analysis and gene expression heatmaps showed clear cohort separation, with a tight clustering of FCT samples, while FEOA samples exhibited greater heterogeneity, suggesting higher biological variability in FEOA. GO Biological Process analysis after subgrouping of genes as upregulated or downregulated revealed that downregulated genes in FEOA samples were linked to ECM synthesis and organization, while upregulated genes were associated with mitochondrial gene expression and RNA processing. PA indicated enrichment of mitochondrial fission-, cell-cycle checkpoint- and mitosis-related genes. Further comparison of DEGs with the CellAge CS gene database from the website genomics.senescence.info identified 20 upregulated and 12 downregulated CS-associated DEGs. These genes were predominantly connected to autophagy, DNA damage repair response and oxidative phosphorylation, implying impeded autophagy as a driver for CS in FEOA. Network prediction suggested activation of IFN signaling as a potential downstream effect of the CS related DEGs.

DISCUSSION & CONCLUSIONS: Collectively, these results indicate that senescence-related mechanisms and autophagy-related pathways are activated during onset of FEOA, which might make prevention of cellular senescence a valuable target for amelioration of FEOA. These findings are currently being validated by qPCR, and subsequent analyses will aim to identify potential pharmaceuticals that target senescent chondrocytes.

ACKNOWLEDGEMENTS: This work was funded by DFG grant AN309/11-1. We also thank EU COST-Actions CA23119: Senescence2030 and CA22170: Tendon Regeneration Network (TENET).

Enhancing Chondrocyte Regulatory Network Accuracy for Multiscale Coupling via Integrated Signalling Pathways

Andreu Pascuet-Fontanet[1] & Jérôme Noailly[1]

[1]*Biomechanics & Mechanobiology, SIMBIOsys Group, BCN MedTech Research Unit, Department of Engineering, Universitat Pompeu Fabra*

INTRODUCTION: While knee osteoarthritis (KOA) is understood at cellular and joint levels, the link between chondrocyte (CC) activity and tissue-scale mechanics remains poorly defined. Current knowledge-based regulatory network models (RNMs) provide a semi-quantitative representation of CC homeostasis, while finite-element models (FEM) track spatiotemporal protein concentrations and strains in cartilage. Yet, multi-scale models are often lacking because robust biochemical and mechanical integration for scale coupling is not considered [1]. Here we address this limitation by enhancing an established CC RNM [2] with literature-derived biochemical and mechano-transduction pathways and integrating them into a bidirectional tissue-level FEM framework [3].

METHODS: The CC RNM was expanded to include: (1) Indian hedgehog (IHH) signalling and its feedback loop with parathyroid hormone-related protein (PTHrP) [4,5], and (2) the chemo-mechano-regulation of integrins. The updated RNM was validated against 79 experimental falsification tests retrieved systematically from PubMed. Success was defined by RNM results matching experimental trends (upregulation, downregulation or maintenance) and statistical significance. Mann-Whitney U tests were used to account for the bimodal computational data distribution (i.e. pro-anabolic and pro-catabolic phenotypes characteristic of the CC RNM) [2]. Finally, the updated RNM was integrated into an in-house multi-scale FEM to enable bidirectional communication between cellular phenotypes and tissue states [3].

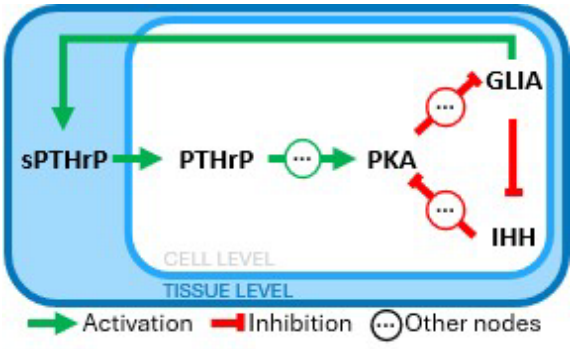

Figure 1. Structural decoupling of IHH-PTHrP feedback into cell and tissue-level nodes.

RESULTS: The refined network comprises 124 nodes and 387 edges. By distinguishing between soluble PTHrP (sPTHrP) and gene expression (see Fig. 1), we avoided cell-level oscillations, ensuring stable phenotype representation within the FEM. Additionally, including auxiliary nodes for mechanical integrin activation preserved essential biochemical sensitivity that would otherwise be lost when an integrin was fully activated by a mechanical load. These structural updates increased the model's predictive accuracy from 48.10% to 75.95%. The updated framework remained consistent when coupled with the tissue-level experimental model that had already been validated [3].

DISCUSSION & CONCLUSIONS: Our findings demonstrate that cell RNM topology shall consider its context of use (e.g. multi-scale simulations). Decoupling extracellular feedback loops and implementing auxiliary mechanical nodes are critical to achieve stable, tissue-scale representations while maintaining biochemical paracrine communication. Mechanistic analysis reveals that discrepancies in falsification tests are likely driven by the effects of interleukin-1β (IL-1β) overriding those of transient receptor potential vanilloid 4 (TRPV4). Incorporating the primary cilia regulation, where these pathways converge [6], may further enhance predictive power. Nevertheless, successfully incorporating the current RNM into the multi-scale model [3] provides a reliable mechanistic bridge between the cell and tissue, offering a powerful tool for unravelling KOA pathogenesis and exploring the potential of simultaneously targeting mechano-transduction and inflammatory pathways.

REFERENCES:

[1] Mukherjee *et al.*, *Front Bioeng Biotechnol.* 2020;8:93
[2] Segarra-Queralt *et al.*, *Front Bioeng Biotechnol.* 2023;11:1006066
[3] Pascuet-Fontanet *et al.*, *Orthop Procs.* 2025;107-B(SUPP_9)
[4] Yoshida & Yoshida, *Anat Sci Int.* 2025;100(2)
[5] Nishimori *et al.*, *Bone.* 2021;142:115709
[6] Sun *et al.*, *Exp Biol Med.* 2025;250:10490

AKNOWLEDGEMENTS

European Commission and Research Council (ERC-2021-CoG-O-Health-101044828); Spanish Government (STRATO-PID2021-126469OB-C21-2, PRE2022-102101).

A Dynamic Whole Knee Joint Culture that Preserves Cartilage Viability

Saskia Funk, Marianna Tryfonidou, Lizette Utomo

Dept of Clinical Sciences, Faculty of Veterinary Medicine, Utrecht University, the Netherlands

INTRODUCTION: Murine models enable comprehensive evaluation of treatment safety and efficacy through diverse readouts, including whole joint histology, which is often not feasible in basic *in vitro* models (1). An *ex-vivo* whole-joint culture model using surplus murine cadavers can reduce the need for live animal experiments in early R&D stages while preserving critical multi-tissue interactions in relatively short-term follow-up studies (2). However, validating such a model requires demonstrating the sustained viability of key joint tissues. The aim is to set up a basic culture system for whole rat knees while maintaining viable articular cartilage tissue.

METHODS: Whole rat knee joints were harvested from surplus female breeding Wistar rats and male Wistar Hannover rats (approximately 10 weeks old). Following dissection, joints were placed in custom 3D-printed culture inserts and maintained under dynamic culture conditions using gentle agitation by a magnetic stirrer for up to 7 days. For comparison, static cultures were performed in 6-well plates and 50ml vented tubes for 7 days. As negative control for each experiment, one knee was devitalized by three freeze-thaw cycles in liquid nitrogen, followed by incubation at 70℃ for 30 minutes.

After culture, articular cartilage (AC) explants were collected and pooled per joint. Metabolic activity was assessed using the Alamar Blue assay, followed by enzymatic digestion and flow cytometry with calcein-AM and propidium iodide staining to distinguish live and dead cells. Uncultured fresh knees were included as controls. For histological analysis, joints were fixed in 4% PFA, decalcified in 10% formic acid, embedded in paraffin, and sectioned (5µm) for Safranin-O/Fast Green staining.

RESULTS: Dynamic culture conditions consistently outperformed both static setups, better maintaining the metabolic activity of AC in cultured knees compared to day 0. However, the AC metabolic activity declined within the first 3 days of dynamic culture and further decreased to ~8% of the baseline by day 7. In contrast, flow cytometry demonstrated that AC cell viability remained high during the first 5 days (94-78% live cells), declining to 69% at day 7.

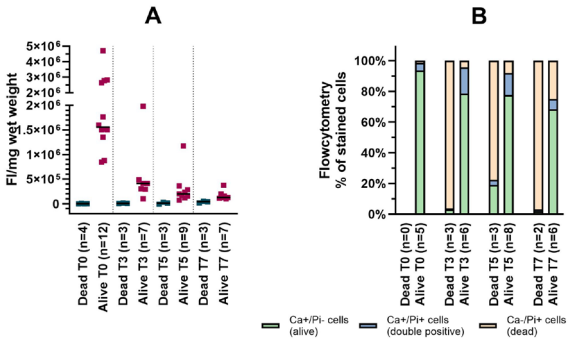

Figure 1 Metabolic activity and cell viability of rat articular cartilage explants over time during ex-vivo whole knee dynamic culture. *(A) Alamar Blue fluorescence normalized to wet weight for alive knees and dead controls. (B) Flow cytometric distribution of alive (Ca^+/Pi^-) double positive (Ca^+/Pi^+) and dead cells (Ca^-/Pi^+).*

DISCUSSION & CONCLUSIONS: This innovative yet minimalistic *ex-vivo* whole-knee dynamic culture model preserves AC viability for at least 5 days. Metabolic activity may be underestimated due to lower sensitivity of the Alamar Blue Assay for small tissues. Compared to static culture, dynamic conditions, generated by stirring of the culture media, enhance metabolic activity and maintained tissue viability. In the future, histological analysis will be done to evaluate microscopic changes during culture. Together, these findings support the use of this platform for cartilage-focused studies and lay the groundwork for future investigations involving additional joint tissues like the synovium and meniscus.

ACKNOWLEDGEMENTS: This work was partially funded by the LSH PPS VHH-MARS project (NSP23-01) supported by ReumaNederland and the National Growth Funds Ombion project (NGFCPBT241). We thank T.H.H. Nguyen (Department of Biology, Utrecht University) and Lydia Wolterman (HU University of Applied Sciences Utrecht) for providing surplus rat tissues.

REFERENCES: (1) Blaker CL, et al. J Orthop Res. 2017;35(3):424–39. (2) Haltmayer E, Ribitsch I, et al. PLoS ONE. 2019 Apr 2;14(4):e0214709.

N-acetylcysteine regulates the endoplasmic reticulum stress response in CEP-like chondrocytes exposed to proinflammatory cytokines

Laura González-Blanco[1,2*], Yousof Farrag[1], Mariam Farrag[1], Jesús Pino[1], Benjamin Gantenbein[2,3], Oreste Gualillo[1]

*[1]*SERGAS (Servizo Galego de Saude) e IDIS (Instituto de Investigación Sanitaria de Santiago), NEIRID Lab, Santiago de Compostela, Spain.*
[2]Tissue Engineering for Orthopaedics and Mechanobiology, Department for BioMedical Research (DBMR), Bern University, Switzerland
[3]Department of Orthopaedic Surgery & Traumatology, Inselspital, Bern University Hospital, Faculty of Medicine, Bern University, Switzerland

INTRODUCTION: Intervertebral disc degeneration (IVDD) is characterized by chronic inflammation and redox imbalance[1], which compromise cartilage endplate (CEP) cells and their organelles such as the endoplasmic reticulum (ER), leading to protein misfolding and altered calcium homeostasis. To counteract this, cells activate the unfolded protein response (UPR) through its main signaling pathways (ATF6α, IRE1α, and PERK/eIF2α)[2]. Due to its antioxidant properties, N-acetylcysteine (NAC) has been proposed as a potential modulator of these stress responses under pro-inflammatory conditions. However, its role in IVDD remains incompletely understood. This study aimed to analyze UPR dynamics and calcium homeostasis in differentiated ATDC5 chondrocytes, used as a CEP-like model, under inflammatory stress, and their modulation by NAC.

METHODS: Murine chondrogenic cell line ATDC5 (300,000 cells/well) was differentiated into mature chondrocytes for 10 days. Cells were then treated for 24 hours with IL-1α, IL-1β, and TNF (1ng/mL), in the presence or absence of NAC (100µM). Cytosolic calcium levels were determined using a colorimetric assay, and the expression of ATF6α, IRE1α, and p-eIF2α was assessed by Western blot. Statistical analysis was performed using one-way ANOVA followed by Tukey's *post hoc* test ($p<0.05$) on data from at least three independent experiments

RESULTS: IL-1α, IL-1β, and TNF significantly increased cytosolic calcium levels ($p<0.05$; Fig.1A), and the ER stress response was more pronounced, showing increased expression of IRE1α ($p<0.01$; Fig.1B), which is involved in the degradation of misfolded proteins, and ATF6α ($p<0.05$; Fig.1C), which regulates chaperone and antioxidant synthesis. No significant differences were observed for p-eIF2α (Fig.1D). NAC restored calcium levels in cells treated with IL-1β and TNF ($p<0.05$) and reduced ATF6α expression ($p<0.05$) under all pro-inflammatory conditions.

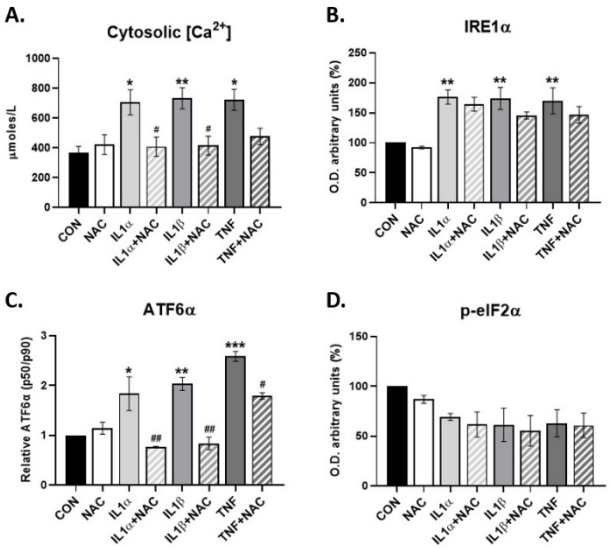

Figure 1. (**A**) Intracellular calcium levels (µmol/L). (**B–D**) Unfolded protein response (UPR) signaling pathways. Semiquantitative optical density of Western blot bands for (**B**) IRE1α, (**C**) ATF6α, and (**D**) p-eIF2α. *p<0.05; **p<0.01; ***p<0.001 *vs.* control; #p<0.05; ##p<0.01 *vs.* respective proinflammatory + NAC**.**

DISCUSSION & CONCLUSIONS: These findings suggest that the selective activation of the IRE1α and ATF6α branches represents an early adaptive response to inflammatory stress, consistent with disc degeneration models and associated with persistent redox imbalance[3]. The lack of changes in p-eIF2α supports differential regulation of UPR pathways. NAC modulates calcium homeostasis and UPR signaling, supporting its role as a regulator of ER stress and its ability to restore redox balance and prevent cytokine-induced cellular dysfunction[4]. Overall, NAC emerges as a potential therapeutic agent to mitigate cellular dysfunction and restore redox balance in CEP-like cells, potentially slowing IVDD progression.

REFERENCES:

[1]Suzuki et al., **2015**. *Arthritis Res Ther* 17:316.
[2]Wang, Kaufman, **2016**. *Nature* 529:326–335.
[3]Huang et al., **2023**. *Front Endocrinol* 13:1094394.
[4]Han et al., **2019**. *Biochem Biophys Res* Commun. 516:1026-1032.

Minimally Invasive Biologic Fusion: Synergistic EP4 and BMP-2/L51P Signaling Promotes Osteogenic Differentiation of Human Annulus Fibrosus Cells (Discfuse): Dose Optimization of KMN-159

Laura González-Blanco[1*], Stefan Zwingenberger[2], Xinggui Tian[2], Christoph E. Albers[3,4], Benjamin Gantenbein[1,2] , Sonja Häckel[1,2]

[*1]*Tissue Engineering for Orthopaedics and Mechanobiology, Department for BioMedical Research (DBMR), Bern University, Switzerland*
[2]*Center for Orthopaedic, Trauma Surgery and Rehabilitation Medicine, University Medicine Greifswald, 17475, Greifswald, Germany*
[3]*Department of Orthopaedic Surgery & Traumatology, Inselspital, Bern University Hospital, Faculty of Medicine, Bern University, Switzerland*
[4]*Spine Unit Sonnenhof Spital Bern, Bern University, Bern, Switzerland*

INTRODUCTION: Intervertebral disc degeneration (IVDD) is a major cause of chronic low back pain and disability worldwide [1]. In advanced cases, spinal fusion is commonly used to restore stability; however, achieving consistent fusion remains challenging, particularly in elderly patients. Promoting osteogenic differentiation within the disc space represents a promising minimally invasive strategy. KMN-159, a selective prostaglandin E2 receptor 4 (EP4) agonist, has been shown to modulate bone formation and inflammation, making it a promising candidate for this purpose. Notably, we previously demonstrated that KMN-159 induces up to a fivefold higher osteogenic response compared to BMP-2 alone, with particularly strong effects in degenerated cells derived from older female patients [2]. This study aimed to identify the optimal concentration of KMN-159 to induce osteogenic differentiation in primary human annulus fibrosus cells (AFCs), with the ultimate goal of reducing the need for spinal fusion surgery.

METHODS: Human AFCs (20,000 cells/well) from two donors were cultured for 21 days in osteogenic medium and stimulated with KMN-159 at concentrations ranging from 10 nM to 2 µM. Osteogenic differentiation was evaluated by measuring alkaline phosphatase (ALP) activity at day 14 and matrix mineralization by Alizarin Red staining at day 21, as previously described by Chen et al. [2]. Cell viability was assessed after 21 days using an XTT assay. Statistical analysis was performed using one-way ANOVA followed by Tukey's *post hoc* test ($p<0.05$) on data from independent experiments.

RESULTS: KMN-159 induced a dose-dependent osteogenic response, with 2 µM consistently producing the strongest effect, despite some variability at intermediate concentrations. This was demonstrated by a significant increase in ALP activity (Fig. 1A; $p < 0.001$) and matrix mineralization (Fig. 1B; $p < 0.001$), without compromising cell viability (Fig. 1C).

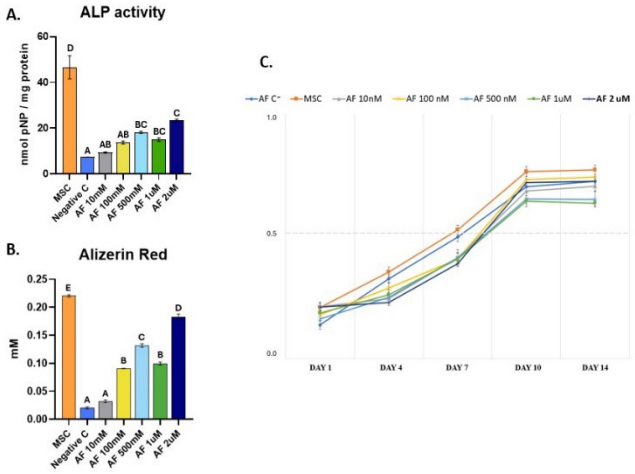

Figure 1. *In vitro* dose optimization of KMN-159 in human AF cells under osteogenic induction. (**A**) ALP activity at day 14. (**B**) Quantification of Alizarin Red staining (mM) at day 21. (**C**) Cell viability was assessed by the XTT assay after 21 days. Different letters indicate statistically significant differences between groups ($p < 0.05$).

DISCUSSION & CONCLUSIONS: KMN-159 induced a dose-dependent osteogenic response in human AFCs, with 2 µM identified as the optimal concentration to enhance ALP activity and matrix mineralization. This profile is consistent with previous *in vivo* data showing that KMN-159 promotes bone regeneration in a dose-dependent manner, reaching a maximal effect at an optimal dose beyond which no additional benefit is observed [3].
Overall, 2 µM KMN-159 represents the most effective concentration for promoting osteogenic differentiation in human AFCs without compromising cell viability, supporting its further evaluation as a candidate for spinal fusion strategies.

REFERENCES:
[1]Ferreira et al., **2021**. *Lancet Rheumatol* 5(6):e316-e329.
[2] Chen et al., **2026**. *Eur Spine J*. 1-11.
[3] Vater et al., **2021**. *Biomedicines* 9(11):1712.

Promoting Intervertebral Disc Fusion Through Combined BMP2, L51P, and EP4 Agonism: In Vitro Evidence from Human Annulus Fibrosus Cells (Discfuse)

Sonja Häckel[1,2] Shuimu Chen[2] Laura González-Blanco[2,3] Stefan Zwingenberger[4] Xinggui Tian[4] Christoph E. Albers[1,4], Spine Science Commission of the German Spine Society (DWG), Benjamin Gantenbein[1,2]

[1] *Department of Orthopaedic Surgery & Traumatology, Inselspital, Bern University Hospital, Faculty of Medicine, University of Bern, CH-3010 Bern, Switzerland.*
[2] *Tissue Engineering for Orthopaedics and Mechanobiology, Department for BioMedical Research (DBMR), University of Bern, Switzerland*
[3] *SERGAS (Servizo Galego de Saude) e IDIS (Instituto de Investigación Sanitaria de Santiago), NEIRID Lab, Santiago de Compostela, Spain.*
[3] *Center for Orthopaedic, Trauma Surgery and Rehabilitation Medicine, University Medicine Greifswald, 17475, Greifswald, Germany*
[4] *Spine Unit Sonnenhof Spital Bern, University of Bern, Bern, Switzerland.*

INTRODUCTION: Spinal fusion remains effective for restoring stability, but in older or comorbid patients it is associated with substantial surgical burden. A minimally invasive biological approach that induces ossification within the disc space could reduce the need for disc removal and interbody implants. Because endogenous BMP antagonists limit osteogenesis in intervertebral disc tissue, we investigated whether combining BMP2 with the BMP antagonist neutraliser L51P and the selective EP4 agonist KMN-159 enhances osteogenic differentiation of human annulus fibrosus cells (AFCs)[1–3]v.

METHODS: Primary human AFCs from 11 donors were cultured for 21 days and exposed to BMP2, L51P, KMN-159, or combination treatments. Cytocompatibility was assessed by viability testing. Osteogenic differentiation was quantified by qPCR for ALP, SP7, and COL1 at day 21; expression of the BMP antagonists NOG, GREM1, and CHRD was analysed in parallel. Functional osteogenesis was evaluated by alkaline phosphatase activity at day 14 and Alizarin Red staining for mineral deposition at day 21.

RESULTS: KMN-159 alone was not cytotoxic but induced weaker osteogenic gene expression than BMP2. In contrast, triple stimulation with BMP2 + L51P + KMN-159 significantly increased ALP expression compared with BMP2-based conditions (5,3-fold increase). This molecular response was accompanied by increased ALP activity at day 14 and more pronounced mineralisation at day 21. SP7 and COL1 showed consistent upward trends without reaching statistical significance. KMN-159 had only minor effects on expression of NOG, GREM1, and CHRD [4].

DISCUSSION & CONCLUSIONS: EP4 receptor activation augments BMP2/L51P-driven osteogenesis in human AFCs and promotes a more mineralising phenotype than BMP2 alone. These findings support the concept of targeted osteoinduction within the intervertebral disc as a potential route toward minimally invasive, implant-sparing fusion. Further ex vivo and in vivo studies are warranted to determine whether this synergistic strategy can be translated into controlled disc-space fusion.

REFERENCES:

1. Albers CE, Hofstetter W, Sebald HJ, Sebald W, Siebenrock KA, Klenke FM. L51P - A BMP2 variant with osteoinductive activity via inhibition of Noggin. *Bone*. 2012;51(3):401-406. doi:10.1016/j.bone.2012.06.020

2. May RD, Frauchiger DA, Albers CE, Benneker LM, Kohl S, Gantenbein B. Inhibitory Effects of Human Primary Intervertebral Disc Cells on Human Primary Osteoblasts in a Co-Culture System. *International journal of molecular sciences*. 2018;19(4). doi:10.3390/IJMS19041195

3. Vater C, Mehnert E, Bretschneider H, et al. Dose-Dependent Effects of a Novel Selective EP4 Prostaglandin Receptor Agonist on Treatment of Critical Size Femoral Bone Defects in a Rat Model. *Biomedicines*. 2021;9(11). doi:10.3390/BIOMEDICINES9111712

4. Chen S, Tian X, Zwingenberger S, Albers CE, Gantenbein B, Häckel S. Promoting intervertebral disc fusion using BMP2, L51P, and the EP4 agonist KMN-159: synergistic osteogenesis in human annulus fibrosus cells. *Eur Spine J*. Published online March 3, 2026. doi:10.1007/s00586-026-09841-0

Sirtuin-6 Therapy: A Promising Concept with Limited Efficacy in Intervertebral Disc Degeneration in Beagle Dogs

S. Amir Kamali[1], Chantal Voskamp[1], Anouk Eversdijk[1], Lisanne T. Laagland[1], Michelle Teunissen[1], Saskia Plomp[1], Anna Tellegen[1], Gerhard Sponder[2], Björn P. Meij[1], Kilian Guse[2], Stanislav Plutizki[2], Marianna A. Tryfonidou[1]

[1]Faculty of Veterinary Medicine, Utrecht University, The Netherlands. [2] Pacira Germany GmbH, Hamburg, Germany

INTRODUCTION: Recent studies report that Sirtuin-6 (SIRT6), a NAD+-dependent deacetylase, plays a crucial role in maintaining a healthy intervertebral disc (IVD). It protects nucleus pulposus cells (NPCs) from apoptosis, cellular senescence and inflammation as shown *in vitro* (human NPCs) and *in vivo* (conditional deletion of SIRT6 in mouse NP and rat annulus fibrosus puncture followed by immediate lentiviral SIRT6 treatment). Expanding on this, we investigated the protective effects of SIRT6 in a large animal model of IVD degeneration and complementary *in vitro* studies. **METHODS:** A high-capacity adenoviral vector (HCAd) was used to deliver SIRT6. Moderate IVD degeneration was induced in Beagle dogs by partial nuclectomy. Six weeks post-induction, degenerated IVDs were injected with HCAd-SIRT6 (40 µL, 2.5 × 10^{10} VPs; N = 5). IVDs were longitudinally followed by MRI (T2 mapping). At 6 months follow up disc tissues were subjected to biochemical and histological analyses, and multiplex ELISA of inflammatory mediators and growth factors. To interpret the *in vivo* findings, beagle dog NPCs (N = 3) were transduced with HCAd-SIRT6, after which the NPC pellets were challenged with IL-1β (1 ng/mL) for 7 days. Outcomes were GAG content, (immuno-) histochemistry, and gene expression analysis.

RESULTS: Moderate IVD degeneration was confirmed by decreased T2 relaxation, a 32% reduction in GAG content, and elevated PGE2, CCL2, IFNγ, and NGF levels vs. native discs ($P<0.05$). HCAd-SIRT6 treatment did not improve gross and histopathological degeneration, nor T2 relaxation on MRI or GAG content, at 6 months post-injection (Fig. 1). Furthermore, no differences were observed in inflammatory or growth factors between treated and untreated discs, except for a 2.5-fold increase in CCL2 in HCAd-SIRT6–treated discs ($P=0.006$). *In vitro*, IL-1β induced a degenerative phenotype in NPC pellets, marked by reduced GAG content, impaired matrix deposition, and increased IL-1β immuno-reactivity. This phenotype was not rescued by HCAd-SIRT6 transduction, mirroring the *in vivo* findings.

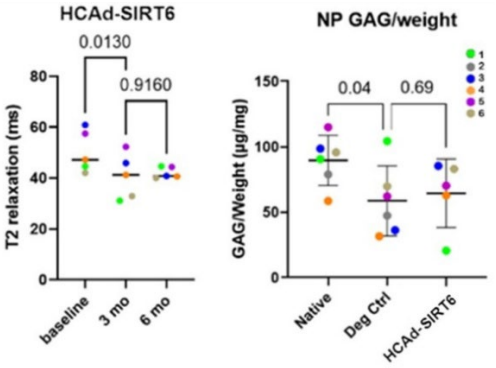

Figure 1. Nucleus pulposus (NP) T2 relaxation over time and GAG content at 6 months following HCAd-SIRT6 treatment.**DISCUSSION & CONCLUSIONS:** Although SIRT6 has been reported to exert anti-catabolic/inflammatory effects in an acute rat disc degeneration model, HCAd-SIRT6 transduction was ineffective in preventing degeneration in dog NPCs under inflammatory conditions or in animal model with established IVD degeneration. This discrepancy may relate to species-specific differences in cell composition with mouse and rat IVDs being rich in notochordal cells, while Beagle IVDs contain non-vacuolated NPCs. Furthermore, we cannot exclude that SIRT6-mediated deacetylation potentially suppresses signaling pathways required for disc repair. Overall, these findings imply that SIRT6 effects are context-dependent.

AKNOWLEDGEMNT: The study was financially supported by Pacira Germany GmbH. We kindly thank Irin Kwananocha for surgical assistance.

Cartilage-on-Chip reveals a translational response to mechanical cues

John Kreutzkamp Joanne[1], van Galen Ivar[1], Lauwers Elsa[2], Surtel Don[1], de Vries Marjolein[1], Cremers Andy[1], Marjolein Caron PhD[1], Paggi Carlo PhD[2,3], Welting Tim PhD[1,4], van den Akker Guus PhD[1]

[1]Department of Orthopedic Surgery, Maastricht University, Maastricht, the Netherlandsand. [2]chiron, chrn on-chip biotechnologies B.V., The Netherlands, [3]BioEngineering, TechMed Center University of Twente, The Netherlands, [4]Department of Orthopedic Surgery, Maastricht University Medical Center+, Maastricht, the Netherlands.

INTRODUCTION: Cartilage-on-chip (CoC) technology represents a promising in vitro system for studying the biomechanical responses of human articular chondrocytes at medium throughput (1). Previous work has demonstrated that prolonged mechanical compression enhances extracellular matrix (ECM) protein production in these cells (2). However, it has also been observed that mechanical compression can suppress overall protein translation for up to eight hours (3). This suggests a disconnect between gene expression, protein synthesis, and ECM production in chondrocyte responses to mechanical stimuli. We therefore hypothesized that mechanical compression regulates protein translation independently of gene expression. To examine this within a physiologically relevant microenvironment, we incorporated human osteoarthritic (OA) synovial fluid into the CoC model and optimized mechanical stimulation conditions for protein translation and ECM production.

METHODS: Human articular chondrocytes (HACs) and synovial fluid (SF) were obtained from surplus cartilage tissue of patients with end-stage osteoarthritis (METC permit 2022-3235). Passage 2 HACs were cultured in DMEM/F12 supplemented with 1% antibiotics and either 10% OA synovial fluid (OASF) or 10% fetal calf serum (FCS). Cells were mixed 1:1 with 4% agarose and loaded into Chiron CoC devices. Mechanical compression was applied for 1 hour at 1 Hz with 10% deformation, either once or multiple times per day with 4-hour rest intervals. Chondrocyte phenotype was assessed using RT-qPCR, global protein translation was measured via a puromycin incorporation (SunSET) assay, and ECM production was evaluated by confocal microscopy and immunoblotting.

RESULTS: Culturing HACs in CoC devices for 7–11 days with OASF, without mechanical stimulation, led to increased expression of COL1A1, SERPINF1, CXCL12, and MMP13 compared to FCS conditions. Cell viability remained above 90% in both groups. To test our hypothesis, HACs were subjected to mechanical compression once, twice, or three times daily, or maintained under static conditions. Puromycin-based immunoblotting showed that a single compression event reduced protein translation, whereas two or three daily compressions enhanced it. Based on these findings, a twice-daily compression regimen was selected for a 5-day stimulation protocol. By day 11, this condition resulted in increased production of collagen types I and II and aggrecan compared to static controls, while collagen VI levels were unchanged. Notably, no corresponding changes were observed in gene expression levels of COL1A1, SERPINF1, CXCL12, MMP13, COL2A1, ACAN, or COL6A1.

DISCUSSION & CONCLUSIONS: Incorporation of OASF into the CoC system successfully recapitulated key aspects of the OA microenvironment, consistent with previous findings in HAC monolayer cultures. Mechanical compression exhibited frequency-dependent effects on global protein translation, with twice-daily stimulation enhancing ECM protein production without altering gene expression at the measured time points. These findings point to a regulatory role of mechanical cues at the level of protein translation. Future studies will focus on elucidating how mechanical stimuli influence ribosomal activity and ECM synthesis. Such insights may inform improved mechanical interventions for preserving articular cartilage in osteoarthritis.

REFERENCES:

1) Paggi CA, et al. oint-on-chip platforms: entering a new era of in vitro models for arthritis. Nat Rev Rheumatol. 2022;18(4):217-31.

2) Paggi CA, et al. Emulating the chondrocyte microenvironment using multi-directional mechanical stimulation in a cartilage-on-chip. Lab on a Chip. 2022;22(9):1815-28.

3) Lomas C, et al. Cyclic mechanical load causes global translational arrest in articular chondrocytes. Eur Cell Mater. 2011;22:178-89.

Biomimetic Composite Hydrogel using Silk Fibres, Hyaluronic Acid, and Collagen type II for Nucleus Pulposus Regeneration

Ashish Kumar[1,2], Parisa Torabi Rahvar[1], Alice Bouduban[1], Michael Wöltje[3], Benjamin Gantenbein[1,4]

[1] *Tissue Engineering for Orthopaedics and Mechanobiology, Bone and Joint Program, Department for BioMedical Research (DBMR) of the Medical Faculty, University of Bern, Bern, Switzerland;* [2] *Graduate School for Cellular and Biomedical Sciences (GCB), University of Bern, Bern, Switzerland,* [3] *Institute of Textile Machinery and High-Performance Material Technology, TUD University of Dresden, Germany,* [4] *Department of Orthopaedic Surgery & Traumatology, Inselspital, Bern University Hospital, Faculty of Medicine, University of Bern, Bern, Switzerland*

INTRODUCTION: Low back pain is a major cause of disability worldwide and is often caused by degeneration of the intervertebral disc (IVD). Current treatments primarily focus on symptom management, failing to offer long-term regenerative solutions. A composite hydrogel comprising silk fibroin, Hyaluronic acid (HA), and Collagen type II (COL-II) has emerged as a promising biomaterial for IVD regeneration due to its excellent biocompatibility and tunable mechanical properties.

METHODS: Human bone marrow-derived mesenchymal stromal cells were expanded to P3 and encapsulated in HA from Bloomage (MW=500kD), COL-II extracted from chicken sternum, and silk fibres-enriched (SF) hydrogels (4×10^6 cells/ml) crosslinked with HRP/H_2O_2. Cell Viability (Live/Dead) using confocal laser scanning microscopy (cLSM) was performed using z-stacks. Metabolic activity, GAG/DNA, gene expression (*ACAN*, *COL1*, *COL-II*, *MMP3*), and collagen and aggrecan immunostaining were assessed. Gene expression was normalised to 18S and GAPDH relative to Day 0.

RESULTS: Live/Dead staining showed high cell viability from Day 1to 14, with HA/COL-II+GDF5 showing the highest viability. Immunofluorescence confirmed ECM deposition, with HA/COL-II/SF-GDF5 and HA/COL-II/SF+GDF5 showing stronger collagen and aggrecan signals. Metabolic activity remained stable across all groups. The HA + GDF5 and HA/COL-II + GDF5 groups demonstrated the highest GAG/DNA ratio by Day 14. Gene expression analysis revealed that the HA/COL-II/SF-GDF5 combination induced high matrix turnover and fibrosis (MMP3/COL1), whereas the HA + GDF5 and HA/COL-II + GDF5 groups promoted chondrogenic stability.

DISCUSSION and CONCLUSION:
The embedded cells maintained viability, metabolic activity, and extracellular matrix production over 14 days. HA + GDF5 and HA/COL-II + GDF5 hydrogels exhibited higher metabolic activity and an increased GAG/DNA ratio, suggesting they are the most promising conditions. Although it was expected that the HA/COL-II/SF + GDF5 hydrogel would promote chondrogenic differentiation, the results indicated that further optimisation is required to achieve consistent chondrogenic outcomes. Moreover, additional replicates are needed to validate these findings statistically.

REFERENCE: P. Torabi Rahvar et al. 2024

Acknowledgment: This work was supported by the SNSF Weave Grant (#320030E_224175) and the DFG (#437213841).

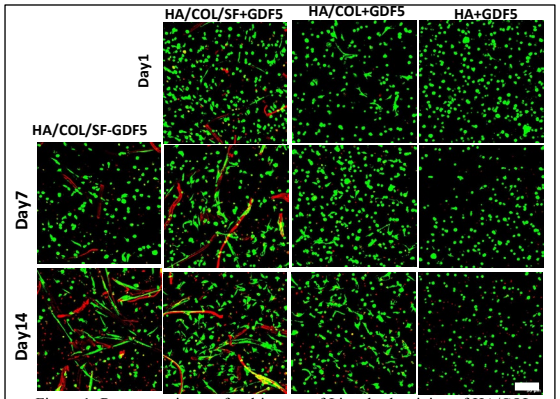

Figure 1: Representative confocal images of Live-dead staining of HA/COL-II/SF-GDF5, HA/COL-IISF+GDF5, HA/COL-II+GDF5, and HA+GDF5 after day 1, 7 and 14. Green colour from Calcein AM represents the live cells, and red colour, Ethidium homodimer, represents the dead cells, Z stacks, (n=1) scale bar=50µm

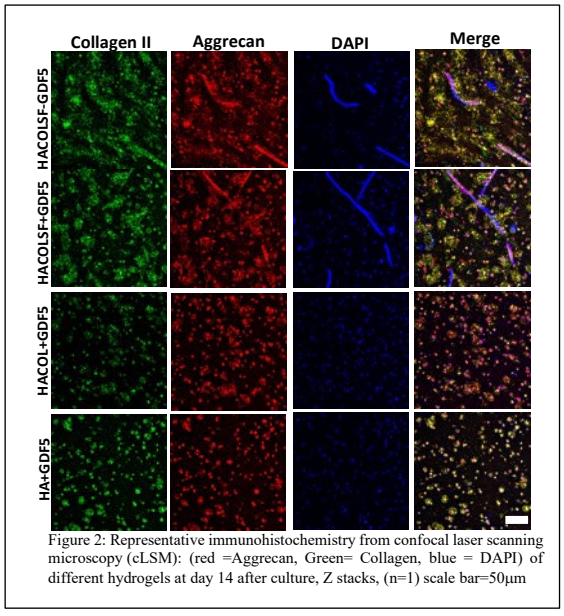

Figure 2: Representative immunohistochemistry from confocal laser scanning microscopy (cLSM): (red =Aggrecan, Green= Collagen, blue = DAPI) of different hydrogels at day 14 after culture, Z stacks, (n=1) scale bar=50µm

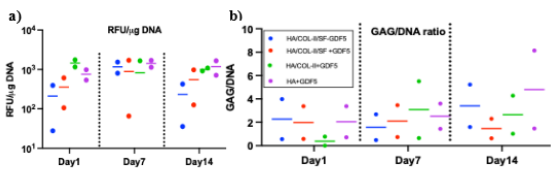

Figure 3: a) Demonstrates the normalized cell metabolic activity over time, measured as relative fluorescence units (RFU/µg DNA) at days 1, 7, and 14, b) This graph shows GAG/DNA ratios over 14 days of culture among the different groups. (n=2)

Advanced Ex Vivo Model Recapitulating the Complexity of Disc Degeneration for pre-clinical Testing of a Next-Generation Gene Therapy

L.T. Laagland[1], S. A. Kamali[1], C. Voskamp[1], E. Salzer[2,3], G. Sponder[4], K. Guse[4], S. Plutizki[4], K. Ito[2], M. A. Tryfonidou[1]

[1]UU. Utrecht, NL, [2]TU/e, Eindhoven, NL, [3]Erasmus MC, Rotterdam, NL, [4]Pacira Germany GmbH, Hamburg, DE

INTRODUCTION: The clinical translatability of regenerative approaches for the degenerate intervertebral disc is challenging. One of the causes is that conventional *in vitro* models, used during preclinical development, fail to adequately recapitulate the complexity of the disc. Building on an established advanced *ex vivo* model allowing for constrained swelling and dynamic loading[1], this study aimed to enhance its pathophysiological relevance by incorporating an inflammatory component. In a fit-for-purpose approach, the therapeutic potency of a high-capacity adenoviral (HCAd) vector encoding for the anti-inflammatory interleukin-1 receptor antagonist (IL-1Ra) was tested.

METHODS: Bovine nucleus pulposus (NP) explants were cultured in confined chambers[1]. GAG loss was induced using chondroitinase ABC (chABC; 0.05U/explant) alone, to reproduce the already established degenerative model, or in combination with 5 ng/mL IL-1β to incorporate an inflammatory component. To evaluate disease-modifying effects, explants were treated with HCAd-IL-1Ra (25 µL; 1.56×10^{10} viral particles; $n = 3$ explants) 3 days after induction using chABC+IL-1β. After 14 days of culture in the bioreactor under diurnal and dynamic loading, explants were harvested for biochemical and histological analyses.

RESULTS: 14 days after culture, the explants induced with chABC alone and in combination with IL-1β showed loss of glycosaminoglycans and brachyury expression compared to native tissue (Fig. 1A+B). Only induction with chABC+IL-1β resulted in IL-1β immune-positivity indicating a pro-inflammatory response (Fig. 1C). Treatment with HCAd-IL-1Ra partly rescued GAG loss, effectively suppressed IL-1β protein expression, and maintained expression of the healthy NP phenotypic marker brachyury after induction using chABC+IL-1β (Fig. 1A-C).

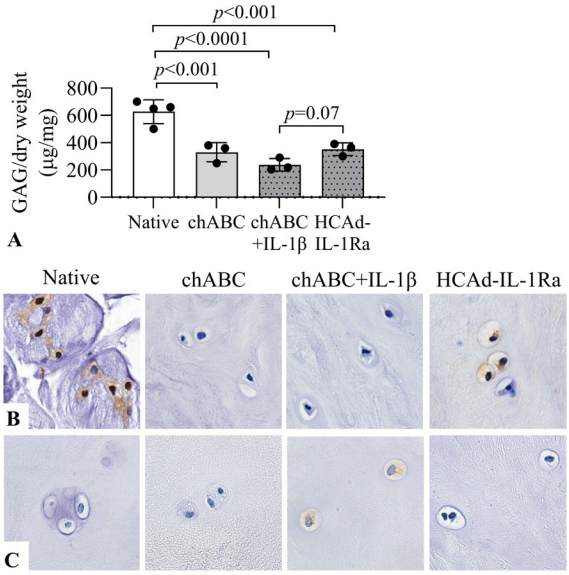

Fig 1. (A) GAG content (One-Way ANOVA + Fisher's LSD), immunostaining for (B) brachyury, and (C) IL-1β of native NP explants and upon 14 days of culture after induction with chABC alone or in combination with IL-1β (dotted bars), untreated or treated with HCAd-IL-1Ra.

DISCUSSION & CONCLUSIONS: Incorporating a pro-inflammatory stimulus enhances the disease-mimicking capacity of the model. HCAd-IL-1Ra treatment partially rescued the degenerative phenotype induced by chABC+IL-1β. Follow up studies including a higher n, increasing the vector dose, and clinically relevant readouts, *e.g.* quantification of multiple inflammatory markers, will further elucidate the translational potential of this model and therapeutic approach.

ACKNOWLEDGEMENTS: Funded by Pacira Germany GmbH and the Osteoarthritis & Reumatoid Arthritis project of the Ombion Centre for Animal-free Biomedical Translation (CPBT) programme in NL financed by the National Growth Fund (no. NGFCPBT241).

REFERENCES: [1]Salzer et al. JOR 40.9 (2022): 2089-2102.

Human Fibroblast-like Synoviocytes Modulate the Inflammatory Response of Human Articular Chondrocytes Across Multiple Patients

Shubo Liu[1,2], Dariel Terrazas[1,2], Stefaan Verbruggen[1,2], Timothy Hopkins[1,2], Martin Knight[1,2]

[1] Centre for Predictive In Vitro Models, Queen Mary University of London, London, UK (www.cpm.qmul.ac.uk), [2] Centre for Bioengineering, School of Engineering and Materials Science, Queen Mary University of London, London, UK

INTRODUCTION: Osteoarthritis (OA) is the most common joint disease in the world, affecting over 240 million people globally. The interaction between cartilage and synovium is thought to play a key role in the onset and progression of OA. While the precise nature of this interaction is yet to be fully elucidated, the crosstalk between these tissues is mediated by their resident cells: fibroblast-like synoviocytes (FLS) and articular chondrocytes (AC). Both the FLS and AC produce, and are activated by inflammatory mediators such as prostaglandin E2 (PGE_2), signifying interacting networks of inflammatory regulation. In the present study, we used a range of in vitro, conditioned media (CM) experiments, to test the hypothesis that factors secreted by FLS regulate the AC inflammatory response.

METHODS: Primary human (h) AC and FLS were isolated from the articular cartilage and synovium of patients undergoing total knee replacement for end-stage OA (n=5). Primary non-OA hAC and hFLS were commercially sourced (n=4). hFLS were cultured in separate monolayer ± interleukin-1β (IL-1β; 10 ng/mL) to generate CM which was collected and applied to hAC ± IL-1β in various configurations, including donor-matched and donor-crossed experiments. PGE_2 release was quantified by ELISA in the CM from hFLS, and in hAC-CM after treatment with hFLS-CM. An inflammatory cytokine profile was generated for the OA hFLS-CM by semi-quantitative array.

RESULTS: Overall, we demonstrated that treatment with hFLS-CM reduced the IL-1β induced PGE_2 release of hAC, in all experimental configurations. This included in donor-matched OA cells (mean reduction: 36%; Fig. 1A), donor-crossed OA cells (mean reduction: 33%; Fig. 1B), donor-crossed non-OA (mean reduction: 58%) and donor-crossed OA/non-OA cells (mean reduction: 28%; Fig. 1C). The cytokine profile of the OA hFLS-CM highlighted commonly expressed cytokines between the five donors: IL-6, MCP-1, GRO, IL-8, RANTES, GRO-a and IL-5 (data not shown).

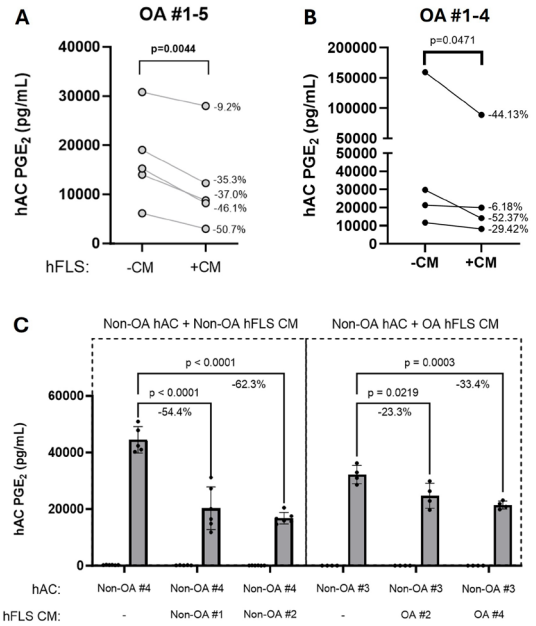

Figure 1. *The % reduction of IL-1β induced hAC PGE_2 release upon the addition of hFLS-CM, in various configurations. (A) Treatment of OA hAC with donor-matched OA hFLS-CM (OA #1-5). (B) Treatment of multiple donor OA hAC (OA #1-4) with OA hFLS CM from a single donor (OA #3). (C) Treatment of non-OA hAC with hFLS-CM from two non-OA (left) and two OA (right) donors.*

DISCUSSION & CONCLUSIONS: The addition of hFLS-CM significantly reduced PGE_2 release in IL-1β-stimulated hACs, regardless of whether the hFLS-CM was from normal or OA donors. This finding suggests that hFLS secrete intrinsic anti-inflammatory molecules. We hypothesize that these may include IL-6, MCP-1, GRO, IL-8, RANTES, GRO-a and IL-5, which were the most highly expressed cytokines in hFLS-CM. Future studies are examining the direct influence of this hFLS cytokine cocktail on hAC PGE_2 release and other markers of inflammation and extracellular matrix degradation.

Sialylation Is a Central Mediator of Osmolarity- and pH-Dependent Ferroptosis and ER Stress in Nucleus Pulposus Cells

Junqiao Lyu[1], Aert Scheper[1], Kieran Joyce[1], Kishor Das[1, 2], Abhay Pandit[1]

[1]CÚRAM Research Ireland Centre for Medical Devices Biomedical Sciences Building, University of Galway, Galway, Ireland, [2]School of Mathematical and Statistical Sciences, University of Galway, Galway, Ireland.

INTRODUCTION: Intervertebral disc degeneration is a major contributor chronic low back pain, characterised by extracellular matrix degradation and altered microenvironment (1). Glycosylation plays a crucial role in extracellular matrix homeostasis in NP cells (2).

METHODS: We applied central composite design (CCD) to optimise NP cell culture conditions, stimulating NP cells with different pH and osmolarity . Glycan profile alterations were assessed using lectin histochemistry,

RESULTS:

Sialylation as the dominant glycosylation pattern. Hyperosmolarity and acid-induced glycosylation changes occurred separately of sialylation upregulation.

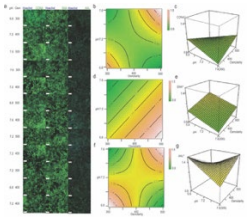

Fig. 1: pH and osmotic conditions influence the presented glycan motifs (mannose, fucose, and sialic acid) in NP cells.

DISCUSSION & CONCLUSIONS: Our results support the hypothesis that alterations in pH and osmolarity contribute to the dysregulation of glycosylation patterns in NP cells. We applied CCD to optimise NP cell culture conditions, establishing sialylation as the most differentially presented glycosylation motif. This work lays the foundation for investigating the glycosylation-mediated regulation of NP cells.

ACKNOWLEDGEMENTS: Research Ireland(13/RC/2073_P2) and China Scholarship Council(202408140011).

REFERENCES:

1. Li F, Shi Y, Chen J, Sun J, Shi J, Sun K, et al. LGR6 modulates intervertebral disc degeneration through regulation of macrophage efferocytosis. Journal of Translational Medicine. 2025;23(1):475.
2. Johnson ZI, Shapiro IM, Risbud MV. Extracellular osmolarity regulates matrix homeostasis in the intervertebral disc and articular cartilage: evolving role of TonEBP. Matrix Biol. 2014;40:10–6.

Single-Cell Resolution Atlas of Glycosylation Heterogeneity in Intervertebral Disc Degeneration

Junqiao Lyu[1], Pablo Rodriguez-Alonso[1], Harry Revill[1] , Abhay Pandit[1]

[1]CÚRAM Research Ireland Centre for Medical Devices Biomedical Sciences Building, University of Galway, Galway, Ireland

INTRODUCTION: In our previous work, we characterized the N-glycoproteomic landscapes of NP and AF tissues and identified aberrant glycosylation as a potential driver of IVDD progression (1). However, the cellular heterogeneity of glycosylation within NP tissues remains largely unexplored. We hypothesize that distinct NP cell subpopulations exhibit unique glycosylation profiles, which differentially regulate extracellular matrix homeostasis and contribute to intervertebral disc (IVD) function.

METHODS: Primary human disc was enriched in $CD24^+$ NP cells using magnetic-activated cell sorting and treated with IL-1β for 3 days to establish an in vitro degenerative model (1). 5 different lectins (SNA, MAL II, GNL, AAL, and CON A) were tagged with DNA oligo barcodes and cells were then incubated with the lectins for multiplexed profiling of the surface glycosylation. Put cells to the 10x Genomics Chromium platform according to the manufacturer's instructions.

RESULTS: A $CD24^+$ NP enriched cell population was successfully obtained from human intervertebral disc (Fig 1).

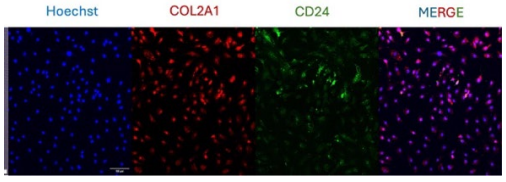

Fig. 1: Immunofluorescence staining of sorted $CD24^+$ NP cells, COL2A1 (red) and CD24 (green) 100 µm, 10X.

DISCUSSION & CONCLUSIONS: Our approach represents a strategy for profiling glycosylation at single-cell resolution in human IVD cells. Mapping the single-cell glycosylation landscape of NP cells, provide new perspectives on the molecular mechanisms driving IVD degeneration.

ACKNOWLEDGEMENTS: Research Ireland (No. 13/RC/2073_P2), European Union (No. 101126640) China Scholarship Council (202408140011).

REFERENCES:

1. Joyce K, Scheper AF, Phyo AM, Flaherty RO, Drake R, Devitt A, et al. Inhibition of Hypersialylation in Human Intervertebral Disc Degeneration Modulates Inflammation and Metabolism. Adv Sci (Weinh). 2025:e06669.

Influence of Fibre Reinforcement on Annulus Fibrosus Mechanics in Finite Element Models

M. Machado[1], R. Gill[1], E. Pegg[2], S. Gheduzzi[1]

[1]University of Bath, Bath, GB, [2] Newcastle University, Newcastle, GB

INTRODUCTION: Characterising the mechanical behaviour of the annulus fibrosus (AF) is challenging due to its complex structure and function. Limitations of in vitro testing have driven the use of numerical approaches, such as Finite Element Analysis (FEA), to predict AF and articular cartilage mechanics [1,2]. Biphasic formulations (e.g. Holmes&Mow, 1990) capture fluid-solid interactions in hydrated soft tissues [3] but require an appropriate description of the solid matrix architecture. This project therefore aims to identify a suitable fibre-reinforcement strategy, accounting for fibre type and orientation, to reproduce the AF mechanical behaviour within a biphasic framework.

METHODS: Biphasic finite element models of the annulus fibrosus (AF) inclusive of superior and inferior cartilaginous endplates (CEPs) were developed in FEBio Studio 3.0. Unconfined compression tests were simulated for three fibre-reinforcement strategies: (1) no fibres, (2) discrete fibres, and (3) a continuous-fibre distribution. A creep protocol was applied using a compressive pressure of 0.14 MPa until steady state, matching in-vitro experimental conditions. A nonlinear permeability response (Eq. 1) from Holmes&Mow (1990) theory and material properties reported for bovine caudal disc tissues, a widely used disc analogue [4], were applied to the material type. Transient analyses quantified lateral deformation, fluid pressure, and solid matrix stress.

$$k(J) = k_0 (J- \varphi_0/1-\varphi_0)^{\alpha} e^{1/2M(J^2-1)} \quad (1)$$

RESULTS: Unconfined compression simulations showed large lateral deformation in the no-fibres and discrete-fibres models, whereas deformation was markedly reduced with the continuous-fibre distribution. Fluid pressure responses also varied across models (Fig. 1A-C). Analyses of the resulting solid matrix stresses was conducted.

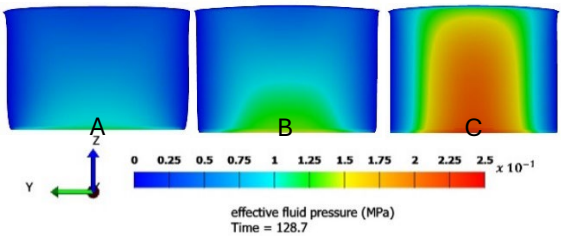

Fig. 1: Interstitial fluid pressure. A) no-fibres, B) discrete-fibres, and C) continuous-fibre distribution.

DISCUSSION & CONCLUSIONS: The time-dependent response was strongly influenced by the solid matrix characterisation within each fibre-reinforced model. Both the no-fibres and discrete-fibres configurations showed pronounced bulging and lower interstitial fluid pressures (≈0.11 and 0.14 MPa, respectively), whereas the continuous-fibre distribution model exhibited reduced bulging and a steeper pressure gradient, reaching ~0.25 MPa, at a comparable time-step. The external pressure is balanced via load sharing between interstitial fluid pressure and solid matrix stress, establishing a higher fluid pressure will have a protective effect on the matrix. Ongoing experiments will further assess creep behaviour and fibrous structure. Accurate representation of fluid-solid interactions and matrix stiffness is therefore critical for predicting AF mechanisms.

ACKNOWLEDGEMENTS: David Parkin Scholarship.

REFERENCES:

[1] DOI: 10.1007/s10439-025-037592
[2] DOI: 10.1016/S0021-9290(97)85606-0
[3] DOI: 10.1007/978-1-4612-3448-7
[4] DOI: 10.3389/fbioe.2021.685799

The actin-binding and -bundling protein plastin-3 (PLS3) and cartilage mechanotransduction

Daniela Maehlich[1], Franziska Busse[2], Nils M. Kronenberg[2], Maxim Vovchenko[3,4], Nele Vaes[3], Hans Van Oosterwyck[3,5], Malte C. Gather[2,6], Anja Niehoff[1,7]

[1]*Institute of Biomechanics and Orthopaedics, German Sport University Cologne, Cologne, Germany,*
[2]*Humboldt Centre for Nano- and Biophotonics, Department of Chemistry and Biochemistry, University of Cologne, Cologne, Germany*
[3]*Biomechanics Section, Department of Mechanical Engineering, KU Leuven, Leuven, Belgium*
[4]*Laboratory for Soft Matter and Biophysics, Department of Physics and Astronomy, KU Leuven, Leuven, Belgium*
[5]*Prometheus Division of Skeletal Tissue Engineering, KU Leuven, Leuven, Belgium*
[6]*Cologne Excellence Cluster on Cellular Stress Responses in Aging-Associated Disease (CECAD), University of Cologne, Cologne, Germany*
[7]*Cologne Center for Musculoskeletal Biomechanics, Medical Faculty, University of Cologne, Cologne, Germany*

INTRODUCTION: Articular cartilage is continuously exposed to mechanical loading. The ability of chondrocytes to sense and respond to these external forces is essential for maintaining cartilage homeostasis. Altered cellular mechanotransduction contributes to cartilage degeneration and the development of osteoarthritis. Force transmission from the extracellular matrix to the cytoskeleton is mediated by focal adhesions and actomyosin networks, whose organization depends on actin-binding and -bundling proteins such as plastin-3 (PLS3) [1]. Here, we investigated whether PLS3 regulates cytoskeletal mechanics and force transmission in chondrocytes which might affect cartilage damage.

METHODS: We studied ubiquitous PLS3 knockout (KO) [2] and PLS3 overexpression (OE) [3] mice in comparison to C57BL/6N wild-type (WT) controls. Atomic force microscopy (AFM) was used to determine Young's modulus of chondrocytes isolated from newborn mice of each genotype. In addition, traction force microscopy (TFM) was performed after 48 h of culture on 5 kPa substrates embedded with fluorescent beads to quantify cell-generated forces. To further access chondrocyte-matrix mechanical interactions, elastic resonator interference stress microscopy (ERISM) [4] was applied at 48 h and 72 h on substrates of different stiffness (5 kPa and 34 kPa) to compare indentation volumes over time. Moreover 5% tensile stress for 30 minutes on three consecutive days (FX-6000 Tension System) was applied to isolated chondrocytes to examine the effect of PLS3 on matrix production in response to mechanical loading.

RESULTS: *Pls3* KO chondrocytes showed a significantly reduced Young's modulus compared to WT cells, while it was elevated in *PLS3* OE ($p < 0.05$). Despite their diminished Young's modulus, *Pls3* KO cells generated higher traction forces with significantly smaller traction foci compared to WT chondrocytes ($p < 0.01$) and exhibited increased normalized indentation volumes on soft substrates at both time points compared to WT and *PLS3* OE chondrocytes. This effect on enhanced deformation of *Pls3* KO cells was reduced on stiff substrates after 48 h, indicating impaired adaptation to matrix stiffness. Consistently, mechanical loading increases collagen II fiber thickness in WT mice while PLS3 imbalance prevented the formation of a robust collagen II matrix independent of mechanical loading especially when PLS3 was missing.

DISCUSSION & CONCLUSIONS: These findings demonstrate that PLS3 might be involved in cartilage mechanotransduction and might be required for focal adhesion reinforcement but not for early adhesion formation. This indicates a specific role of PLS3 in the formation of force-bearing adhesions which are necessary for mechanotransduction to maintain cartilage integrity.

REFERENCES:

[1] Martino et al. (2018). Front Physiol, 9: 824.
[2] Ackermann et al. (2013). Hum Mol Genet, *22*(7), 1328-1347.
[3] Neugebauer et al. (2018). Hum Mol Genet, *27*(24), 4249-4262.
[4] Kronenberg et al. (2017), Nat Cell Biol, *19*(7), 864-872.

Deploying iPSC-derived M2 Macrophages to Mitigate PTOA in 2D, 3D and in vivo Models

Nadia Mahmoudi,[1,2] Lea Zila,[1,2] Julia Sheyn,[1,2] Jacob Wechsler,[1,2] Sarah Mohyeddinipour,[1,2] Dean Roell,[,2] Minoo Bastani,[1,2] Mia Orr,[1,2] Andrew Spitzer,[3], Sean Rajaee[3], Melissa Chavez,[1,2], Namdev More,[1,2], Rachel Lev Gur,[1,2], Wafa Tawackoli,[1,2,3,4,5] Dmitriy Sheyn,[1,2,3,4,5]

[1]Orthopaedic Stem Cell Research Laboratory, [2]Board of Governors Regenerative Medicine Institute, [3]Department of Orthopedics, [4]Department of Surgery, [5]Department of Biomedical Sciences, Cedars-Sinai Medical Center, Los Angeles, CA

INTRODUCTION: PTOA, a degenerative disease caused by traumatic injury, is a major cause of joint pain and disability. An imbalance between pro-inflammatory M1 macrophages and anti-inflammatory M2 macrophages has been proposed as a central disease driver characterized in several local cell types including articular chondrocytes and fibroblast like synoviocytes (FLS). iPSC-derived M2 macrophages (iMac-M2) offer a promising therapeutic approach to slow or even halt the progression of PTOA. To evaluate their treatment efficacy 2D, 3D and in vivo models can be employed and provide complementary insights. We hypothesized that iMac-M2 therapy would decrease inflammatory markers and limit degeneration.

METHODS: To evaluate iMac-M2 treatment efficacy, several models were employed: 2D and 3D co-culture models as well as in vivo rat model to assess translational impact. Human iPSCs were differentiated into iMonocytes and into iMacs over 5 days. The iMacs were then further polarized into iMac-M2s over two additional days. Expression of M1 and M2-associated genes were measured under varying inflammatory media compositions and timepoints to evaluate the phenotypic stability of the iMac-M2s. The anti-inflammatory effects of the cells were subsequently tested using an in vitro 2D model: iMac-M2s were co-cultured separately with chondrocytes and FLS that had been inflamed with IL-1β and LPS for 24 hours. Pro-inflammatory markers in chondrocytes and FLS were assessed after 24 hours using gene expression. Gene expression of catabolic markers was also assessed after 14 days in the FLS cells and 28 days in the chondrocyte culture. To validate the translational efficacy of iMac-M2 treatment, an in-vivo rat model was performed: cells were injected into a DMM injured rat knee 1-week post injury. Disease progression was assessed through gait analysis and weight bearing. Subchondral bone changes were monitored using μCT. For additional validation of iMac-M2 treatment, an additional 3D model will be assessed: Chondrocytes and FLS will be printed onto a petri dish surface using bioink, however, sharing media, mimicking a shared joint environment. The iMAC-M2s will then be co-cultured and gene expression on anabolic and catabolic markers will be performed to assess co-culture effects.

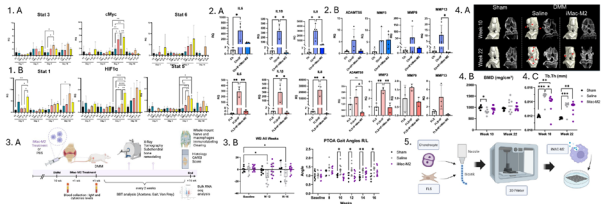

Fig. 1. Phenotypic stability of iMac-M2 macrophages under inflammatory conditions: (**A**) Gene expression of M2-associated genes across the same inflammatory conditions and timepoints. (**B**) Gene expression of M1-associated genes showing a dynamic regulation depending on stimulus and duration. Data are presented as relative

RESULTS: The phenotypic stability of the iMac-M2 cells was assessed to determine if they maintain their anti-inflammatory phenotype under stressful conditions. Gene expression of M2-associated genes (Stat3, cMyc, and Stat6) and M1-associated genes (Stat1, HIF1α, and Stat5) showed a dynamic regulation that was dependent on inflammatory media type and duration (**Fig. 1**). In the 2D model, iMac-M2 treatment in chondrocyte and FLS co-culture (**Fig. 2**) led to a reduction in gene expression levels of pro-inflammatory markers as well as a decrease in catabolic markers. In the rat model, iMac-M2 treated rats exhibited a more normal gait pattern and weight distribution (**Fig. 3**). μCT analysis showed that iMac-M2 treated rats maintain subchondral bone structure over time when compared with the saline-treated group (**Fig. 4**). For the projected 3D co-culture model with chondrocytes, FLS, and iMac-M2s, we hypothesize that treatment will reduce inflammatory and catabolic markers in both cell types (**Fig. 5**).

CONCLUSIONS: We show that iMac-M2s retain plasticity under varying inflammatory conditions and timepoints but preserve an anti-inflammatory phenotype even under some inflammatory stress. In a 2D in vitro culture, iMac-M2 treatment reduced catabolic and pro-inflammatory gene expression in chondrocyte co-culture as well as FLS co-culture, suggesting they have a direct influence on inflammatory signaling and matrix degradation mechanisms. In vivo, treated rats exhibited improved gait and weight distribution, as well as preservation of subchondral bone structure, supporting a disease-modifying trajectory in PTOA. Future work in 3D joint modelling may allow for more cell type integration and can more closely mimic the joint structure and environment. Developing iMac-M2s as a cell therapy offers a minimally invasive option for both symptom alleviation and disease course alteration for PTOA by targeting inflammatory processes that contribute to the disease. Using a complementary 2D, 3D and in vivo model approach allows for more thorough treatment validation across the translational spectrum.

Evaluation of Clinically Relevant Lipid Nanoparticles for mRNA delivery in Osteoarthritic Joint Models

Jordi A.J. Martens[1], Aida Varela Moreira[1], Anouk Eversdijk[1], Raymond Schiffelers[2], Marianna A. Tryfonidou[1], Lizette Utomo[1]

[1]*Regenerative Orthopedics group, Department of Clinical Sciences, Faculty of Veterinary Medicine, Utrecht University,* [2]*CDL Research, University Medical Center Utrecht, Utrecht, The Netherlands.*

INTRODUCTION: Osteoarthritis (OA) is a complex multifactorial joint disease characterized by chronic pain, articular cartilage degeneration, and low-grade, chronic inflammation. Current treatments such as NSAIDs and intra-articular steroid injections provide symptomatic relief but are associated with systemic side effects. Local administration of nucleic acid loaded delivery platforms could enhance therapeutic efficacy, minimizing off target effects. Here, we evaluate the intrinsic transfection capacity of clinically available lipid nanoparticle (LNP) formulations, using enhanced green fluorescent protein (eGFP) mRNA, in *in vitro* models of increasing complexity.

METHODS: Three LNP formulations composed of different ionizable lipids: ALC-0315 (Pfizer/BioNTech), SM-102 (Moderna) and Dlin-MC3-DMA (Alnylam) were compared for their mRNA delivery efficiency. Transfection was assessed *in vitro* in canine articular chondrocytes (ACs) in monolayer culture, 3D in AC pellets, and *ex vivo* in bovine articular cartilage. Synovial fibroblasts (SFs) and synovial tissue explants served as joint-resident controls. To mimic an OA microenvironment, cells, pellets, and explants were pre-stimulated with pro-inflammatory cytokines (i.e., rc IL-1β for ACs and rc IFNγ+TNF for SFs) before exposure to *eGFP*-mRNA-loaded LNPs. Cartilage degeneration and inflammation were evaluated by glycosaminoglycans (GAGs) and nitric oxide (NO) release, respectively. Transfection efficiency was quantified 24 hours post-transfection using flow cytometry (FCM) and GFP immunohistochemistry (IHC).

RESULTS: Pro-inflammatory stimulation induced an OA-like phenotype, evidenced by increased GAG release from AC pellets and AC explants, together with elevated NO production in AC pellets as well as in cartilage and synovium explants compared to non-stimulated controls. FCM showed that SFs and ACs in monolayers were transfected by all LNP formulations, with formulation- and cell type-dependent differences in efficiency (Fig 1). GFP immunopositivity was not detected in AC pellets. In contrast, FCM of digested synovial explants demonstrated measurable transfection (approximately 20%). Analysis of cartilage explants is ongoing.

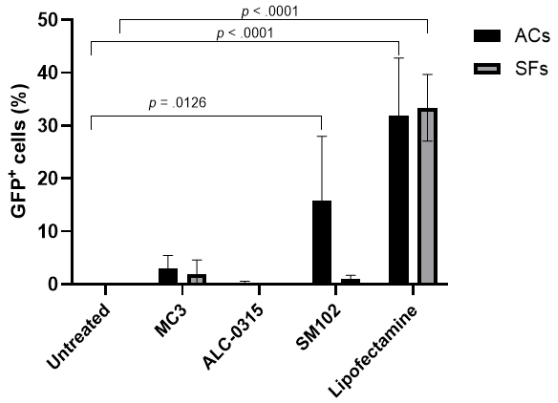

Fig 1: percentages of GFP$^+$ ACs and SFs after mRNA delivery using different LNP formulations, with and without stimulation. Lipofectamine was used as transfection control. A two-way ANOVA with Tukey's post hoc test was used.

DISCUSSION & CONCLUSION: Differences in transfection efficiency between monolayer cultures and OA-like 3D models suggest that the extracellular matrix (ECM) plays a critical role in LNP uptake and mRNA translation in joint tissues. The absence of detectable eGFP signal in AC pellet cultures, despite successful monolayer transfection suggests that the cartilaginous ECM may pose a substantial barrier to LNPs, while the synovial tissue may be more permissive to LNP-mediated mRNA delivery evidenced by measurable transfection in synovial explants. Together with ongoing targeting studies, these findings will help determine which clinically used LNP platforms are suitable for cartilage, synovial membrane or combined targeting approaches.

ACKNOWLEDGEMENTS: Funded by ReumaNederland and Health Holland (grant-id NSP23-01).

Clinically Meaningful Machine Learning: The Role of Feature Selection in Knee Osteoarthritis

Ida Maruotto[1], Federica Kiyomi Ciliberti[1], Halldór Jónsson jr[1], and Paolo Gargiulo[1,2]

[1]*Institute of Biomedical and Neural Engineering, Reykjavik University, Iceland*
[2]*Department of Science, Landspitali University Hospital, Reykjavik, Iceland*

INTRODUCTION: Osteoarthritis (OA) is a leading cause of disability worldwide, characterized by heterogeneous clinical presentation[1]. Advances in machine learning (ML) offer opportunities to improve early diagnosis and personalized management. However, the high dimensionality of healthcare data poses challenges for model performance, interpretability, and clinical adoption. From a clinical perspective, the integration of feature selection[2] into ML pipelines offers several advantages. First, it enhances transparency, allowing clinicians to better understand and trust model outputs; and second, it facilitates the development of scalable tools that can be implemented in routine care settings. This study explores the application of advanced feature selection strategies to optimize ML models in the context of OA, with a focus on extracting clinically meaningful features.

METHODS: The dataset is composed of a total of 102 knees from both healthy (61) and OA patients (41). From MRI, femoral, lateral tibial, medial tibial, and patellar cartilages were manually segmented and then reported on the CT. Radiomics features are image derived features that allow extract pixel-based information, and they were extracted from both CTs and MRIs cartilages. The final sets are: *a)* radiomics features from MRI (radMRI = 581) *b)* radiomics features from CT (radCT = 420) *c)* morphological and densitometric features (MoDe = 16).
A ML pipeline[3] was implemented to select a subset of features that retains high OA classification accuracy. The different feature sets are tested using Random Forest (RF) and Support Vector Machines (SVM) on 5-folds stratified cross validation, that ensures the same healthy/OA balance in both training and validation set in each fold, using F1 score as evaluation metric. Moreover, the parameters of the pipeline are tuned to further refine the feature sets.

RESULTS: The first round of feature reduction results in a reduction to 50% for MoDe (16 to 8 features), 41% for radMRI (581 to 237) and 36% for radCT (420 to 150).
In all cases, the reduction allows an increase of F1 score and reduced standard deviation across folds. The best performance is reached by radMRI with SVM going from 0.85±0.08 to 0.92±0.06. The worst performance is from MoDe using RF from 0.67±0.13 to 0.73±0.08.
However, the further tuning of parameters lead to the huge reduction of features to only 29 with 0.96±0.03 in the case of radMRI with SVM.

DISCUSSION & CONCLUSIONS: In all the considered subsets, the reduction in features led to increases in F1 scores and decreased variability across folds, indicating enhanced generalizability and reduced overfitting. Although MoDe is reduced to the smallest subset, it showed the lowest predictive performance, suggesting the limited complexity may restrict the ability to capture the full variability of OA.
Notably, radMRI demonstrated the greatest performance gains and the biggest reduction, suggesting that these features capture more discriminative information related to OA compared to MoDe or radCT.
SVM achieved higher performance, particularly radMRI, suggesting stronger ability of discrimination healthy/OA compared to RF.
These suggest that MRI-derived radiomics features combined with SVM can provide a reliable assessment of OA, supporting their integration into clinical decision support systems for improved diagnosis.

REFERENCES:

1. Sharma, L. (2021). Osteoarthritis of the knee. *New England Journal of Medicine*, *384*(1), 51-59.
2. Guyon, I., & Elisseeff, A. (2003). An introduction to variable and feature selection. *Journal of machine learning research*, *3*(Mar), 1157-1182.
3. Maruotto, I., Ciliberti, F. K., Gargiulo, P., & Recenti, M. (2025). Feature selection in healthcare datasets: Towards a generalizable solution. *Computers in Biology and Medicine*, *196*, 110812.

Bioactive And Load-Bearing Calcium Phosphates For Developing Biomimetic Spine Fusion Implants

Massel B.F.[1], Truckenmüller R.[1], Habibović P.[1], Tahmasebi Birgani Z.N.[1]

[1] Department of Complex Tissue Regeneration, MERLN Institute of Technology-Inspired Regenerative Medicine, Maastricht University, Universiteitssingel 40, 6229 ER Maastricht, Netherlands, beatricefrancesca.massel@maastrichtuniversity.nl

INTRODUCTION:

Intervertebral disc (IVD) degeneration is a major cause of chronic back pain and a substantial global health burden. When conservative treatment fails, spinal fusion with cage implants remains the standard surgical option. However, commonly used cages made of titanium or polyetheretherketone are bioinert and non-degradable, which can limit osseointegration, osteoinductivity, and long-term compatibility with surrounding bone. These shortcomings may contribute to delayed fusion, implant failure, and degeneration of adjacent vertebral segments.

Calcium phosphate biomaterials, such as hydroxyapatite and tricalcium phosphate, are promising candidates for bone regeneration because of their similarity to native bone and their osteoconductive properties. Yet, their brittleness limits application in load-bearing settings like spinal fusion. This study aims to develop bioactive and mechanically competent calcium phosphate porous scaffolds as biomimetic candidates for spine fusion implants.

METHODS:

Porous calcium phosphate scaffolds were fabricated from mixtures of in-house synthesized β-tricalcium phosphate nanofibers and hydroxyapatite nanowires. The total solid content was varied to adjust scaffold stiffness while preserving some elasticity. Scaffold morphology and phase composition were characterized using electron microscopy and X-ray diffraction. Mechanical performance was assessed by uniaxial and cyclic compression testing. Planned biological evaluation will assess human mesenchymal stem cell compatibility and osteogenic differentiation.

RESULTS:

Preliminary analyses confirmed successful synthesis of hydroxyapatite nanowires and β-tricalcium phosphate nanofibers and their incorporation into fibrous porous scaffolds. Increasing solid content resulted in higher scaffold stiffness. The fibrous microarchitecture appeared to reduce the brittleness typically associated with ceramic biomaterials, suggesting improved mechanical adaptability for spinal fusion applications.

CONCLUSION

These findings indicate that fibrous calcium phosphate scaffolds may provide a promising platform for spinal fusion by combining bioactivity with mechanically relevant behavior. This approach could support future development of bone graft substitutes aimed at improving fusion outcomes and reducing implant-related complications.

A High-Throughput Cartilage-on-Chip Model Reveals Mechanosensitive Chondrogenic Responses in Human MSCs

Laura Mecchi [1,2], Marjolein M. J. Caron[2], Tim J. M. Welting[2,3], Martin J. Stoddart [1]

[1]AO Research Institute Davos, Davos Platz, Switzerland, [2]Laboratory for Experimental Orthopedics, Department of Orthopedic Surgery, Caphri School for Public Health and Primary Care, Maastricht University, Maastricht, the Netherlands, [3]Laboratory for Experimental Orthopedics, Department of Orthopedic Surgery, Maastricht University Medical Center, Maastricht, the Netherlands

INTRODUCTION: Osteoarthritis (OA) is increasingly prevalent in an aging population and lacks effective regenerative treatments[1]. Human mesenchymal stromal cells (hMSCs) represent a promising autologous cell source due to their chondrogenic potential[2]. Cartilage-on-chip (CoC) platforms enable controlled, high-throughput investigation of cartilage biology[3]. Mechanical loading is a key feature of articular joints and should be reflected in in-vitro models[4]. Therefore, this study aimed to assess the feasibility of using hMSCs in a mechanically loaded CoC system.

METHODS: hMSCs from four donors (72.25 ± 1.48 years old, all female) were expanded and seeded (25 million cells/mL) into agarose-based CoC devices. Three conditions were tested over 7 days: static chondro-permissive medium (CP-FS), mechanically loaded chondro-permissive medium (CP-L; uniaxial dynamic compression, 1 h/day), and static chondrogenic medium supplemented with TGF-β1 (CG-FS). Samples were collected 4 h after the final loading session. Cell viability was assessed via live/dead staining. Gene expression analysis included mechanosensitive (*COX2*) and differentiation (*SOX9, RUNX2*) markers. Data was analyzed using linear mixed-effects models with donor as a random effect.

RESULTS: High cell viability (CP-FS: 74.36 ± 7.73%; CP-L: 76.78 ± 2.84%; CG-FS: 76.76 ± 6.83%) was maintained across all conditions (Figure 1). *COX2* expression was ~ 4.7-fold higher in CP-L compared to CP-FS and CG-FS ($p = 0.016$ and 0.032 respectively, Figure 2A). *SOX9/RUNX2* ratio was ~ 5-fold higher in CP-L compared to both controls ($p = 0.025$ vs CP-FS and $p = 0.012$ vs CG-FS, Figure 2B).

DISCUSSION & CONCLUSIONS: To our knowledge, this is one of the first studies demonstrating the feasibility of integrating hMSCs into this mechanically loaded CoC model. Mechanical stimulation induced a chondrogenic transcriptional response without compromising viability, supporting its relevance for cartilage mechanobiology studies. Future studies should focus on extending culture duration and optimizing conditions to enhance chondrogenesis, achieve robust matrix formation and functional tissue development, thereby advancing this platform as a tool to study cartilage mechanobiology and develop regenerative strategies for OA.

ACKNOWLEDGMENTS: Cartilage-on-chip devices were purchased from *chrn on-chip biotechnologies B.V.* This project has received funding from the European Union's Horizon 2020 research and innovation programme under the Marie Skłodowska-Curie grant agreement No. 101034412.

REFERENCES:

1. Kloppenburg, M., *et al.*, *Lancet* (2025) **405** (10472), 71
2. Monaco, G., *et al.*, *Front Bioeng Biotechnol* (2022) **10**, 998774
3. Paggi, C. A., *et al.*, *Lab on a Chip* (2022) **22** (9), 1815
4. Melo-Fonseca, F., *et al.*, *Bio-Design and Manufacturing* (2023) **6** (3), 340

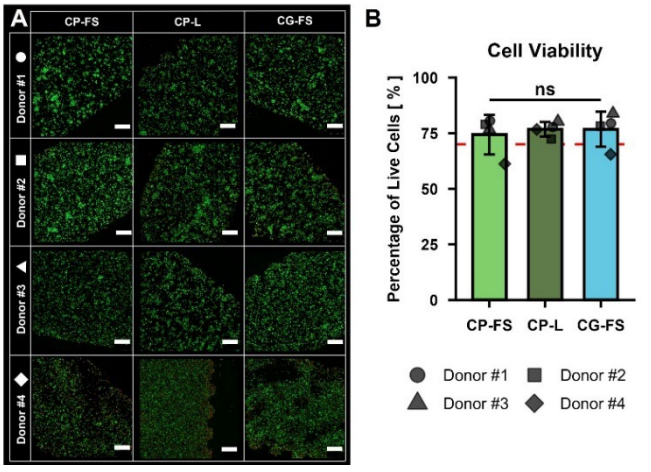

Figure 1: (A) Representative images of live/dead staining, scale bar = 200 µm (B) Live/dead staining quantification.

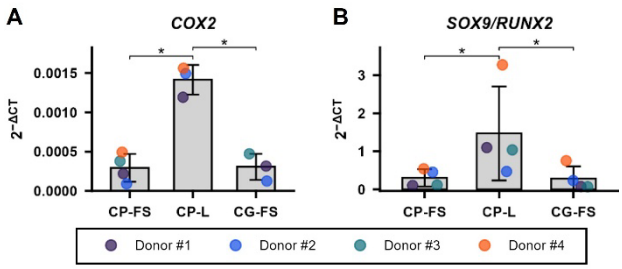

Figure 2: (A) *COX2* and (B) *SOX9/RUNX2* ratio gene expression.

Antibiotic-loaded hyaluronic acid-tyramine hydrogel to prevent bacteria-mediated disc degeneration and Modic type 1 changes of herniated discs

Danilo Menghini[1,2,3,4], Elian Kuhn[3], Marcia Muerner[3], Oliver Distler[4], Mazda Farshad[1], Sibylle Grad[2,3], Matteo D'Este[3], T. Fintan Moriarty[3], Jess G. Snedeker[1,2], Stefan Dudli[4]

[1]Dept. of Orthopedics, Balgrist Univ. Hospital, Univ. of Zürich, Zürich, CH; [2]Inst. for Biomechanics, ETH, Zürich, CH; [3]AO Research Institute Davos, Davos, CH; [4]Center of Exp. Rheum Univ. of Zürich, Zürich, CH

INTRODUCTION: Intradiscal *Cutibacterium acnes* (*C. acnes*) is a risk factor for Modic type 1 changes (MC1) after microdiscectomy.[1,2] Oral antibiotics (amoxicillin-clavulanate) have shown significant clinical benefits in MC1 patients.[3] Microdiscectomy may enable local antibiotic application to prevent bacteria-induced degeneration and MC1. We propose an antibiotic-loaded hyaluronic acid-tyramine (HA-Tyr) hydrogel combined with annulus fibrosus repair using a mechanically interlocking patch (iPatch), previously shown to restore biomechanics and reduce re-herniation.[4] This study investigates (i) antibiotic choice and loading in relation to antibacterial efficacy, cytocompatibility, and hydrogel viscoelasticity, and (ii) for the lead candidate, cytocompatibility in 3D culture and release profile.

METHODS: HA-Tyr was loaded with amoxicillin-clavulanate, clindamycin, or doxycycline (0.1, 1.0, 10.0 mg/ml). Rheology was assessed by amplitude sweep tests (n=3/group). Antibacterial activity against *Staphylococcus aureus* (*S. aureus*) ATCC25923, *Escherichia coli* (*E. coli*) MG1655, and *C. acnes* (patient isolate) was evaluated using disk diffusion assay (n=5/group). Released antibiotics from HA-Tyr were applied to human disc cells in monolayer (n=3) to assess cytotoxicity (lactate dehydrogenase) and metabolic activity (resazurin). The cytocompatibility of the selected drug was further evaluated using human disc cells cultured in alginate beads. Release kinetics were quantified at different doses by high-performance liquid chromatography (n=3/group).

RESULTS: Storage modulus was maintained across all antibiotic concentrations with clindamycin, but not for the other antibiotics. Clindamycin had the largest zones of inhibition against *S. aureus* and *C. acnes*, while doxycycline was the least effective. Amoxicillin-clavulanate and doxycycline outperformed clindamycin against *E. coli*. Amoxicillin-clavulanate and clindamycin displayed acceptable cytocompatibility (>75% activity and <25% cytotoxicity vs. control) up to 1 mg/ml. Clindamycin was selected as the lead candidate (*Table 1*) and confirmed cytocompatibility in 3D up to 10 mg/ml. Clindamycin release followed a rapid profile, plateauing at 62.2% after 6.6 hours.

		Amoxicillin/ Clavulanate			Clindamycin			Doxycycline		
[mg/ml]		0.1	1	10	0.1	1	10	0.1	1	10
Viscoelasticity Retention		✓	✓	✗	✓	✓	✓	✓	✗	✗
Antibiotic Cytotoxicity		✓	✓	✓	✓	✓	✗	✗	✗	✗
Antibacterial Growth Activity (z-score)	*C.acnes*	-0.70	0.14	0.62	-0.33	0.73	1.51	-1.94	-0.47	0.44
	S.aureus	-0.32	0.11	1.25	-0.29	0.44	1.47	-1.80	-0.78	-0.07
	E.coli	-0.85	0.62	1.35	-1.39	-1.06	0.11	-0.48	0.47	1.23

Table 1: Interpretation table showing that amoxicillin-clavulanate at 1 mg/ml is the best candidate against *E. coli*, and clindamycin against *S. aureus* and *C. acnes*. Values are presented as z-scores, indicating the standardized deviation from each line mean, with higher values corresponding to stronger effects relative to the average.

DISCUSSION & CONCLUSIONS: Clindamycin preserved HA-Tyr structural integrity, showed strongest activity against a known disc pathogen (*C. acnes*), and showed to be cytocompatible. Its prolonged release supports the suitability of clindamycin-loaded HA-Tyr as a local delivery system. Treating microdiscectomy patients with clindamycin-loaded HA-Tyr and iPatch, holds potential of preventing bacteria-caused disc degeneration and MC1, while preventing re-herniation and improving disc biomechanics.

REFERENCES:

1. Albert HB et al. (2013) *Eur Spine J*, 22(4):690-696.
2. Capoor MN et al. (2021) *Int J Mol Sci*, 22(5):1-16.
3. Bråten LCH et al. (2019) *BMJ*, 367:15654.
4. Menghini D et al. (2025) *Eur Spine J*, 34(6):2301-2310

HTRA1-driven disc matrix fragmentation propagates Modic-like pathology across the disc-endplate-marrow axis

T. Menigs[1,2], J. Devan[1,2], A. Nüesch[1,2], P. Hatt[1,2], I. Heggli[1,2,3], B. Roschitzki[4], A. Laimbacher[1,2], N. Herger[1,2], M. Farshad[5], F. Brunner[2], O. Distler[1,2], S. Dudli[1,2]

[1]Center of Experimental Rheumatology, Department of Rheumatology, University Hospital Zurich, University of Zurich, CH. [2]Department of Physical Medicine and Rheumatology, Balgrist University Hospital, Balgrist Campus, University of Zurich, CH. [3]Department of Orthopedics, Icahn School of Medicine at Mount Sinai, New York, USA. [4]Functional Genomics Center Zurich University and ETH Zurich, CH. [5] Department of Orthopedics, Balgrist University Hospital, University of Zurich, CH.

INTRODUCTION: Modic changes (MC) are painful vertebral bone marrow lesions adjacent to degenerated discs. Although MC are increasingly viewed as a disorder of the disc–endplate–marrow unit, the molecular signals that cross a compromised endplate and initiate marrow remodelling remain insufficiently defined. We therefore profiled disc proteolysis in MC and tested whether disc-derived proteins and proteolytic products are sufficient to trigger endplate failure and marrow inflammation.

METHODS: We determined the proteome and degradome of surgical disc tissue (MC1, MC2, degeneration-matched nonMC, n =21-33) using N-TAILS mass spectrometry. To link degradome features to activity of a candidate protease emerging from the proteome, we generated an ex vivo reference degradome by digesting a minimally degenerated human disc with recombinant HTRA1 and compared reference degradome to the MC degradome. To test sufficiency in vivo, HTRA1 or its in vitro-generated disc matrix digestion products were injected into rat caudal discs (sham: PBS-injection). Lesion development and endplate failure was assessed by serial MRI and endpoint histology (n=8/group). To connect disc degradome to MC pathology, we quantified COMP, a main MC disc degradome component, in human MC1 marrow, and tested COMP-induced NF-κB activation in myeloid cells.

RESULTS: Proteomics revealed increased HTRA1 in MC1 discs (Fig.1a) and degradomic identified an MC1 proteolysis-high state with increased ECM-derived neo-N-termini, dominated by fragments from FN1, COL1A1, COMP, CILP1 (Fig.1b). Ex vivo HTRA1 digestion reproduced the MC1 degradome (Fig.1c). In rats, intradiscal recombinant HTRA1 or HTRA1-generated matrix digestion products induced MC-like marrow changes on MRI and histology (Fig.1d,e) and caused endplate failure (Fig.1f). COMP was increased in human MC-adjacent marrow (Fig.1g) and activated NF-κB signaling in human myeloid cells (Fig.1h), supporting COMP as a downstream marrow-facing effector cue.

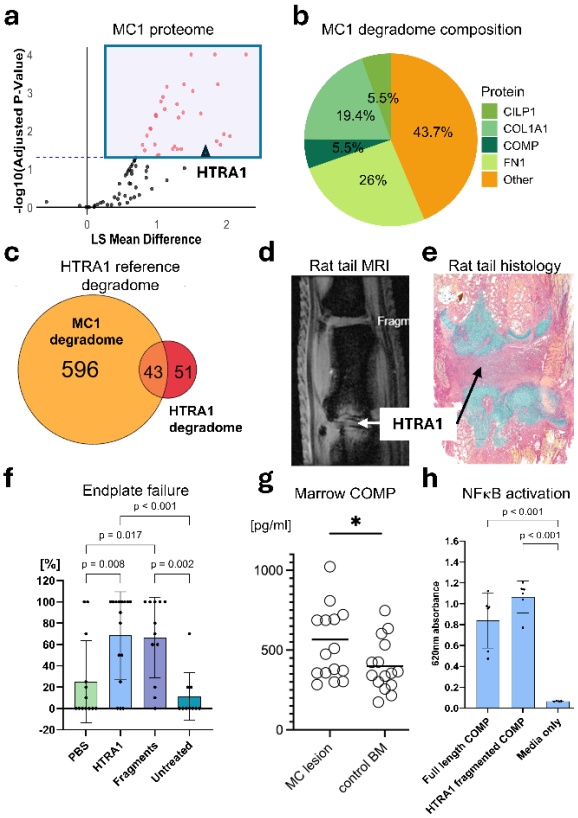

Fig.1. *HTRA1-linked disc degradome and COMP effector signaling connect MC1disc proteolysis to endplate failure and MC-like marrow pathology.*

DISCUSSION & CONCLUSIONS: These findings position HTRA1-linked disc matrix fragmentation as a mechanism coupling disc proteolysis to endplate barrier failure and downstream marrow inflammatory signaling in MC1. It highlights the HTRA1–fragment axis as a tractable therapeutic entry point in MC1.

Human-relevant chondroprogenitor-based models of cartilage injury to study regulated cell death after surgical debridement

Diana Mock. [1] Monica De Luise. [1] Andrea Barbero. [1].

[1] *Department of Biomedicine, University Hospital Basel, University of Basel, Basel, Switzerland.*

INTRODUCTION: Current treatment for cartilage defects, including the implantation of engineered grafts, often fail to achieve durable repair. Surgical debridement with tools like curettes, while necessary to prepare the wound bed, causes collateral damage to surrounding chondrocytes. This injury can compromise graft integration and matrix integrity, undermining long-term therapeutic success. Understanding how debridement procedures trigger cell death pathways, particularly those linked to osteoarthritis, is therefore crucial. Given the limitations of bovine cartilage models and the scarcity of healthy articular cartilage, developing human-relevant models for studying mechanical injury is essential. This study aims to establish a human chondroprogenitor-based platform, using spheroids and engineered cartilage disc (ECD), to model curette-induced injury. We characterize neo-hyaline cartilage formation, and provide a robust system for downstream analysis of regulated cell death and potential therapeutic interventions.

METHODS: Human chondroprogenitors (ChP) were isolated from osteoarthritic specimens of patients undergoing total knee replacement using the established fibronectin adhesion assay. ChP were differentiated in a defined serum-free chondrogenic medium either as spheroids (0.05 x 10^6 cells / spheroid, 21 days) or as engineered cartilage discs (ECDs) in transwell inserts (2 x 10^6 cells / ECD, 42 days). To simulate clinical lesion preparation, ECDs were subjected to curette debridement. Spheroids were treated with compounds to activate specific regulated cell death pathways (Ras-selective lethal 3, RSL3 for ferroptosis and staurosporine for apoptosis), followed by inhibition with pathway-specific inhibitors (ferrostatin-1, Fer-1 and z-VAD(OH)-FMK, z-VAD). Generated tissues were assessed histologically and by immunofluorescence.

RESULTS: Both models reproducibly generated mature human neo-hyaline cartilage with abundant extracellular matrix positive for Safranin-O (Fig. 1A) and collagen II. Mature ECDs measuring 7 mm in diameter were successfully injured with curette debridement. TUNEL staining at day 7 post-injury revealed positive cells near the injury edge, confirming injury-induced cell death (Fig. 1B). The spheroid model enabled pathway-specific validation. Ferroptosis and apoptosis were successfully induced by RSL3 and staurosporine, respectively, and inhibited by ferrostatin-1 and z-VAD, as shown by cleaved caspase 3 (cCas3) and the 4-Hydroxynonenal (4-HNE) immunofluorescence staining (Fig. 1C, D).

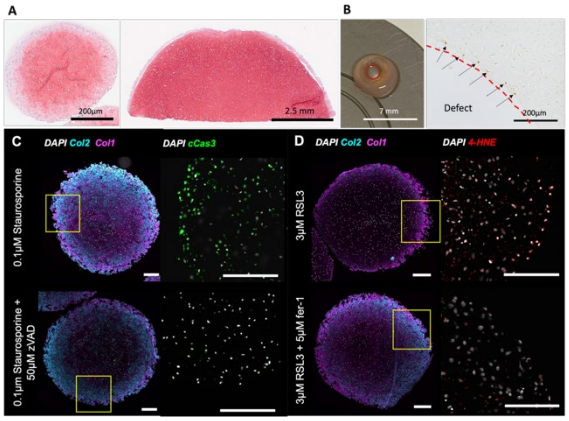

Fig. 1 (**A**) Safranin-O/Fast Green staining of spheroid (left) and ECD (right). (**B**) Macroscopic image (left) and TUNEL staining 7 days post-injury (right) of curette-injured ECD. (**C**) Spheroids treated with 0.1µM staurosporine, 0.1µM staurosporine + 50µM zVAD stained with collagen 1 (Col1, cyan), collagen 2 (Col2, magenta), cCas3 (green) and DAPI (white). (**D**) Spheroids treated with 3µM RSL3, 3µM RSL3 + 5µM fer-1 stained with collagen 1 (Col1, cyan), collagen 2 (Col2, magenta), 4-HNE (red) and DAPI (white). Scalebars in (**C**) and (**D**) represent 200µm.

DISCUSSION & CONCLUSIONS: We established two complementary human ChP models, a 21-day spheroid system and a 42-day ECD, which reproducibly generate mature neo-hyaline cartilage. Together, these platforms provide a robust foundation for investigating how curette debridement affect chondrocyte viability, matrix integrity and repair responses, as well as for evaluating potential chondro-protective interventions.

REFERENCES:

https://doi.org/10.1530/EOR-2024-0083
https://doi.org/10.1016/j.joca.2002.12.001
https://doi.org/10.1038/s41598-023-49089-y

CRISPR-Engineered MSC-Derived Extracellular Vesicles: From TSG-6 Overexpression to Subpopulation Characterization

Lucia Morales[1], Iker Martinez-Zalbidea[1], Liam Brown[1], Varun Puvanesarajah[2], Karin Wuertz-Kozak[1]

[1] *Department of Biomedical Engineering, Rochester Institute of Technology (RIT), Rochester, NY USA.*
[2] *Department of Orthopedics and Rehabilitation, University of Rochester Medical Center, Rochester, NY USA.*

INTRODUCTION: Mesenchymal stem cell-derived extracellular vesicles (MSC-EVs) hold considerable promise as acellular immunomodulatory therapeutics, but their inherent heterogeneity remains a key obstacle to rational engineering and clinical translation[1]. We have developed CRISPR-based strategies to enhance and characterize MSC-EV potency, with a focus on degenerative disc disease.

METHODS: An immortalized human MSC line (ASC52telo) was transduced with a CRISPR-dCas9 lentiviral activation system targeting TSG-6. EVs were isolated by differential ultracentrifugation and characterized by nanoparticle tracking analysis, electron microscopy, and Western blot. Immuno-modulatory activity was assessed in human IVD cells and THP-1-derived M1 macrophages using qPCR and ELISA. To examine size-based subpopulation differences, ultracentrifugation protocols were adapted to achieve separation of small and large EV fractions.

RESULTS: CRISPR-dCas9 activation of TSG-6 in MSCs led to significant alterations in EV cargo composition, including a distinct microRNA and protein profile, and attenuated inflammatory responses in both human IVD cells and macrophages *in vitro*. Separation of small and large EV fractions revealed that small EVs are released in substantially greater numbers. When applied to M1 macrophages at equivalent particle-to-cell concentrations, both subpopulations demonstrated immune-modulatory activity, suggesting that a mixed population may represent a pragmatic and effective therapeutic approach. In future steps, miRNA and/or protein profiling will be used to investigate cargo differences between subpopulations that may underlie or further distinguish their respective bioactivities.

DISCUSSION & CONCLUSIONS: To enable more precise subpopulation characterization going forward, we are expanding our CRISPR toolkit to include endogenous knock-in fluorescent tagging of tetraspanins (CD63, CD9) in MSCs, allowing FACS-based isolation of phenotypically defined EV subpopulations without antibody-related artifacts, with systematic testing of subpopulation-specific bioactivity and cargo profiles planned. Together, these findings advance a CRISPR-driven framework for engineering and characterizing MSC-EVs as next-generation immune-modulatory therapeutics for inflammatory musculoskeletal conditions, including degenerative disc disease.

REFERENCES:

[1] Maumus et al., Front Bioeng Biotechnol, 2020 (doi: 10.3389/fbioe.2020.00997)

The Protective Effect of Microgel Cell Delivery for Intervertebral Disc Regeneration Therapy

Namdev More,[1,2], Tiffany Lee[1,2], Anoushka Prasad[1,2], Sarah Mohyeddinipour[1,2], Julia Sheyn[1,2], Giselle Kaneda[1,2], Melissa Chavez, [1,2] Dean Roell, [1,2] Lea Zila[1,2], Danial Khorsandi[4], Matthew Grol,[5], Mehmet Dokmeci,[4] Dror Seliktar, PhD[3], Wafa Tawackoli, [1,2,6,7,8,9], Dmitriy Sheyn,[1,2,6,7,9]

[1]Orthopaedic Stem Cell Research Laboratory, [2]BOG Regenerative Medicine Institute, Cedars-Sinai Medical Center (CSMC), Los Angeles, CA, [3]Technion, Israel[4]Terasaki Institute, Los Angeles, CA, Physiology and Pharmacology, Western University Ontorio.[6]Department of Orthopedics, [7]Department of Surgery, [8]Department of Biomedical Sciences, [9]Biomedical Imaging Research Institute, CSMC, Los Angeles, CA.

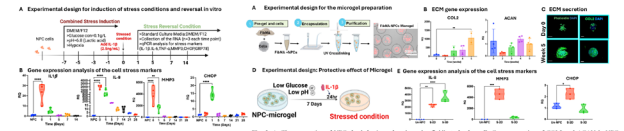

Fig. 1. A. Experimental design: NPCs were cultured in stressing conditions followed by recovery in standard culture conditions. B. Analysis of stress markers under both stress and recovery conditions demonstrates stress induction and recovery of the NPC in normal culture.

Fig. 2. A. The preparation of NPCs-loaded microgels using microfluidic technology. B. Gene expression of COL2 and ACAN in NPCs encapsulated in microgels over time. C. Immunofluorescence images show the distribution of NPCs within the microgel and the secretion of ECM after 5 weeks of culture. D. Experimental design for examining the protective effect of microgels on NPCs in stressful culture conditions. E. Stress markers indicates that microgels protect NPCs from environmental stressors.

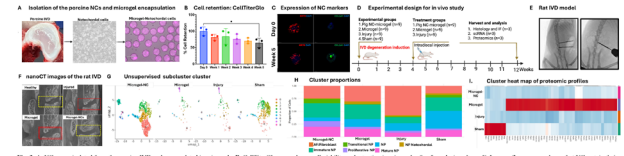

Fig. 3. A. NCs were isolated from the porcine IVD and encapsulated in microgels. B. CellTiterGlo assay shows cell viability and retention in microgels after 5 weeks in culture. C. Immunofluorescence shows that NCs retain their phenotype up to week 5. D. Experimental design for the efficacy study of the Microgel-NC injected in degenerated rat IVD model. E. X-ray images show induction IVD injury F. High-resolution nanoCT images show structural retention following microgel-NC cell injection, similar to that of a healthy disc G. SubCluster analysis shows expression of IVD markers, with increased regenerative NP markers and reduced fibrotic tissue formation compared to the saline-treated group. H. Stacked bar plots showing the relative abundance of NP and AF cell subtypes across the four groups: Microgel-NC, Microgel, Saline, and Sham. I. Heatmap showing differential gene expression across groups. Clustering reveals distinct expression patterns, with Microgel-NC displaying upregulation of regenerative and protective markers compared to Saline, while Sham shows enrichment of baseline homeostatic markers.

INTRODUCTION: One of the main causes of low back pain (LBP) is intervertebral disc (IVD) degeneration. Despite advancements in IVD degeneration treatments, the prognosis remains poor. In IVD tissue, the microenvironment is compromised, characterized by acidic pH, low glucose, and elevated levels of inflammatory mediators. Direct intradiscal delivery of the cells exposes them to a stressed microenvironment and leakage, resulting in poor survival and limited regeneration. To overcome these challenges, we developed an injectable microgel system that protects them from stress conditions. In the cell-based approach, notochordal cells (NCs) are considered progenitors for NPC and are essential for maintaining disc homeostasis. Their early loss in humans is closely linked to the onset of degeneration, making them an attractive target for regenerative strategies. Encapsulation of NCs or NPCs within our microgel system provides both protection from the compromised environment and an effective delivery system, highlighting its potential as a promising platform for IVD regeneration.

METHODS: NPCs were isolated from human surgical samples. To simulate a degenerative IVD environment, cells were cultured under stressor conditions **(Fig. 1A).** Stress induction was assessed using qPCR. Subsequently, stressed cells were transferred to standard culture media, and recovery was analyzed. NPCs were encapsulated within FibMA microgels prepared using microfluidic technology **(Fig. 2A)**. ECM marker expression was analyzed by qPCR, and cell distribution and ECM secretion were examined by IF. The protective effect of the microgel was assessed by culturing Microgel-NPCs under simulated degenerative conditions and analyzing stress marker gene expression. Since NCs are progenitors for NPCs, we isolated NCs from healthy porcine IVDs and encapsulated in FibMA microgels **(Fig. 3A).** NC phenotype was validated by IF. The efficacy of the developed Microgel-NC system was evaluated in vivo using a rat IVD degeneration model. IVD regeneration was assessed by nanoCT, single-cell transcriptomics, tissue proteomics, and histology.

RESULTS: NPCs cultured under simulated degenerative conditions (low glucose, hypoxia and low pH, **Fig. 1A**) exhibited cell stress, as evidenced by increased expression of IL-1β, IL8, MMP3, and CHOP. However, when the stressed cells were transferred to standard culture conditions, stress reversal was observed **(Fig. 1B)**. NPCs were successfully encapsulated in microgels **(Fig. 2A)**, showing >75% retention after 5 weeks (data not shown). Encapsulated cells expressed COL2 and ACAN **(Fig. 2B)** and secreted ECM **(Fig. 2C)**. Under simulated degenerative conditions, Microgel-NPCs exhibited reduced stress marker expression compared to 2D culture **(Fig. 2E)**. Like human NPCs, porcine NCs encapsulated in FibMA microgels **(Fig. 3A)** exhibited >65% retention after 5 weeks **(Fig. 3B)** and confocal imaging confirmed retention of the NC phenotype **(Fig. 3C)**. To evaluate the therapeutic efficacy in vivo, an IVD degeneration was induced at L3-L4 and L4-L5 levels in a rat model **(Fig. 3E)**. NanoCT analysis showed that Microgel-NC treatment restored IVD structure similar to healthy controls **(Fig. 3F)**. Single-cell RNA sequencing revealed that the Microgel-NC approach promoted non-fibrotic regeneration with proliferative NP populations, whereas the saline-only and microgels only groups exhibited fibrotic tissue formation **(Fig. 3G-H)**. Same confirmed with proteomics analysis shows Microgel-NC shows more ECM remodeling (increased expression of ECM protein COL23A1 and structural protein PKP2, CUZD1**, Fig. 3I)**.

CONCLUSION: NPCs exposed to degeneration undergo stress but recover their native phenotype when returned to standard culture, indicating their capacity to regain function after disc regeneration. The FibMA microgel, along with NPC or NC fabricated successfully, allowing for high-quality cell encapsulation without compromising cell viability. The microgel system promotes ECM secretion and shields NPCs from low pH, low glucose, and IL-1β. In the rat IVD model, microgel-loaded NCs promoted superior disc regeneration compared to the injury and bare microgel groups. The regenerative effect may be attributed to NCs enhancing NP cell populations and reducing fibrotic tissue formation, while simultaneously activating strong metabolic activation for tissue remodeling**.** The cell-loaded microgels provide effective cell delivery with a protective effect for encapsulated cells. This approach offers strong clinical potential for cell therapy to regenerate the IVD and treat discogenic LBP.

The Role and Mechanism of Matrix Sulfation in Regulating Chondrocyte Cell Cycle Abnormalities in Osteoarthritis

Bowei Ni[1], Chao Zheng[1], Liu Yang[1]

[1]*Institute of Orthopedic Surgery, Xijing Hospital, Fourth Military Medical University, Xi'an, China.*

INTRODUCTION: The cartilage matrix is a critical determinant of chondrocyte phenotype and fate [1]. During osteoarthritis (OA), quiescent chondrocytes re-enter the cell cycle [2], forming pathological cell clusters [3]. However, the mechanisms underlying chondrocyte cell cycle entry in OA remain elusive.

METHODS: We performed multi-species histological analyses of cell cycle, sulfation modifications, and apoptotic markers in OA cartilage from mice, Bama miniature pigs, and humans. Single-cell data from OA cartilage were analyzed to evaluate the transcriptional activity of sulfation and cell cycle genes. Using mRNA sequencing, we investigated the specific biological processes affected by impaired sulfation and identified key pathogenic mechanisms. We established an OA large animal model and administered a PROTAC molecule targeting the key pathogenic factor to assess therapeutic efficacy.

RESULTS: Here we show that sulfation, a chemical modification essential for the functional activity of matrix molecules, is significantly diminished in the pericellular regions of pathological chondrocyte clusters in OA cartilage from both humans and Bama miniature pigs. Consistently, single-cell data from OA patients reveal that proliferative chondrocytes exhibit high cell cycle gene activity but low sulfation-related gene expression. To functionally validate this observation, we generated a mouse model with impairment of cartilage matrix sulfation (*Col2α1-Cre; Slc35b2*$^{fl/fl}$). These conditional knockout mice developed spontaneous OA, characterized by active chondrocyte cell cycle progression at 3 months of age and significantly upregulated chondrocyte apoptosis at 6 and 9 months. Mechanistically, we found that reduced sulfation led to decreased focal adhesion, which promoted the nuclear translocation of FAK. Nuclear FAK mediated the suppression of E2F7, a negative regulator of the cell cycle, at both transcriptional and post-translational levels via MDM2 and FZR1, respectively. Targeted degradation of MDM2 using a PROTAC molecule Oridonin-Oridonin significantly restored E2F7 expression, inhibited the formation of pathological cell clusters, and normalized chondrocyte cell cycle regulation and COL2A1 secretion in the Bama miniature pig ACLT model, thereby alleviating cartilage degeneration.

DISCUSSION & CONCLUSIONS: Collectively, our findings demonstrate that decreased matrix sulfation downregulates the expression of E2F7, a negative regulator of the cell cycle, thereby inducing aberrant chondrocyte cell cycle entry. Our findings provide new insights into the pathogenesis of OA and lay the groundwork for the clinical translation of PROTAC technology.

REFERENCES:

[1] Pueyo Moliner A, Ito K, Zaucke F, et al. Restoring articular cartilage: insights from structure, composition and development. Nat Rev Rheumatol. 2025;21(5):291-308. https://doi.org/10.1038/s41584-025-01236-7

[2] Fan, Yue et al. Fan Y, Bian X, Meng X, et al. Unveiling inflammatory and prehypertrophic cell populations as key contributors to knee cartilage degeneration in osteoarthritis using multi-omics data integration. Ann Rheum Dis. 2024;83(7):926-944. https://doi.org/10.1136/ard-2023-224420

[3] Danalache M, Kleinert R, Schneider J, et al. Changes in stiffness and biochemical composition of the pericellular matrix as a function of spatial chondrocyte organisation in osteoarthritic cartilage. Osteoarthritis Cartilage. 2019;27(5):823-832. https://doi.org/10.1016/j.joca.2019.01.008

Bacteria-induced Epigenetic Modification in Intervertebral Disc Cells

A. Nüesch[1,2], E. Ezen[1,2], T. Mengis[1,2], P. Bitterli[1,2], O. Distler[1,2], C. Seiler[1,2], S. Dudli[1,2]
[1]Center of Experimental Rheumatology, Department of Rheumatology, University Hospital, University of Zurich, Switzerland, [2]Department of Physical Medicine and Rheumatology, Balgrist University Hospital, University of Zurich, Switzerland

INTRODUCTION: Innate immune memory, the capacity of innate immune cells to undergo epigenetic reprogramming following initial stimuli, has emerged as a key mechanism in chronic inflammatory diseases[1]. Emerging evidence suggests that non-immune cells may also acquire such memory. The intervertebral disc (IVD), despite being considered immune-privileged, expresses pattern recognition receptors and responds to microbial signals. Whether bacterial presence in the IVD is associated with epigenetic changes in disc cells remains unexplored.

METHODS: Matched IVD samples with 16S rRNA gene sequencing[2] and RRBS methylation data were analyzed (n=17). Microbiome data were aggregated to genus level, filtered for prevalence, and transformed using centered log-ratio (CLR), with parallel presence/absence tracking. Methylation regions were filtered for coverage and variance. Exploratory analyses included PERMANOVA and Covariate-adjusted Spearman rank correlations were computed between CLR-transformed genus abundances and methylation beta values, with residualization for sex and age. Multiple testing was corrected using Benjamini-Hochberg FDR. Genera of interest were selected based on variance explained and number of significant correlations. Confirmatory analyses were performed using limma, comparing high vs. low abundance and presence vs. absence. Differential methylation was defined by adjusted FDR < 0.1 and $\Delta\beta \geq 0.10$. Results were summarized at the gene and promoter level. To further investigate the findings of the bioanalysis, primary human disc cells from six donors were co-cultured with *Acinetobacter baumannii* (MOI 10) for 2 h, followed by gentamicin treatment to eliminate extracellular bacteria. Samples were collected at 6 h and 24 h post-infection alongside matched controls, and RNA sequencing was performed.

RESULTS: PERMANOVA analysis identified Acinetobacter as the only genus significantly associated with global DNA methylation variation in both promoter ($R^2 = 10.8\%$, $p = 0.022$) and gene body regions ($R^2 = 11.4\%$, $p = 0.014$). Genome-wide Spearman correlation analysis between Acinetobacter CLR-transformed abundance and gene body methylation identified 949 genes with significant associations (FDR < 0.10), predominantly showing negative correlations (hypomethylation with increasing Acinetobacter abundance). Top hits included DDX41 ($\rho = -0.84$, FDR = 0.018), APTR ($\rho = -0.85$, FDR = 0.017), and MAP3K14-AS1 ($\rho = -0.91$, FDR = 0.003). Differential methylation analysis comparing Acinetobacter-present (n = 7) versus absent (n = 10) samples revealed similar patterns, with gene body regions showing more pronounced effects than promoters. The majority of differentially methylated genes showed hypomethylation in the presence of Acinetobacter.
RNA-seq validation is underway to assess functional consequences of identified methylation changes.

DISCUSSION & CONCLUSIONS:
Our exploratory analysis reveals a significant association between *Acinetobacter* presence and DNA methylation patterns in human IVD tissue, suggesting that bacterial colonization may be linked to epigenetic changes in disc cells. The observed predominance of hypomethylation. Notably, *DDX41*, a cytosolic DNA sensor involved in innate immune signaling via the STING pathway, emerged among the top correlated genes, pointing toward a possible mechanistic link between bacterial sensing and methylation changes. However, these correlational findings from clinical samples cannot establish causality. Ongoing RNA sequencing will assess whether methylation patterns correspond to transcriptional changes, and functional experiments will determine whether *Acinetobacter* can induce observed epigenetic changes. If confirmed, these findings could implicate immune memory mechanisms in IVD pathology and identify novel therapeutic targets for disc degeneration.

REFERENCES:
1 Netea, M. G. *et al.* Trained immunity: A program of innate immune memory in health and disease. *Science (80-.).* **352**, 427 (2016). 2 Mengis, T. *et al.* Intervertebral disc microbiome in Modic changes: Lack of result replication underscores the need for a consensus in low-biomass microbiome analysis. *JOR Spine* **7**, e1330 (2024).

I Like to move it: Robotic microsystem approaches for musculoskeletal disease modelling

Mario Rothbauer[1]

[1.]Karl Chiari Lab for Orthopaedic Biology, Department of Orthopedics and Trauma Surgery, Medical University of Vienna, Währinger Gürtel 18-20, 1090 Vienna, Austria,

INTRODUCTION: Musculoskeletal diseases are a leading cause of disability, yet current models fail to capture human-specific physiology and mechanobiology. Robotic microsystems, integrating precise actuation and control, recreate physiological forces and enable deeper insight into disease mechanisms, with potential to accelerate therapy development.

METHODS: Additive manufacturing, soft lithography and stop flow lithography was employed to develop a microfluidic soft robotic platform. Using 520 nm laser illumination at a power of 1 Watt, PNIPAM based structures containing gold nanoparticles were actuated by thermal changes, resulting in collapse of the polymer constructs.

RESULTS: Hexagonal soft robots were mass-produced via stop-flow lithography, and a laser-based platform actuated four biochips in parallel. Light intensity, frequency, and area enabled cyclic loading up to 30% compression exploring geometry effects and coupling PNIPAM actuation to biocompatible hydrogels to convert compressive collapse into tensile loading of cell-laden compartments.

DISCUSSION & CONCLUSIONS: This work presents a scalable soft robotic microsystem for controlled, light-driven mechanical stimulation in microfluidic environments. By enabling tunable cyclic actuation, it addresses the lack of physiologically relevant mechanobiological cues in vitro. Robotic microsystems represent a promising path toward predictive musculoskeletal models, with potential to advance mechanistic insight and accelerate therapeutic development.

Figure.7¿Example.of.soft.robotic.system.inside.a.microfluidic.chip¡

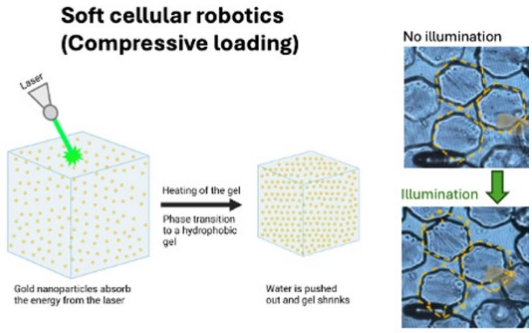

REFERENCES: None

Modelling Osteoclast–Chondrocyte Interactions in a 3D Human Organoid System

Fatemeh Safari[1], Sibylle Grad[1], Martin J. Stoddart[1], Zhen Li[1]

[1]*AO Research Institute Davos, Davos Platz, Switzerland*

INTRODUCTION: Interactions between the immune system and cartilage play a crucial role in maintaining tissue homeostasis. Osteoclasts (OC), as immune derived cells residing in skeletal tissues, localize to the hypertrophic zone of cartilage, suggesting that they may directly or indirectly regulate chondrocyte responses to biological and biochemical cues. Furthermore, osteoarthritis (OA) occurs more frequently in women, indicating potential intrinsic sex specific differences in chondrocyte biology. This study aims to elucidate how OCs interact with chondrocytes, determine whether OCs alter chondrocyte responses to inflammatory stimuli, and investigate whether these interactions differ between male and female derived cells.

METHODS: A human osteoclast–chondrocyte organoid model was established using primary chondrocytes isolated female femoral heads and OCs generated by differentiating $CD14^+$ monocytes isolated from buffy coats using CSF-1 and RANKL (30 ng/mL). Organoids were generated at a 3:1 chondrocyte-to-OC ratio (150'000/50'000 cells). Monocultures of chondrocytes served as controls (200'000 cells). qPCR, Live/Dead staining and histological analyses were performed to assess cell function, organization, and gene expression. Culture conditions were supplemented with TGF-β1 (1 ng/mL), CSF-1 and RANKL (30 ng/mL) under healthy conditions and additionally treated with IL-1β and TNF (1 ng/mL) to generate an inflammatory model.

RESULTS: After 7 days of culture, organoids formed a self-organized structure characterized by a central chondrocyte core surrounded by a peripheral OC layer. TRAP staining confirmed the presence and localization of OC (n=4, Fig1A). Live/Dead staining confirmed cell viability in both mono- and co-culture organoids after 7 days of culture (n=4, Fig. 1B). qPCR analysis revealed increased expression of *ADAMTS5*, *COL1A1*, *COL10*, and *ACAN* in chondrocyte monocultures compared with co-cultures with OC (n=2). Inflammatory condition led to a further increase in *ADAMTS5* and *COL1A1* in chondrocytes monocultures. *COL2* and *MMP13* expression were not affected by the presence of OC (n=2).

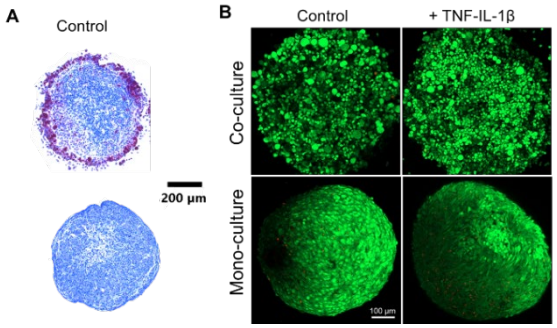

Figure 1. Spatial organization and viability of osteoclast–chondrocyte organoids. (A) TRAP staining (red: TRAP; blue: hematoxylin). (B) Live/Dead staining (green: Calcein AM; red: ethidium homodimer).

DISCUSSION & CONCLUSIONS: These findings demonstrate an *in vitro* spatial arrangement resembling *in vivo* tissue architecture, where OCs and chondrocytes maintain distinct yet interacting layers. High cell viability in both mono- and co-culture systems supports the suitability of this model for mechanistic studies. Osteoclast presence modulated chondrocyte phenotype, by decreasing hypertrophic and catabolic gene expression, suggesting a potential regulatory role rather than induction of hypertrophy for OC. In contrast, expression of the anabolic marker ACAN was reduced in the co-culture model, indicating osteoclast-mediated regulation of matrix synthesis. Ongoing work includes investigation of male donor cultures and spatial transcriptomic profiling to map cell-type-specific gene expression, enabling identification of intrinsic sex-associated differences independent of systemic hormonal effects.

Funding: This project was funded by the Swiss National Science Foundation (SNF), SPARK program, CRSK-3_229034.

Synergistic Effects of Mechanical Loading and Inflammation on Chondrocyte Gene Expression in a Cartilage-on-Chip Model

Z. Sarmadian[1], J. Henriques[1], V. Peitso[1], C.A. Paggi[2], E. Lauwers[2], M. Risteli[1], A. Mobasheri[1]

[1] Research Unit of Health Sciences and Technology, Faculty of Medicine, University of Oulu, Oulu, FI, [2] Chiron (chrn-on-chip biotechnologies B.V.), Maastricht, NL

INTRODUCTION: Osteoarthritis (OA) is a highly prevalent joint disease driven by dysregulated mechanobiological and inflammatory signaling. Cartilage-on-chip (CoC) platforms, as advanced microfluidic joint-on-chip models, more closely recapitulate the joint microenvironment and dynamic mechanical forces, enabling the study of OA progression under near-physiological conditions. This study investigated OA-related gene expression in response to mechanical loading and inflammatory stimulation using a CoC system.

METHODS: Primary bovine chondrocytes were isolated from bovine articular cartilage. Next, cells were injected in combination with a 2% agarose hydrogel into CoC devices and were cultured at 37 °C for 5 days; cells rested for the first two days, followed by sinusoidal dynamic mechanical loading (300 mbar, 1 hour/day) on days 3 and 4, with or without pro-inflammatory cytokine stimulation (TNF-α and IL-1β, 10 ng/mL each). On day 5, total RNA was extracted, and relative gene expression was assessed by real-time quantitative PCR and normalized to β-actin *(ACTB)*. Statistical analysis was performed using the Kruskal-Wallis test followed by Dunn's post hoc test.

RESULTS: Dynamic mechanical loading differentially regulated mechanosensitive, matrix, and inflammatory gene expression. Mechanosensitive ion channel *TRPV4* was significantly reduced under dynamic loading and cytokine stimulation compared with dynamic loading alone ($p = 0.003$), whereas integrin beta-1 (*ITGB1*) expression was increased under dynamic loading compared with static cytokine-treated conditions ($p = 0.03$). Dynamic loading, combined with cytokine stimulation, resulted in the upregulation of *IL-6* and *TNF-α*, and a significant increase in the expression of the fibrotic marker *COL1A1*, indicating an interaction between mechanical and inflammatory cues ($p = 0.02$, $p = 0.01$, and $p = 0.01$, respectively). *TNF-α* was significantly upregulated under static cytokine-treated conditions but reduced by dynamic loading alone ($p = 0.02$). In contrast, the extracellular matrix gene aggrecan (*ACAN*) expression showed a modest but significant increase under dynamic loading relative to static control ($p = 0.02$). The catabolic enzyme gene *ADAMTS5* showed no significant differences over the 5-day culture period.

CONCLUSIONS: These findings demonstrate that this CoC platform captures mechanosensitive and inflammatory interactions relevant to OA, providing a robust *in vitro* model to study how biomechanical loading modulates inflammatory cartilage responses on bovine chondrocytes.

ACKNOWLEDGEMENTS: This research was supported by the Academy of Finland (Profi6, 336449) and the Orion Research Foundation sr.

DISCLOSURES: Carlo Alberto Paggi is the Co-Founder and employee, and Elsa Lauwers is an employee of Chiron (chrn-on-chip biotechnologies B.V.).

Intra-articular α-MSH analogs attenuate cartilage degradation and systemic inflammation in a murine osteoarthritis model

Nicole Schäfer[1,2], Patrick Pann[1,3], Matthias Rudolph[4], Nicolas Pere[4], Hauke Clausen-Schaumann[4], Markus Böhm[5], Susanne Grässel[1,2]

[1]Dept. of Orthopedic Surgery, Experimental Orthopedics, Centre for Medical Biotechnology (ZMB), Bio Park 1, University of Regensburg, Germany. [2]Dept. of Orthopedic Surgery, Asklepios clinic, University of Regensburg, Germany. [3]Dept of Trauma Surgery, University Regensburg, Germany. [4] Center for Applied Tissue Engineering and Regenerative Medicine (CANTER), University of Applied Sciences Munich, Germany. [5]Dept. of Dermatology, University of Münster, Germany.

INTRODUCTION: Osteoarthritis (OA) is a progressive inflammatory disease characterized by cartilage degradation and joint-wide structural damage. To investigate its pathogenesis, the murine destabilization of the medial meniscus (DMM) model serves as highly relevant proxy for human OA due to its cross-species biomechanical similarities. The neuropeptide α-melanocyte-stimulating hormone (α-MSH) exhibits potent anti-inflammatory and chondroprotective properties, primarily through the melanocortin 1 receptor (MC1R). This study evaluated whether intra-articular supplementation with the stable analog NDP-α-MSH or the derivative KdPT can modulate anti-inflammatory and senescence-associated pathways to delay OA progression.

METHODS: OA was induced in 12-week-old male wild type (C57Bl/6J) mice via destabilization of the medial meniscus (DMM) surgery, with sham-operated mice serving as controls. Animals received intra-articular injections of NDP-α-MSH, KdPT (tripeptide derivate from □□MSH), or PBS at 1, 4, 8, and 12 weeks post-surgery. After 8 and 16 weeks post DMM/Sham surgery, evaluation included nighttime locomotion monitoring, histological assessment of cartilage degradation, and immunohistochemical analysis of MC1R- and TUNEL-positive chondrocytes. Additionally, cartilage stiffness is quantified via atomic force microscopy (AFM), and systemic inflammatory markers were measured using Luminex multiplex ELISA.

RESULTS: DMM surgery induced significant cartilage degradation, which was markedly inhibited by NDP-α-MSH and KdPT treatment 16 weeks post-surgery compared to PBS controls. While MC1R-positive chondrocytes decreased in NDP-α-MSH treated DMM mice relative to sham controls, plasma levels of pro-inflammatory markers (CRP, IL-1β, IL-6, IL-18) were significantly reduced in the NDP-α-MSH group at 8 and 16 weeks post-surgery. Furthermore, KdPT administration resulted in greater total distance moved and longer moving times, yet it significantly reduced average locomotor velocity, indicating a pattern of persistent but slower-paced exploration compared to other treatment groups.

DISCUSSION & CONCLUSIONS: These findings demonstrate that intra-articular applied α-MSH analogs effectively mitigate cartilage loss and systemic inflammation following joint destabilization. The reduction in circulating cytokines and the preservation of joint integrity suggest that targeting melanocortin signaling offers a viable therapeutic strategy for disease-modifying OA treatment.

Experimental Workflow

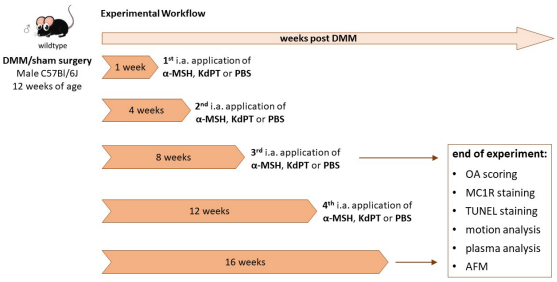

Application of an Electric Current in the Developing Chicken Embryo Induces Spinal Deformity

Thomas P. Schaer[1], Jacob V. Jordan[2,3], Guiseppe Orlando[4], Andrea Ketschek[5], Gianluca Gallo[5], Jason Anari[2,3], Brian D. Snyder[6], Patrick J. Cahill[2,3]

[1]Department of Clinical Studies New Bolton Center, University of Pennsylvania School of Veterinary Medicine, Kennett Square, PA; [2]Department of Orthopedic Surgery, Children's Hospital of Philadelphia, Philadelphia PA;[3]Perelman School of Medicine at the University of Pennsylvania, Philadelphia PA; [4]Casilino Hospital, Rome, Italy; [5]Shriners Hospitals Pediatric Research Center, Lewis Katz School of Medicine at Temple University, Philadelphia PA; [6]Boston Children's Hospital and Beth Israel Deaconess Medical Center, Harvard Medical School, Boston, MA

INTRODUCTION: Congenital scoliosis is a relatively rare condition, affecting 1 in 1000 live births, where vertebral anomalies present at birth involve either a failure of vertebral formation, such as a hemivertebra, or a failure of vertebral segmentation, such as a unilateral unsegmented bar, where different parts of the vertebral body and posterior elements can be affected to varying extent creating complex spinal deformity. Our understanding of congenital spinal deformity is limited by the lack of relevant animal models to study the mechanisms underlying congenital spinal pathoanatomy, including intervertebral disc behavior. The purpose of this study is to examine the effects of applying targeted electric current on the formation and location of congenital spinal deformities in the developing chicken embryo. **METHODS:** 57 specific pathogen-free (SPF) eggs were incubated at standard conditions (99.5 F, 50-55% RH) to embryonic day 3 (E3), after which eggs were windowed for intervention. Electroporation parameters were set to 50V, 3 pulses, 50 ms duration, 950 ms interval. Plasmid DNA constructs were not used. Current was delivered through electrodes placed superiorly (n=13), inferiorly (n=14), and in an oblique orientation to the vitelline vessels (n=19) in the treatment arm (Fig 1). Controls (n=11) underwent a sham procedure where no current was applied. Eggs were then sealed and re-incubated to E10/E11, after which embryos were sacrificed, and gross observations were made. Fisher's exact test was used to compare the proportions of deformities and survivability across groups. Histologic sections stained with Alcian Blue and Picrosirius Red were also prepared from representative specimens. **RESULTS:** Our protocol yielded high survival (n=33/46, 79%) and spinal deformity rates (n=29/33, 88%) with region-specific defects based on electrode placement (Table 1). Control embryos showed 100% survival (11/11) with no deformity development (0/11), demonstrating a significant difference in deformity rates between experimental and control groups ($p<0.0001$). Curves were isolated to the cranial end in the superior group, to the caudal end in the inferior group, and in the oblique group complex multi-region curves were produced (Fig 2), Upon histologic assessment of the region of interest in representative specimens, segmentation defects between adjacent cartilaginous vertebral anlage were observed, not present in controls**.** **DISCUSSION:** By inducing regionally specific vertebral segmentation failures, we have established and optimized a method to model congenital scoliosis in the developing chicken embryo, achieving 88% survival across specimens. The ability to produce region-specific thoracolumbar malformations that persist through late-stage development provides a valuable platform for investigating disease progression, biomechanical consequences, and potential therapeutic interventions. Moreover, as the popularity of non-fusion spinal deformity correction (vertebral tethers) increases, this model may provide mechanistic insight into how intervertebral disc growth is modulated in the growing axial skeleton.

ACKNOWLEDGEMENTS: The Wyss / Campbell Center for Thoracic Insufficiency Syndrome (Children's Hospital of Philadelphia).

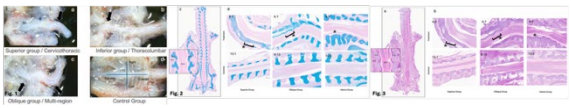

Figure 1. Shows representative gross specimens from the dissection of the superior group (a), the inferior group (b), and the oblique group (c). Each display coronal plane structural curves. Control specimens (d) showed no signs of scoliosis. Fig. 2 & 3 Display coronal H&E (a, b) and Alcian blue / Picrosirius Red (c, d) sections from the respective groups, illustrating abnormal vertebral morphology. In the superior group, sections are taken from the cervical/cervicothoracic region; in the oblique group, from the thoracic region; and in the inferior group, from the thoracolumbar region. Adjacent segments in the scoliotic region of interest show fusion of the vertebral cartilaginous anlagen, not seen in controls, indicating vertebral failure of segmentation as the structural cause of scoliosis observed at gross dissection. Sample normal, unoperated embryos (a, c) were used for relevant comparisons (s.c. (spinal cord); v.c. (vertebral cartilage); n.r. (nerve root); *Areas of abnormal morphology).

Impact of Digestion Time and Tissue Size on the Isolation of TIE2+ Nucleus Pulposus Progenitor Cells

Leon Schlagenhof [1,2], Anja Stirnimann [2,3], Fabian Ille [3], Benjamin Gantenbein [1,4]

[1]Department for BioMedical Research, Bone & Joint Program, University of Bern, Bern, Switzerland; [2]Graduate School for Cellular and Biomedical Sciences, University of Bern, Bern, Switzerland; [3]Center of Competence in Aerospace Biomedical Science and Technology, Lucerne University of Applied Sciences and Arts, Hergiswil, Switzerland; [4]Department of Orthopedic Surgery & Traumatology, Inselspital, University of Bern, Bern, Switzerland

INTRODUCTION: Worldwide the leading cause of disability is low back pain, with intervertebral disc (IVD) degeneration (IDD) as a significant contributor. The effectiveness of current therapies, such as conservative or surgical treatment, remains debatable. Novel approaches focus on cell-based therapies to mitigate IDD and aim to further rejuvenate and regenerate the degenerated IVD. Therefore, the autochthonous angiopoietin receptor-1 (TIE2) positive nucleus pulposus progenitor cells (NPPCs^{TIE2+}) have come into focus, a cell population residing within the nucleus pulposus (NP). While NPPCs^{TIE2+} were investigated in animal studies, the isolation protocols vary among laboratories. Different research groups reported between <1% and >80% NPPCs^{TIE2+} among the NP cell populations. The published protocols varied in the type of digestion enzyme used, their concentrations and incubation times, and in the type and concentration of antibodies. Finally, they were differing regarding whether a recovery phase and whole tissue culture before cell isolation vs. direct cell isolation was applied. Furthermore, the size of the of the digested NP pieces was not disclosed all the protocols. In this research we investigated the effect of changing the parameters of tissue digestion on the detection of NPPCs^{TIE2+} using flow cytometry (FCM).

METHODS: For every replicate, ten to twelve coccygeal bovine NPs of two to three animals were pooled. NP tissue was minced by hand using a scalpel into fragments of three different diameters: small (~2-4 mm), medium (~ 4-6 mm) or large (~6-10 mm). Cells were then isolated by sequential digestion with pronase (1h) and collagenase type II (12h or 16h). Following digestion cells were directly stained with an anti-TIE2 antibody (Bioss, bs-1300R-BF488) and analysed by FCM using the BD FACSDiscover™ S8 Cell Sorter (Becton & Dickinson, Brussels, Belgium).

RESULTS: FCM showed clear differences between experimental groups: Both the digestion time and the NP tissue size impacted overall cell yield (Fig. 1A) and NPPCs^{TIE2+} percentages (Fig. 1B). While overall cell yield increased with smaller tissue size and longer digestion time (Fig. 1A), NPPCs^{TIE2+} percentages increased with bigger tissue size and shorter digestion time (Fig. 1B). NPPCs^{TIE2+} percentages varied between <1% and >40%.

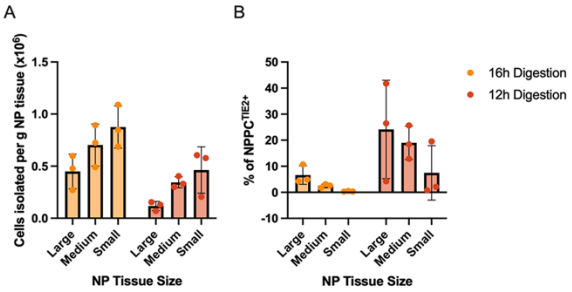

Figure 1: Bovine NP tissue was enzymatically digested using pronase and collagenase type II. Therefore, different digestion times and tissue fragment sizes (small [~2-4 mm], medium [~4-6 mm] or large [~6-10 mm]) were investigated. Digestion was followed by anti-TIE2 antibody staining and FCM analysis. A) Number of cells (x10^6) per gram tissue isolated after enzymatic digestion of NP tissue. B) Percentage of NPPCs^{TIE2+} after FCM analysis. Abbreviations: Angiopoietin receptor-1 positive nucleus pulposus progenitor cells (NPPCs^{TIE2+}), nucleus pulposus (NP), flow cytometry (FCM).

DISCUSSION & CONCLUSIONS: We showed here that NP tissue size and digestion time impacted overall cell yield and also the percentages of NPPCs^{TIE2+}. Although more replications are needed to obtain robust statistical analysis, this highlights the need of further standardization of the basic NPPCs^{TIE2+} isolation protocols. Our results suggest that the high variance in cell number of NPPCs^{TIE2+} across different labs might arise through unfixed sensitive parameters in cell isolation.

REFERENCES:

[1] Sakai et al. **2012** *Nat Commun*. 2012;3:1264.

[2] Basatvat et al. **2023** *JOR Spine*. 2023;6(1):e1238.

[3] Lee et al. 2015 . *J Orthop Res*. 2015;33(12):1743-1755.

A Comparison of Bovine Adipose-Derived Mesenchymal Stromal Cells With Nucleus Pulposus Progenitor Cells: Exploring Extracellular Vesicle Therapy for Intervertebral Disk Regeneration

Leon Schlagenhof [1,2], Carla Raffaele [1], Cristina Zivko [3,4], Paola Luciani [4], Ali Hashemi Gheinani [5,6], Benjamin Gantenbein [1,7]

[1]Department for BioMedical Research, Bone & Joint Program, University of Bern, Bern, Switzerland; [2]Graduate School for Cellular and Biomedical Sciences, University of Bern, Bern, Switzerland; [3]Department for BioMedical Research, Center for Extracellular Vesicle Research, University of Bern, Bern, Switzerland; [4]Department of Chemistry, Biochemistry and Pharmaceutical Sciences, Pharmaceutical Technology, University of Bern, Bern, Switzerland; [5]Functional Urology, Department for BioMedical Research, University of Bern, Bern, Switzerland; [6]Department of Urology, Inselspital, Bern, Switzerland; [7]Department of Orthopedic Surgery & Traumatology, Inselspital, University of Bern, Bern, Switzerland

INTRODUCTION: Intervertebral disc (IVD) degeneration is a major contributor to low back pain (LBP), the leading global cause of disability. Current conservative and surgical treatments remain of limited efficacy. Emerging strategies target a nucleus pulposus (NP) progenitor cell population expressing angiopoietin receptor-1 (TIE2), known for regenerative and proliferative potential. Extracellular vesicles (EVs), key mediators of cellular communication, are gaining interest as cell-free therapies for LBP. Recent work shows that NP cell (NPC)-derived EVs enhanced proliferation in degenerated NPCs compared with mesenchymal stromal cell-derived EVs. Here, we compared EVs from bovine NPCs^{TIE2+}and NPCs^{TIE2-} regarding vesicle number, size distribution, membrane potential, proteomics and transcriptomics.

METHODS: NPCs were isolated from four bovine tails. Before seeding, NPCs were sorted using fluorescence-activated cell sorting to obtain NPCs^{TIE2+} and NPCs^{TIE2-}. After one passage and culturing to 80% confluency, standard medium was replaced with EV-free medium for two days before collecting cells and EVs for proteomic and transcriptomic analyses. EVs were isolated from conditioned media by ultracentrifugation and size-exclusion chromatography.

RESULTS: Nanoparticle tracking analysis revealed EV populations averaging 191nm (NPCs^{TIE2+}) and 193nm (NPCs^{TIE2-}) in size, with mean zeta potentials of -29.2mV and -27.6mV, respectively. Proteomic and transcriptomic analysis showed fewer highly differentially regulated proteins and genes between NPCs^{TIE2+} and NPCs^{TIE2-} than between their respective EVs (Fig. 1). TIE2 protein was not detected, while its gene *TEK* showed no difference between cell types or EVs, though it appeared more abundant in EVs. CD24 mRNA was only detected in NPCs^{TIE2-}, and B4GALNT1, encoding the GD2-synthesizing enzyme, was modestly upregulated in EVs from NPCs^{TIE2-} compared with NPCs^{TIE2+}.

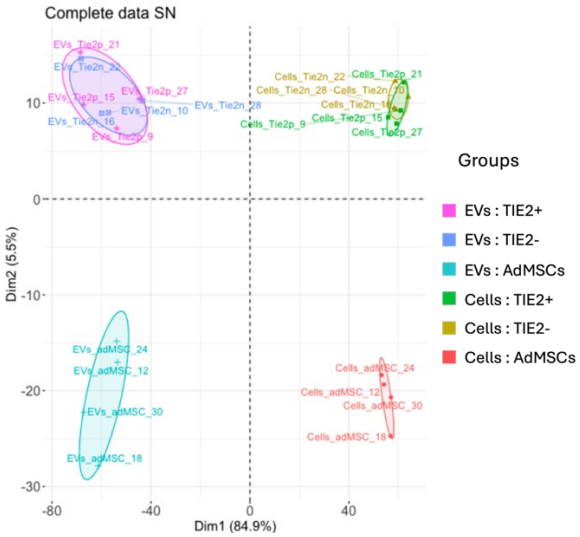

Figure 1: Proteomics: Principal component analysis of the log2-transformed Spectronaut intensity (SN), depicting three different cell types: TIE2+ and TIE2- nucleus pulposus cells, and adipose-derived mesenchymal stromal cells (AdMSCs), along with their corresponding extracellular vesicles (EVs).

DISCUSSION & CONCLUSIONS: Here, EVs were successfully isolated from healthy donor-matched bovine NPCs and AdMSCs. Bovine NPCs^{TIE2+} derived EVs were chosen as a pre-clinical model to investigate their regenerative potential compared to other targeted cell sources. The bovine source allows testing of EVs regenerative effect in a bovine *ex vivo* IVD organ culture model.

REFERENCES:

[1] Sakai et al. **2012** *Nat Commun*. 2012;3:1264.
[2] Ambrosio et al. **2024** *Eur Spine J*. 2024;33(5):1713-1727.
[3] Samanta et al. **2025** *PLoS One*. 2025;20(5):e0324179.

Mechanical loading of 3D-printed thermoplastic polyurethane scaffolds promotes chondrogenic differentiation of human mesenchymal stromal cells without exogenous TGF-β1 while limiting hypertrophy

Maja Schlittler[1], Laura Mecchi[1,2], Martin J. Stoddart[1]

[1]AO Research Institute Davos, Davos Platz, Switzerland. [2]Laboratory for Experimental Orthopedics, Department of Orthopedic Surgery, Caphri School for Public Health and Primary Care, Maastricht University, Maastricht, the Netherlands

INTRODUCTION: Articular cartilage has limited intrinsic repair capacity, and current clinical treatments rarely restore durable, functional tissue. Tissue engineering using human mesenchymal stromal cells (MSCs) presents a promising alternative but requires scaffolds capable of delivering appropriate biochemical and mechanical cues to guide chondrogenic differentiation. In this study, we developed and characterised a 3D-printed thermoplastic polyurethane scaffold and evaluated its ability to activate latent TGF-β1 under mechanical load, as well as its capacity to support mechanically induced chondrogenesis in a custom bioreactor. Importantly, this approach avoids the supraphysiological concentrations of exogenous TGF-β1 typically used to drive chondrogenesis, enabling a more physiological, mechanically mediated activation of endogenous TGF-β1.

METHODS: MSCs from seven donors were seeded into fibrin-filled scaffolds and cultured for 28 days under one of three conditions: free swelling in a typical in vitro chondrogenic medium containing 10 ng/mL TGF-β1 (CG-FS), free swelling in TGF-β1-free medium as a negative control (CP-FS), or mechanical loading consisting of combined shear and compression applied twice daily for 1 h in TGF-β1-free medium (CP-L). Medium was collected throughout the culture period, and scaffolds were harvested after 28 days for biochemical analyses.

RESULTS: Mechanical loading stimulated the secretion and activation of latent TGF-β1 (Fig. 1), increased the expression of downstream chondrogenic markers including *ACAN*, *SOX9*, *COMP*, and the *SOX9/RUNX2* ratio (Fig. 2), and enhanced the production of sulphated glycosaminoglycans in both scaffolds and medium compared with CP-FS ($p = 0.018$). While the chondrogenic outcomes of CP-L were comparable in magnitude to those induced by exogenous TGF-β1, a key difference emerged regarding hypertrophy: CG-FS caused a significant upregulation of *COL10A1* and *ALPL*, whereas mechanically induced chondrogenesis did not alter their expression compared with CP-FS (Fig.2).

DISCUSSION & CONCLUSIONS:
Taken together, our results indicate that mechanically induced activation of endogenous TGF-β1 in 3D-printed scaffolds can support a stable, non-hypertrophic chondrogenic phenotype. By applying physiologically relevant loading, this approach overcomes key limitations of conventional TGF-β1-based induction protocols and provides a basis for growth-factor-free cartilage engineering strategies.

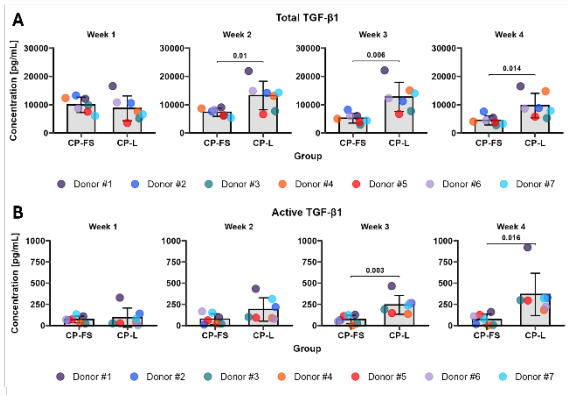

Fig. 1.: (**A**) Total (latent and active) and (**B**) active TGF-β1 released into the medium over 4 weeks of loading.

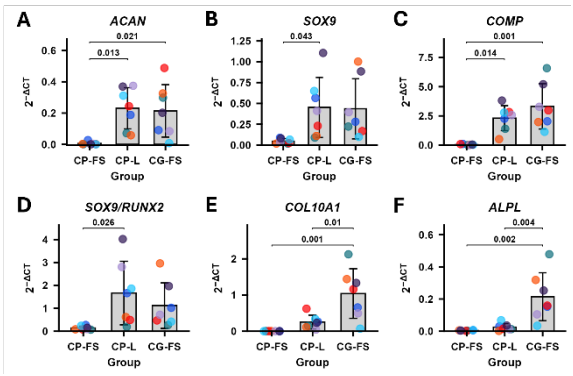

Fig. 2.: Expression of chondrogenic (**A-D**) and hypertrophic (**E-F**) genes after 4 weeks.

L.M. was supported by the EU Horizon 2020 programme under the Marie Skłodowska-Curie grant No. 101034412.

Bridging Biomechanical and Biochemical Profiles in Whole-Organ Intervertebral Disc Degeneration Models

D.Schnyder[1,2*], M. Muerner[1,2*], N. Fischlin[1,2*], C. Honz[1,2], M. Santolini[1,2], P. Schwarzenberg[1], S. Grad[1,2]

*[1]AO Research Institute, AO Foundation, Davos, CH, [2]Swiss Federal Institute of Technology Zurich, Zurich, CH, * contributed equally*

INTRODUCTION: Chemonucleolysis is a well-established method to model intervertebral disc (IVD) degeneration, yet studies typically focus on either biology in whole-organ cultures or biomechanics using cadaveric tissue, but rarely both. As a result, multidimensional changes in tissue composition and mechanics in *ex vivo* organ culture studies remain poorly understood. This study examined the biochemical and biomechanical effects of papain, collagenase II, and chondroitinase ABC (chABC) at three distinct doses to evaluate how enzymes and concentrations affect IVD features and their interrelations, with the goal of identifying the most informative parameters for improved disease model selection.

METHODS: Bovine coccygeal IVDs (Ø 17.3 ± 1.9 mm, height 12.2 ± 2.0 mm) were treated with low, medium, or high doses of papain, collagenase II, or chABC (100 µL/injection, n = 6/group) to generate distinct degeneration profiles (Table 1). Discs underwent three days of physiological compressive loading (0.02–0.2 MPa, 0.2 Hz, 2 h/day) in a uniaxial bioreactor. Mechanical parameters (height changes, stiffness, creep, and hysteresis) were tracked over time, and nucleus pulposus (NP) and annulus fibrosus (AF) biochemical changes (hydration, GAG, collagen, DNA) were quantified at endpoints. Data was analysed using basic statistics, Pearson correlations, regression analysis, and supervised classification approaches.

Table 1. Enzymes and their activities (U/mL) used in this study.

U/mL	Papain	Collagen. II	chABC
Low	5	5	5
Medium	30	70	30
High	60	310	60

RESULTS: All enzymes markedly reduced NP GAG content, with collagenase II only reaching significant reduction at the high dose. Collagen, DNA, and hydration showed no significant differences in NP and AF. Disc height loss increased over loading days, most notably in all papain groups and the high-dose collagenase II group. The strongest correlations between biochemical and biomechanical parameters observed were NP collagen content, which was negatively correlated with creep, while AF collagen content positively correlated with stiffness. NP GAG content positively correlated with disc height loss, reswelling, hysteresis and creep, and AF DNA content correlated with linear stiffness. Additionally, NP DNA negatively correlated with disc height loss and disc reswelling. Regression models only had low predictive power ($r^2 \leq 0.36$), while combining biochemical and biomechanical features improved classification; the best model (random forest) reached a macro F1 of 0.61 (~60% correct group assignments).

DISCUSSION & CONCLUSIONS: Notably, varying enzyme concentrations did not produce the expected differential effects on tissue biochemistry. Histological staining will be added to assess dose dependence and determine whether this reflects methodological limitations or genuinely similar effects across doses. NP GAG content was the most sensitive marker of enzyme-induced disc degeneration, consistent with the known GAG-degrading effects of papain and chABC. Individual biomechanical features correlated with biochemical changes in biologically expected ways, but their combined predictive power in regression was limited. Classification analyses showed that integrating biochemical and biomechanical data improved discrimination of enzyme-specific degeneration profiles. Overall, although dose dependence needs further investigation, this study demonstrated that integrating biochemical and biomechanical data enhances the characterization of IVD degeneration models, underscoring the value of combining both data types for *ex vivo* disease model analysis.

ACKNOWLEDGMENTS: This work was funded by the SNSF within the grant 310030L_212196 and supported by the AO Foundation Fellowship from the ETH Foundation.

Extracellular vesicles from spontaneously calcifying chondrocytes stimulate chondrocyte and matrix calcification

Andrea Schwab[1], Carolin Schneider[1], Severin Gylstorf[1], Claudia Göttsch[2], Agnieszka Halm-Pozniak[1], Christoph H Lohmann[1], Jessica Bertrand[1]

[1]*Medical Faculty, Otto-von-Guericke University Magdeburg,* [2]*Medical Faculty Carl Gustav Carus, TU Dresden*

INTRODUCTION: Extracellular vesicles (EVs) are lipid-bound particles released by cells and contain proteins, lipids and nucleic acids. EVs act as messenger in cellular communication by transporting these bioactive molecules and thereby modulating cell function, extracellular matrix (ECM) production and immune response. Current literature lacks knowledge on whether EVs play an active role in cartilage calcification. Ectopic cartilage calcification is one hallmark in osteoarthritis (OA) and correlates with the disease severity. The aim of this study was to characterize EVs derived from calcifying chondrocytes and to investigate the potential of the EVs to stimulate chondrocyte calcification *in*

METHODS: β-Glycerophosphate (10 mM, βGP) enriched media was used to calcify C28 chondrocytes (n=3) and chondrocytes isolated from cartilage of OA patients (n=6 patients) *in vitro*. EVs were harvested from the cell culture supernatant and size-characterized using the Nanosight. Calcein staining was used to visualized and characterize the amount of calcium-containing crystals in EVs. Hydroxyapatite crystals were visualized using OsteoImage staining. We used Western Blot analysis to characterize the cargo (CD9, CD63, TSG101, HSP70, Flotilin, Sortilin, TNAP) of the EVs.

In a second step, we stimulated human OA chondrocytes (n=5 patients) with the characterized C28-derived EVs for 21 days *in vitro* in absence of βGP. To additionally study the contribution of the cell derived ECM on the *in vitro* calcification, the cultured chondrocytes (7 days) were freeze-thawed to induce cell death before stimulated with EVs. Alizarin Red staining was used to compare the calcification between the viable cells+ECM and freeze-thawed dead cells+ECM samples.

RESULTS: C28 and human OA chondrocytes calcified in response to the phosphate source βGP with an increase in Alizarin Red staining on day 14 and day 21 compared to the donor-matched day 1 samples (C28: $p<0.05$, human OA chondrocytes p=n.s.). The size of the EVs from ranged between 100-300 nm (Figure 1A). We identified calcium-containing crystals in the EVs from the chondrocyte cultures with a tendency of a stronger staining in the larger EVs compared to the smaller EVs (Figure 1A). The intensity of calcein stained EVs normalized to total protein content increased with increasing culture time (C28: $p<0.05$ comparing day 21 vs day 7, human OA chondrocytes: p=n.s.). Calcium-crystals in EVs were positive stained for OsteoImage (Fig.1). EVs isolated from the *in vitro* calcified C28 chondrocytes and human OA chondrocytes were positive for the protein biomarkers CD9, CD63, TSG101, HSP70, Flotilin, Sortilin and TNAP from day 7 on.

Next, we investigated the potential of the characterized and C28-derived EVs on the *in vitro* calcification of human OA chondrocytes. Viable OA chondrocytes with their *in vitro* synthesized ECM and dead cells+ECM underwent calcification based on the increase in Alizarin Red staining after 21 days of culture in media containing calcified EVs compared to the respective control group (viable cells+ECM: $p<0.05$, dead cells+ECM $p<0.01$). However, the extent of the matrix-associated calcification was lower compared to the donor-matched viable cells+ECM group.

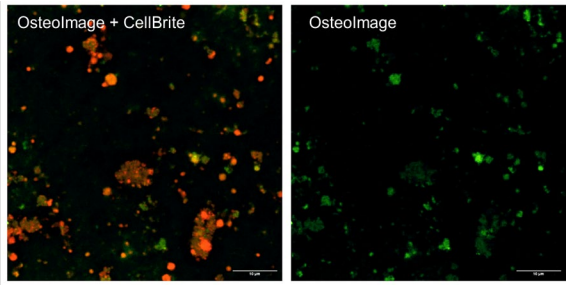

Figure 1: C28-derived EVs at day 21. Hydroxyapatite crystals (green) are co-localized with the lipid stain (red) of the EV membrane. Scale bar 10 µm.

DISCUSSION & CONCLUSIONS: Our data shows that EVs isolated from spontaneously calcifying and βGP stimulated chondrocytes contain hydroxyapatite crystals (Fig.1). The presence of TNAP and Sortilin as well as the potential of hydroxyapatite containing EVs to drive OA chondrocyte calcification suggest a role of EVs in tissue calcification. The results of our study suggest an active role of EVs in stimulating chondrocytes and cell-derived ECM to undergo calcification. This highlights the relevance of EVs in the pathogenesis of calcification in OA tissue.

Deoxycholic Acid Links Gut Microbiota to a Novel Pro-Inflammatory Adipocyte Phenotype in Modic Type 1 Changes

F. Schulze[1,2], J. Devan[1,2], T. Mengis[1,2], LP. Hatt[1,2], M. Farshad[3], O. Distler[1,2], S. Dudli[1,2]

[1]Center of Experimental Rheumatology, University Hospital Zurich, University of Zurich, CH. [2]Department of Physical Medicine and Rheumatology, Balgrist University Hospital, Balgrist Campus, University of Zurich, CH. [3]Department of Orthopedics, Balgrist University Hospital, University of Zurich, CH.

INTRODUCTION: Modic changes (MC) are vertebral bone marrow lesions associated with chronic low back pain. Prior histology indicates altered adipocyte frequency and adipocyte necrosis in MC, but the functional contribution of marrow adipocytes to MC pathophysiology remains unclear. We profiled marrow adipocyte transcriptomes and bone marrow lipidomes in MC type 1 (MC1) and type 2 (MC2) to define adipocyte states and metabolic drivers.

METHODS: Bone marrow aspirates (n=20) were obtained during spinal fusion surgery from patients with MC1, MC2, or no MC (Ctrl). Adipocyte-containing fat layers were isolated by centrifugation and stored at −80°C. RNA-seq was performed on purified high-quality adipocyte RNA (RIN>8; n=2/4/7 for MC1/MC2/Ctrl). Differentially expressed genes (DEG) were defined as FDR<0.05 and |log2FC|>0.5, followed by overrepresentation analysis (ORA). Lipidomics was performed on methanol-extracted, LC-purified lipids using Orbitrap mass spectrometry (n=4/5/11 for MC1/MC2/Ctrl); differential abundance was defined as FDR<0.05 and |log2FC|>1.

RESULTS: Adipocyte transcriptomics identified 1001 DEG in MC1 vs Ctrl, but only 1 DEG in MC2 vs Ctrl, indicating an MC1-selective transcriptional shift. Principal component analysis separated MC1 along PC2 (Fig.1a). Genes loading positively on PC2 were enriched for hepoxilin and arachidonic acid metabolism. ORA of MC1-upregulated genes showed a strong inflammatory signature, including leukotriene metabolic processes, neutrophil chemotaxis, T-cell activation, necroptosis, and regulation of superoxide (Fig.1b). Within the leukotriene axis, PLA2R1 (a scavenger receptor for PLA2) was downregulated, consistent with increased bioavailable PLA2 for leukotriene synthesis. Lipidomics quantified 371 lipids in 20 classes and revealed 3 lipids enriched in MC1 vs Ctrl: deoxycholic acid (DCA), LPE O-18:0, and LPE O-18:1 (Fig.1c). In MC2 vs Ctrl, seven membrane-associated lipids were enriched.

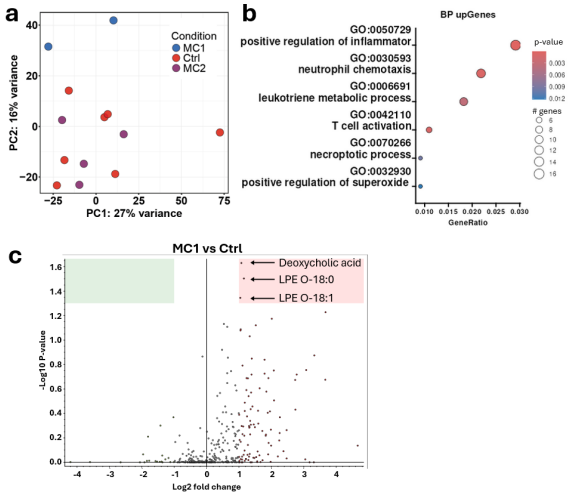

***Fig.1. (a)** Principal component analysis of bone marrow adipocyte transcriptome from MC1, MC2, and non-MC bone marrow (Ctrl). **(b)** Overrepresented biological processes in MC1 vs Ctrl adipocytes. **(c)** Vulcano plots of differentially abundant lipids in MC1 vs Ctrl.*

DISCUSSION & CONCLUSIONS: MC1 marrow adipocytes exhibit a pro-inflammatory, leukotriene phenotype that aligns with chemotactic and necroptotic programmes. The concurrent enrichment of DCA, a secondary bile acid produced by gut bacteria and a known adiponecrotic factor, supports a the notion of a gut–spine metabolic axis that may promote adipocyte stress/necrosis and PLA2–leukotriene pathway activation. LPE O-18:0/1 enrichment may reflect phospholipid remodeling and antioxidant responses downstream of inflammation. Together, these data implicate marrow adipocytes as active contributors to MC1 inflammation and suggest a role of DCA to mediate the gut-spine axis.

Notochordal & mesendoderm progenitor cells as potential cell sources for disc degeneration-associated back pain

Joseph W Snuggs[1], Shaghayegh Basatvat[1], Josette van Maanen[2], Markus Templin[3], Marianna Tryfonidou[2] and Christine Le Maitre[1]

[1]The University of Sheffield, UK, [2]Utrecht University, Netherlands [3]NMI, Reutlingen, Germany

INTRODUCTION: During disc degeneration the central nucleus pulposus (NP) is broken down due to increased degradation and cell loss. It has been proposed that notochordal (NC) cells, embryonic precursors within the disc, could be utilised for mediating regeneration as they have the potential to increase anti-catabolic factors and matrix synthesis. This study investigated the co-culture of porcine NC cells with degenerate human NP cells to determine the anti-catabolic effects NC cells potentially provide to NP cells. Also, due to the lack of availability of NC cells as a viable treatment strategy, we also investigated the effects of iPSC-generated mesendoderm progenitor cell (MEPC–precursors to NC cells) co-culture with human NP tissue, to determine the potential regenerative capacity of MEPCs.

METHODS: Porcine NCs (pNC) and human NP cells were encapsulated seperately in 3D alginate beads and co-cultured in conditions mimicking the healthy and degenerate disc. Subsequently, iPSCs were differentiated into MEPCs and injected into degenerate human NP tissue. Viability, gene expression, protein expression and secretion were investigated.

RESULTS: No significant differences were seen in phenotypic marker expression in NCs cultured in any media. Co-culture of NP cells with pNC cells showed significantly reduced production of MMP3, IL-8, VEGF-A and CXCL1 (Figure 1). Following culture, MEPCs were identified within NP tissue, and their viability was maintained. Luminex and IHC determined the production of secreted and factors and expression of proteins within the tissue.

DISCUSSION & CONCLUSIONS: Studying the in vitro behaviour of NCs in conditions that mimic the in vivo IVD environment has enabled a better understanding of their regenerative potential. Degenerate conditions had slight adverse effects on pNC viability but did not have any effect on their phenotypic markers' gene expression levels. This indicates that within the degenerate IVD environment NCs retain their phenotype and are able to modulate the production of catabolic proteins from degenerate NP cells when co-cultured together. This highlights that NC cells, or certain factors they produce, provide anti-catabolic effects which may alter the course of IVD degeneration. The ability of NC cells to provide anti-catabolic effects on degenerate NP cells indicates that the underlying pathophysiological causes of IVD degeneration can be modulated when targeted, and the generation of MEPC precursors from iPSCs can enable the production of NC-like cells, whereas previously the use of NC cells for IVD regeneration has not been considered due to their lack of availability.

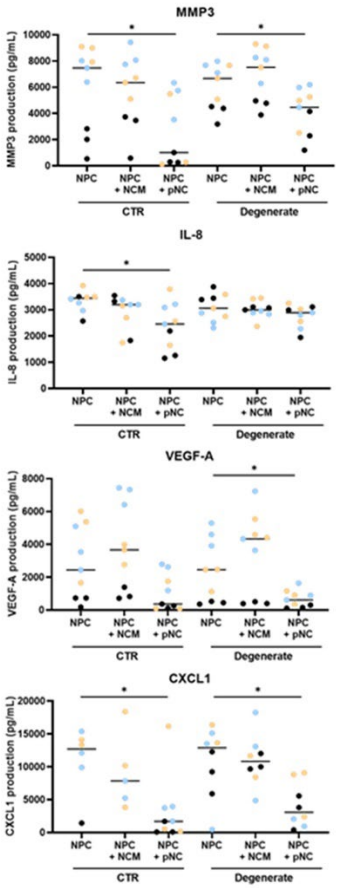

Figure 1. Production of proteins in cell culture supernatant from NP cells (NPC), NPC + notochordal cell conditioned media (NCM) and NPC + porcine notochordal cell (pNC) co-culture determined by Luminex. Treatment groups were cultured for 7d in control media (CTR) or media mimicking degenerate conditions + 100pg/mL IL-1β. Significance determined using Kruskall-Wallis with Dunn's multiple comparison tests $p \leq 0.05$. Different colour points represent individual patients (n=3). Horizontal lines represent the median value.

Targeting cellular senescence to combat osteoarthritis and intervertebral disc degeneration

Joseph Snuggs, Diane Swift, Heather Wilson, Endre Kiss-Toth, J Mark Wilkinson, Christine Le Maitre

The University of Sheffield, UK.

INTRODUCTION: Osteoarthritis and intervertebral disc (IVD) degeneration are leading causes of disability worldwide, leading to substantial pain, decreased mobility and major impacts on individuals' quality of life. However, current treatments do not target the underlying biological causes. Both diseases share several commonalities. We hypothesise that by targeting a common pathway in the development of osteoarthritis and IVD degeneration known as cellular senescence, where cells no longer divide but continue to produce catabolic factors that drive degeneration, we will be able to halt the progression of both diseases. This study, aimed to test a range of anti-senescence drugs (senolytics) and novel compounds to target and remove the dysfunctional cells within human knee and IVD tissue explant culture models.

METHODS: Osteochondral explants and synovium co-cultures and IVD tissue explants were treated for up to 3w with previously known senolytic drugs: quercetin, o-vanillin or RG-7112, and novel compounds to target senescent cells and their secretory phenotype. Cell viability, secretome analysis, gene and protein expression were utilised to determine the effects of senolytics on tissues.

RESULTS: Co-cultures were viable for 3w in culture. Following senolytic treatment, the secretion of specific senescence and catabolic markers was observed for all compounds tested. Particularly, 1w quercetin treatment caused decreased secretion in the greatest number of SASP markers including IL-6, M-CSF, CXCL1, CCL5, MMP3, MMP9, sclerostin and osteopontin compared to untreated controls (Figure 1).

DISCUSSION & CONCLUSIONS: Treatment with senolytic compounds decreased the production of the SASP within our human ex vivo osteoarthritis and IVD degeneration models. This indicates that these compounds target the senescent cell populations within our relevant human model systems and provide potentially disease-modifying effects. The development of a human osteoarthritis co-culture model will also enable the rapid testing of other novel therapies within a physiologically relevant *ex vivo* system.

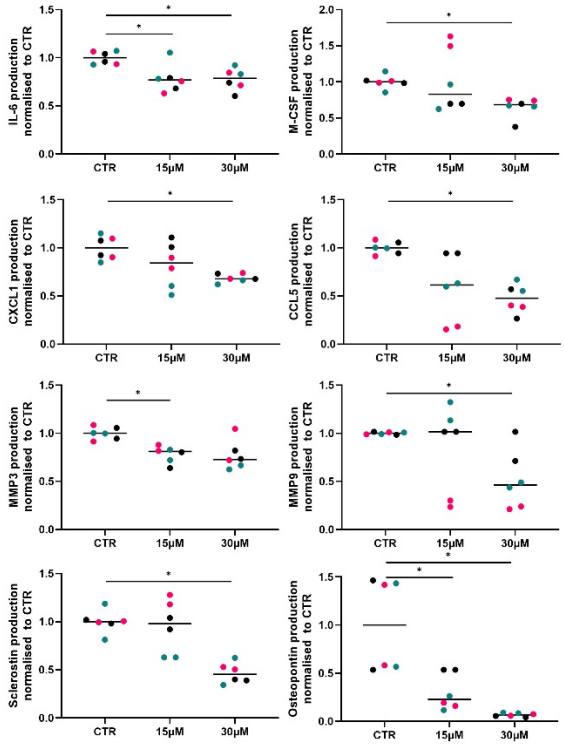

Figure 1: Changes to the secretome of osteochondral + synovium explants following 1 week quercetin (15, 30μM) treatment versus untreated controls (CTR). Each colour represents individual patients (n = 3). Horizontal bars represent median values. $P \leq 0.05$.

TGF-β-driven Interleukin-6 production by human fibroblast-like synoviocytes is OA patient-specific and is regulated by multiple active sites within the IL-6 promoter.

Jessica SJ Steijns[1], Guus GH van den Akker[1], Roderick HMJ Stassen[1], Laura CW Peeters[1], Marjolein MJ Caron[1], Tim JM Welting[1,2]

[1]Laboratory for Experimental Orthopedics, Department of Orthopedic Surgery, Caphri School for Health and Primary Care, the Netherlands. [2]Laboratory for Experimental Orthopedics, Department of Orthopedic Surgery, Maastricht University Medical Centre, the Netherlands.

INTRODUCTION: Osteoarthritis is driven by a cytokine imbalance within the synovial joint. While the synovial membrane normally nourishes the articular cartilage, it can also release inflammatory factors, such as interleukin-6 (IL-6). IL-6 is a key driver of structural damage and a contributor to OA pain. Transforming growth factor-beta (TGFβ) is highly elevated in OA synovial fluid and has been shown to induce IL-6 in chondrocytes [1-3]. However, it remains unknown whether TGFβ also stimulates IL-6 production in fibroblast-like synoviocytes and, if so, by what molecular mechanisms.

METHODS: Fibroblast-like synoviocytes obtained from patients with end-stage knee OA (K&L 3-4; METC: 2022-3235) were seeded at 30.000 cells/cm^2 and stimulated with varying concentrations of TGFβ3. IL-6 secretion and transcriptomic changes were quantified by ELISA and gene expression analysis, respectively. To identify signalling pathways driving IL-6 expression, cells were treated with inhibitors (SB505124, Oxozeanol, SB203580, Parthenolide). The human FLS cell line SW982 was transduced with lentiviral IL-6 promoter truncations and mutations driving Nanoluciferase expression. These were used to pinpoint key regulatory active sites in the IL-6 promoter. Statistics were performed in GraphPad Prism 10.

RESULTS: While all TGFβ isoforms increased IL-6 secretion by FLS, TGFβ3 was the most potent. This induction was found to be driven at the transcriptional level, showing TGFβ3 dose- and time-dependent increases in both mRNA expression and promoter activity. Mechanistically, we found that TGFβ3 stimulates IL-6 expression through the ALK5-TAK1-p38-NFκB pathway and depends on specific transcription factor-binding sequences in the proximal IL-6 promoter (GRE2, GRE1, IRF1, CREB, C/EBP, and NFκB). Screening 24 end-stage OA FLS donors revealed patient-specific IL-6 responsivity to TGFβ3. While a high TGFβ3 dose (1 ng/ml) universally induced IL-6, at a lower concentration (0.1 ng/ml), stratified FLS donors into distinct responders (n=9) and non-responders (n=15). Finally, analysing synovial fluid samples from 60 knee OA-donors supported an inter-molecular relation between IL-6 and TGFβ3. Distinct high-IL-6/ high-TGFβ3 and low-IL-6/low-TGFβ3 profiles were found, with a strong correlation between TGFβ3 and IL-6 levels in OA synovial fluid (Spearman r=0.9982).

DISCUSSION & CONCLUSIONS: This study demonstrated that TGFβ3 is a driver of synovial inflammation in osteoarthritis by transcriptionally upregulating IL-6 via the ALK5-TAK1-p38-NFκB axis and specific IL-6 promoter transcription factor binding sites. The finding that low TGFβ3 levels distinguish OA FLS into responder and non-responder IL-6 phenotypes is supported by the strong correlation between TGFβ3 and IL-6 concentrations in OA synovial fluid patient samples. Together, this suggests that patient-specific sensitivity to TGFβ signalling determines, at least in part, the state of synovial inflammation. Identifying OA patient-specific molecular signalling thresholds offers a novel concept for future OA patient endotyping and targeted anti-inflammatory interventions.

REFERENCES:

[1] Wiegertjes, R., et al. (2019). TGF-β dampens IL-6 signalling in articular chondrocytes by decreasing IL-6 receptor expression. Osteoarthritis and cartilage, 27(8), 1197-1207.

[2] Punzi, L., et al. (2003). Transforming growth factor-beta levels in synovial fluid of osteoarthritis with or without calcium pyrophosphate dihydrate crystals. *The Journal of Rheumatology*, *30*(2), 420-420.

[3] van der Kraan, P. M. (2022). Inhibition of transforming growth factor-β in osteoarthritis. Discrepancy with reduced TGFβ signalling in normal joints. *Osteoarthritis and Cartilage Open*, *4*(1), 100238.

Impact of TGF-beta and physioxic culture conditions on periosteal chondrogenesis

Matthew Stewart [1], Maja Schlittler[2], Severine Flück[2], Martin Stoddart[2]

[1]*Veterinary Clinical Medicine, University of Illinois, Illinois, USA,* [2]*AO Research Institute, Davos, Switzerland*

INTRODUCTION: Periosteal cells are the primary cell contributors to both cartilaginous and ossified callus formation during fracture repair (1,2). Time course studies have demonstrated that TGF-beta ligands are up-regulated throughout fracture repair (3). Further, chondrogenic differentiation of mesenchymal progenitor cells is stimulated by low oxygen conditions, as occur at vascularly compromised fracture sites (4,5). This study addressed the hypotheses that periosteal cell chondrogenesis is stimulated by (1) TGF-beta supplementation, and (2) physioxic (5%) oxygen culture conditions.

METHODS: Periosteum was collected from the medial tibial and dorsal metacarpal surfaces of healthy, adult horses. Periosteal cells were isolated by collagenase digestion and seeded in low glucose DMEM/10% FBS at low density in physioxic (5% O_2) or normoxic (21% O_2) conditions. Primary cells under both conditions were passaged to P2 then transferred to either non-adherent, aggregate cultures or pellet cultures. Pellet cultures were maintained in chondropermissive (CP) medium (DMEM, sodium pyruvate, L-ascorbic acid 2-phosphate, dexamethasone, ITS+, 1% non-essential amino acids) or chondrogenic (CG) medium (CP medium + 10 ng TGF-b1/ml) for up to 21 days. Aggregate cultures were maintained in CG medium only. At days 7, 14 and 21, samples were collected for measurements of DNA, secreted sGAG, matrix-associated sGAG, cell-associated ALP activity, and histology.

RESULTS: In aggregate cultures, DNA was stable, while CG pellet cultures increased DNA content by approximately 50%. In contrast, pellets in CP medium reduced DNA content by approximately 50% over 21 days. Oxygen concentrations had no effect on DNA content.

Under normoxic conditions, sGAG values in the cell-associated matrix remained stable during the 21 days of culture. In contrast, cultures under physioxic conditions increased matrix-associated sGAG content four-fold; a significant difference at day 21. Matrix-associated sGAG content was negligible in CP pellet cultures under both physioxic and normoxic conditions.

Secreted sGAG concentrations showed a similar profile. Significantly more sGAG was secreted into the medium after 7 days in physioxic conditions, under all three culture conditions. This was also significant at day 14 in CP pellet cultures and at day 21 in CG pellet cultures. Of note, secreted sGAG concentrations were 2- to 6-fold higher in CG medium than CP medium at each time point. The increase in sGAG production under physioxic conditions was impressively reflected in differential alcian blue staining of day 21 cultures (fig 1).

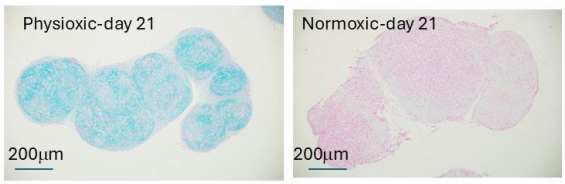

Figure 1: *Alcian blue staining of aggregate cultures maintained under physioxic or normoxic conditions for 21 days.*

In contrast to sGAG synthesis, ALP activity was significantly higher in CG cultures under normoxic conditions, compared to physioxic cultures. ALP activity in CP cultures was consistently lower CG cultures at each time point

DISCUSSION & CONCLUSIONS: This study demonstrates that TGF-beta is necessary for robust periosteal chondrogenesis (Ho1 accepted) and that physioxic conditions dramatically increase proteoglycan synthesis, sGAG deposition in cell-associated matrix and secretion into medium (Ho2 accepted).

Physioxic conditions do appear to delay hypertrophy, based on lower ALP activities at each timepoint. Ongoing gene expression analyses should increase our understanding of the roles of TGF-beta signaling and oxygen concentrations on periosteal chondrogenesis as this relates to early callus formation.

REFERENCES: 1. Wang T et al (2017) J Cell Physiol 232:913–921. **2.** Colnot C (2009) J Bone Miner Res 24:274–2822. **3.** Gerstenfeld LC, et al (2003) J Cell Biochem. 88: 873–8844. **4.** Meyer EG et al (2010) J Biomech 17:43:2516-23 **5.** Henderson JH, et al (2010) Tissue Eng Part A. 16:1585-93.

Optimizing Cartilage Tissue Engineering Using Simulated Microgravity and Pulsed Electromagnetic Fields

A. Stirnimann [1, 2, 3], R. Bischof [1], G. Cerretti [1], L. Beeler [1], M.Egli [1], F. Ille [1]

[1] Lucerne University of Applied Sciences and Arts, School of Engineering and Architecture, Institute of Medical Engineering, Space Biology Group, Hergiswil, Switzerland; [2] Tissue Engineering for Orthopaedics and Mechanobiology, Bone and Joint Program, Department for BioMedical Research (DBMR) of the Medical Faculty, University of Bern, Switzerland.; [3] Graduate School for Cellular and Biomedical Sciences (GCB), Universtiy of Bern, Switzerland.

INTRODUCTION: Articular cartilage (AC) has limited intrinsic repair capacity, and autologous chondrocyte transplantation (ACT) is constrained by chondrocyte dedifferentiation [1,2]. Simulated microgravity (SM) and pulsed electromagnetic fields (PEMF) are promising biophysical stimuli to improve cartilage tissue engineering (TE) outcomes [2,3,4], yet their combined effects remain poorly understood. We hypothesized that cartilage TE cultures yield improved outcomes under combined SMPEMF exposure, as PEMF may enhance proliferation and extracellular matrix (ECM) production, while SM may reduce differentiation changes and promote a more hyaline-like phenotype.

METHODS: Chondrocytes isolated from healthy and degenerated cartilage regions were cultured and exposed to 1g, PEMF, SM, or SMPEMF for 10 days. 10-minute PEMF exposure took place six hours after plating at 4-day intervals. Outcomes included proliferation, ECM formation (*COL2A1/ COL1A1*, *ACAN/ VCAN*, and GAG/ DNA), and differentiation status using combinatorial marker analysis.

RESULTS: SM was the predominant driver of transcriptional changes, inducing upregulation of *SOX9, COL2A1, FGFR3, COL10A1*, and *SPP1*, and downregulation of *COL1A1*. PEMF effects were smaller and primarily detectable in degenerated chondrocytes (increased *SOX9, COL2A1, FGFR3,* and *SPP1* expression). *COL2A1/ COL1A1* and *ACAN/ VCAN* ratios decreased under 1g and PEMF compared to native controls, but were maintained or increased under SM and SMPEMF. GAG/ DNA ratio was preserved under PEMF, increased under SM, and further increased under SMPEMF. Functionally, SM reduced, and PEMF increased proliferation compared to 1g, and their combination partially mitigated the SM-associated proliferation slowdown.

DISCUSSION & CONCLUSIONS: These preliminary data suggest complementary effects of SM and PEMF: SM promotes a more hyaline-like phenotype and enhances ECM accumulation, while PEMF supports proliferation. Combined SMPEMF stimulation may further improve tissue quality while maintaining proliferative capacity. Notably, degenerated chondrocytes were more responsive to PEMF in combinatorial marker analysis, indicating a health-dependent stimulation sensitivity that should be considered in translational cartilage repair strategies.

ACKNOWLEDGEMENTS: We thank Dr. med. Carlo De Simoni and Martina Kunz for patient recruitment and for providing clinical samples to the study. We thank Chris Zumbühl, Gilbert Menth, and Dominique Bovey for developing the PEMF device.

REFERENCES: 1. Mistry H, et al. *Health Technol Assess.* 2017;21:1–294. **2.** Wuest SL, et al. *Int J Mol Sci.* 2018;19:E1289. **3.** Mayer-Wagner S, et al. *Bioelectromagnetics.* 2011;32:283–290. **4.** Stamenković V, Keller G, Nesic D, Cogoli A, Grogan SP. *Tissue Eng Part A*. 2010;16:1729–1736.

Targeting VGLL4 maintains extracellular matrix homeostasis and mitigates osteoarthritis.

Jinlong Suo[1], Duo Wang[2], Jinghui Wang[2], et al.

[1]*Institute of Microsurgery on Extremities, Department of Orthopedic Surgery, Shanghai Sixth People's Hospital Affiliated with Shanghai Jiao Tong University School of Medicine, Shanghai, China.* [2]*CAS Center for Excellence in Molecular Cell Sciences, Shanghai Institute of Biochemistry and Cell Biology, Chinese Academy of Sciences, Shanghai, China*

INTRODUCTION: Osteoarthritis (OA) is a chronic degenerative joint disease characterized by progressive destruction of articular cartilage and disruption of extracellular matrix (ECM) homeostasis[1-3]. However, the molecular mechanisms that preserve hyaline cartilage matrix integrity remain incompletely understood. VGLL4, a transcriptional cofactor in the Hippo pathway[4], was found to be highly expressed in chondrocytes but markedly decreased after cartilage injury and aging, suggesting a potential role in cartilage homeostasis and OA progression[5].

METHODS: Single-cell RNA sequencing datasets from mouse epiphysis and human articular cartilage were analyzed to define VGLL4 expression patterns in chondrocytes. Cartilage injury and aging models were established using destabilization of the medial meniscus (DMM) surgery and aged reporter mice. Chondrocyte-specific *Vgll4* conditional knockout mice were generated to evaluate the *in vivo* role of VGLL4 in cartilage ECM homeostasis and OA progression. Histological staining, immunofluorescence, transcriptomic profiling, in vitro chondrogenic differentiation assays, co-immunoprecipitation, GST pull-down, and structural modeling were performed to investigate the molecular mechanism. Therapeutic efficacy was tested by intra-articular delivery of adeno-associated virus encoding VGLL4 or SMAD3.

RESULTS: VGLL4 was broadly expressed in human and mouse chondrocytes, but its expression significantly declined following cartilage injury and aging. Loss of Vgll4 impaired chondrocyte anabolism, reduced expression of ECM-associated genes including *Col2a1*, *Acan*, *Prg4*, *Eln*, and *Fbln5*, and disrupted collagen and elastin formation. Chondrocyte-specific deletion of *Vgll4* caused ECM disorganization, enhanced hyaline cartilage fibrosis, and exacerbated OA phenotypes after DMM surgery. Mechanistically, VGLL4 did not directly bind SMAD3; instead, TEAD4 mediated formation of a VGLL4–TEAD4–SMAD3 ternary complex that promoted cartilage matrix synthesis. Structural and mutational analyses identified key residues required for the interaction, and mutants defective in complex formation lost their protective effects. Importantly, intra-articular delivery of *Vgll4* or *Smad3* effectively alleviated OA pathology *in vivo*.

DISCUSSION & CONCLUSIONS: These findings identify VGLL4 as a critical regulator of cartilage ECM homeostasis and a suppressor of cartilage fibrosis during OA progression. By forming a functional complex with TEAD4 and SMAD3, VGLL4 promotes anabolic gene expression and preserves hyaline cartilage integrity. Targeting the VGLL4-centered transcriptional complex may therefore represent a promising therapeutic strategy for OA and related cartilage degenerative disorders.

REFERENCES:

1 Tang, S. *et al.* Osteoarthritis. *Nat Rev Dis Primers* **11**, 10, doi:10.1038/s41572-025-00594-6 (2025).

2 Liu, Q. *et al.* DDX5 inhibits hyaline cartilage fibrosis and degradation in osteoarthritis via alternative splicing and G-quadruplex unwinding. *Nat Aging* **4**, 664-680, doi:10.1038/s43587-024-00624-0 (2024).

3 Suo, J. *et al.* Accelerated aging in articular cartilage by ZMPSTE24 deficiency leads to osteoarthritis with impaired metabolic signaling and epigenetic regulation. *Cell Death Dis* **14**, 336, doi:10.1038/s41419-023-05856-3 (2023).

4 Suo, J. *et al.* VGLL4 promotes osteoblast differentiation by antagonizing TEADs-inhibited Runx2 transcription. *Sci Adv* **6**, doi:10.1126/sciadv.aba4147 (2020).

5 Suo, J. *et al.* Targeting VGLL4 maintains extracellular matrix homeostasis and mitigates osteoarthritis in a preclinical model. *Nat Commun* **16**, 9325, doi:10.1038/s41467-025-64361-7 (2025).

Single-cell Analysis identifies Lining Fibroblasts and Macrophages as Key Contributors to Persistent Synovial Inflammation after Cartilage Injury in Experimental Canine Osteoarthritis

M. Teunissen[1,2], F.M. Riemers[1,2], B.A.C. Housmans[3], L. Winkel[2], S.G.M. Plomp[1,2], S.C.M. Mastbergen[2,4], B.P. Meij[1], T.J.M. Welting[3], M.A. Tryfonidou[1,2]

[1]Faculty of Veterinary Medicine, Utrecht University, Utrecht, NL, [2] Regenerative Medicine Center Utrecht, NL, [3] Maastricht University, Maastricht, NL, [4] University Medical Center (UMC) Utrecht, NL

INTRODUCTION: Low-grade synovial inflammation drives osteoarthritis (OA) progression. The mechanisms by which the synovium influences cartilage in OA pathology remain incompletely understood. Experimental animal models with a defined cartilage injury trigger can provide insight into these mechanisms. Using the groove model to induce OA, we performed single-cell transcriptomic analysis of the dog synovial membrane. We examined whether a defined cartilage injury induces persistent synovial alterations and which cell populations and signaling pathways are associated with this response

METHODS: Synovial tissue samples from clinically normal dogs and at 18 and 28 weeks post-OA induction with the groove model (1) were assessed by histology, immunohistochemistry, cytokine/chemokine secretion and in vitro functional assays. Functional analysis was integrated with cellular profiling by single-cell RNA sequencing (scRNA-seq). Phenotypic analyses were performed at 18 and 28 weeks, and scRNA-seq was performed at 28 weeks post-OA.

RESULTS: Histological evaluation confirmed the presence of OA, with higher OARSI scores in OA synovial membranes compared to clinically normal controls at both timepoints. scRNA-seq at 28 weeks identified seven major cell populations in the canine synovial membrane, including sublining fibroblast-like synoviocytes (FLS), lining FLS, endothelial cells, vascular smooth muscle (VSMc), macrophages, and a small unidentified population. Marker gene expression supported these identities, with *THY1, CD34*, and *MFAP5* expressed by sublining FLS; *PRG4, CD55*, and *HBEGF* by lining FLS; *PECAM1* and *VEGFR2* by endothelial cells; *ACTA2* and *MYH11* by VSMc; and *IL1β*, *CD68*, and *CD14* by macrophages. OA and clinically normal cells did not form distinct disease-specific clusters, but OA cells showed population-specific transcriptional changes. This included upregulation of *COL1A1* and *COL3A1* across populations, downregulation of *DDIT4* and *COL28A1* in sublining FLS, and increased *INHBA* expression in lining FLS. Cell–cell communication analysis using CellChat indicated enhanced lining FLS– and macrophage-driven signaling, including activin, IL-1/IL-6, and VEGF signaling. Consistent with these transcriptional and signaling changes, conditioned medium from OA synovium collected from both time points induced catabolic responses in clinically normal chondrocytes, accompanied by persistent activation of JNK/ATF4 and IL6/STAT3 signaling pathways.

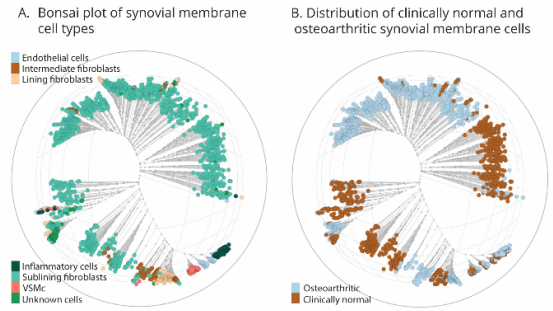

***Fig. 1**: Single-cell transcriptomic landscape of the canine synovial membrane showing (A) the major cell populations identified and (B) the distribution of cells from clinically normal and OA synovial membranes.*

DISCUSSION & CONCLUSIONS: Cartilage injury induces persistent low-grade synovial inflammation in experimental canine OA. Single-cell analysis implicates lining fibroblasts and macrophages as major contributors to this response and highlights activin-related signalling as a new candidate pathway involved in synovitis following cartilage injury.

REFERENCES: (1) doi.org/10.1016/j.jot.2022.09.003

ACKNOWLEDGMENTS: This project was financially supported by NWO Domain AES (P15-23) and the K.F.Heinfonds.

Biomimetic Nucleus Pulposus-on-Chip for Intervertebral Disc Degeneration Research

Parisa Torabi Rahvar[1], Laura González-Blanco[1,2], Benjamin Gantenbein[1,3]

[1]Tissue Engineering for Orthopaedics and Mechanobiology, Department for BioMedical Research (DBMR), Faculty of Medicine, University of Bern, Bern, Switzerland. [2]IDIS (Instituto de Investigación Sanitaria de Santiago), NEIRID Lab, Santiago de Compostela, Spain. [3]Department of Orthopaedic Surgery & Traumatology, Inselspital, Bern University Hospital, Faculty of Medicine, University of Bern, Bern, Switzerland.

INTRODUCTION: Intervertebral disc degeneration is a major contributor to chronic low back pain, impacting hundreds of millions of individuals globally. Degenerative changes often originate in the nucleus pulposus, where a decline in cell density and disruption of the extracellular matrix is observed. Although organ-on-chip technologies present a powerful platform for modeling disc degeneration and testing therapeutics, many existing systems rely on overly simplistic hydrogels that do not adequately reflect the native nucleus pulposus environment. Moreover, replicating the complex mechanical loading and tissue interactions of the intervertebral disc *in vitro* remains a significant challenge.

METHODS: A biomimetic hydrogel composed of hyaluronic acid and collagen type II was functionalized with tyramine groups and enzymatically crosslinked using horseradish peroxidase and hydrogen peroxide. Human nucleus pulposus cells were encapsulated and introduced into a microfluidic chip. Constructs were cultured statically for one week, followed by one week of cyclic mechanical loading. After 14 days, protein content was quantified.

RESULTS: The engineered hydrogel supported uniform cell distribution and stable incorporation within the microfluidic device. Importantly, the constructs withstood repeated dynamic compression without structural damage, indicating adequate mechanical resilience. Protein quantification revealed comparable total protein levels between mechanically stimulated and non-stimulated samples. Furthermore, sufficient protein was recovered from the constructs to enable downstream analytical techniques such as Western blotting.

DISCUSSION & CONCLUSIONS: The developed nucleus pulposus-on-chip model successfully combines biomimetic extracellular matrix components with controlled mechanical stimulation, maintaining structural integrity under dynamic loading. The system enables reliable protein recovery, supporting its use for downstream molecular analyses. No differences in total protein content were observed between conditions, and the platform provides a robust and physiologically relevant environment for studying mechanobiology. Overall, this model represents a promising tool for investigating intervertebral disc degeneration and evaluating potential therapeutic strategies.

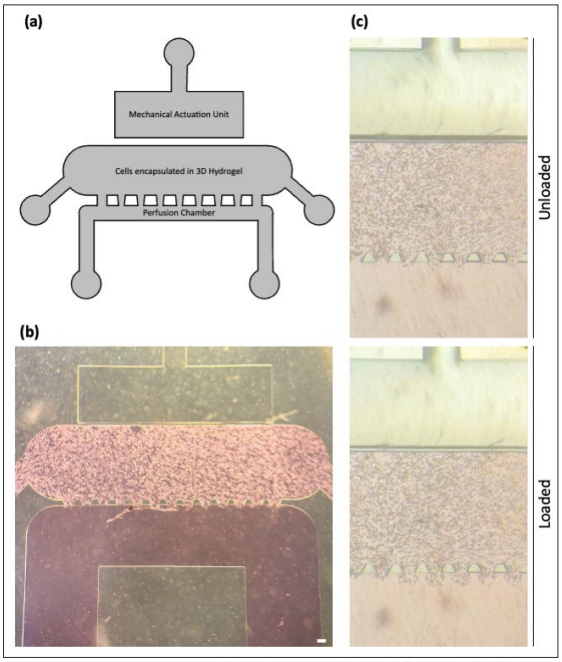

Figure 1. Human nucleus pulposus (hNP) cells encapsulated in a hyaluronic acid (HA)/collagen type II (COL II) hydrogel. **(a)** Schematic illustration of the microfluidic chip design. **(b)** Transmitted light image of the chip loaded with hNP cells at a density of 8×10^6 cells/mL. **(c)** Transmitted light images of the chip under unloaded and loaded conditions. Scale bars: 250 µm.

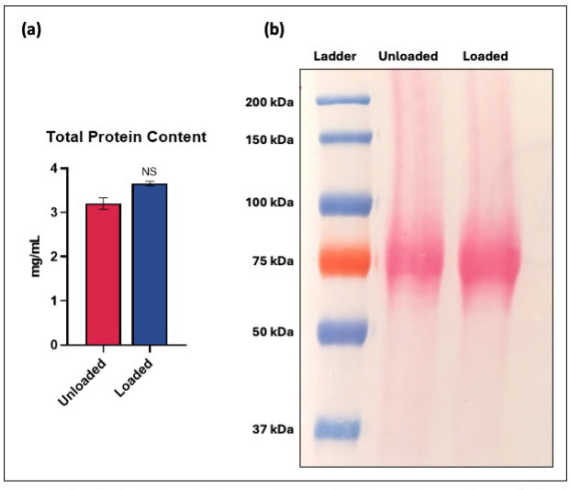

Figure 2. (a) Total protein content measured by Bradford assay (expressed as mg/ml) of cell-encapsulated samples extracted from the chips. (b) Ponceau S staining in nitrocellulose membranes. Data are represented as mean ± SEM from two independent experiments.

Acknowledgment: This work was supported by the SNSF Weave Grant (#320030E_224175) and the DFG (#437213841).

SIRNA–LIPID NANOPARTICLES ENABLE EXTENSIVE GENE SILENCING IN PRIMARY HUMAN MACROPHAGES AND OSTEOARTHRITIC PATIENT-DERIVED CHONDROCYTES

Daniela Pereira de Vasconcelos[1,2] Marina Couto[1], Elise Bonvin[3], Beatriz Ribeiro[1], Bernardo Osório de Valdoleiros[1,4], Antónia Nóbrega[1,2], Ángela Moncada-Pazos[5], Gwendal Guerin[3], Florent Poulhes[3], Sofia Slaoui[3], Olivier Zelphati[3], Manuel Ribeiro da Silva[1,6], Damien Dupin[5], Meriem Lamghari[1]

[1]i3S - Instituto de Investigação e Inovação em Saúde, Universidade do Porto, Portugal, Rua Alfredo Allen, 208. 4200-135 Porto, Portugal. [2]ISEP – Instituto Superior de Engenharia do Porto, Instituto Politécnico do Porto, Rua Dr. António Benardino de Almeida, 431. *4249-015 Porto, Portugal. [3]OZ Biosciences – 163 Avenue de Luminy, Zone Entreprise, Case 922, 13288 Marseille cedex 09, France. [4]FCUP, Faculdade de Ciências da Universidade do Porto, Rua do Campo Alegre s/n, 4169-007 Porto, Portugal. [5]CIDETEC Basque Research & Technology Alliance (BRTA) - Parque Científico y Tecnológico de Gipuzkoa, P° Miramón 191, 20014 Donostia-San Sebastian, Spain. [6]Faculdade de Medicina da Universidade do Porto, Porto, Portugal*

INTRODUCTION: Osteoarthritis (OA) is the most prevalent degenerative joint disease, characterized by painful swelling and irreversible joint damage [1]. Among its key pathogenic drivers, interleukin-1β (IL-1β) and nerve growth factor (NGF) are markedly upregulated in joint tissues and synovial fluid of OA patients, contributing to inflammation and pain [2-3]. Current treatments, including nonsteroidal anti-inflammatory drugs (NSAIDs) and NGF-targeting monoclonal antibodies, provide symptomatic relief but are associated with significant adverse effects, highlighting the urgent need for safer and more effective therapeutic strategies [4]. RNA interference (RNAi) using small interfering RNA (siRNA) offers a highly specific approach to post-transcriptional gene silencing [5]; however, its application in primary cells, particularly macrophages, remains challenging due to their intrinsic resistance to transfection.

METHODS: We present SS23, a novel class of ionizable lipids for lipid nanoparticle (LNP) formulation, enabling efficient siRNA delivery to overcome transfection barriers and reduce OA-related inflammation and pain. LNP uptake and intracellular localization were confirmed in OA patient-derived chondrocytes and primary human macrophages using fluorescent labeling and confocal microscopy. Functional delivery was confirmed by RT-qPCR and cytokine assays following siRNA-mediated silencing of *IL1B* and *NGF*.

RESULTS: We developed a highly effective SS23-based LNP platform for siRNA delivery to primary human cells. These LNPs exhibit optimal physicochemical properties, minimal pro-inflammatory activity, and excellent biocompatibility, while enabling efficient siRNA delivery and robust gene silencing in challenging cell types, including primary human macrophages and OA patient-derived chondrocytes. Functionally, SS23_siIL1B significantly inhibited *IL1B* gene expression in LPS-stimulated macrophages, reducing IL-1β protein availability that could potentially mitigate chondrocyte activation, which may help preserve ECM homeostasis and slow OA progression. Likewise, SS23_siNGF demonstrated safety in OA patient-derived chondrocytes and effectively decreased NGF expression at both transcript and protein levels, addressing pathological innervation associated with OA pain-inflammatory activity.

DISCUSSION & CONCLUSIONS: Together, these findings underscore the therapeutic potential of targeting inflammatory cytokines and neurotrophic factors to modulate OA progression and reduce cartilage degradation. Looking ahead, SS23-LNPs represent a promising platform for RNA-based interventions in early OA. Combining these LNPs with a hydrogel delivery system could enable sustained intra-articular co-delivery of anti-inflammatory siIL1B and pain-modulating siNGF, offering a novel disease-modifying strategy for OA and other inflammatory conditions.

REFERENCES:

[1]Lancet Rheumatol, 5 (2023);[2]Arthritis Rheumatol, 67 (2015); [3] Pharmacol Ther, 211 (2020); [4]Nat Rev Rheumatol, 17 (2021). [5]BMJ, 328 (2004)

The effect of osteoarthritis on the peripheral nerves of the dorsal root ganglions in dogs

P. Virankabutra[1,2], S. Plomp[1,2], M. A. Tryfonidou[1,2], M. Teunissen[1,2]

[1] *Department of Clinical Science, Faculty of Veterinary Medicine, Utrecht University, Utrecht, NL*
[2] *Regenerative Medicine Centre Utrecht, Utrecht, NL*

INTRODUCTION: Osteoarthritis (OA) affects the quality of life of both humans and companion animals. OA pain originates from the affected joint and often persists even after local inflammation has resolved. This implies that additional mechanisms are involved. In this context, the dorsal root ganglion (DRG) modulates pain and plays a key role in chronic OA pain development. Rodent models used to study OA pain do not translate well to human clinical outcomes. In contrast, dogs develop natural OA and better reflect human joint pathology and hence offer a promising approach for translational OA pain research. As a first step, this study aims to explore at which spinal level DRGs are involved in knee OA nociception and determine the DRG molecular responses.

METHODS: DRG from spinal levels L4-S2 were collected from five experimental dogs at 45 weeks follow-up after surgical induction of OA [1], with the contralateral stifle serving as a healthy control. Calcitonin gene-related peptide (CGRP), a marker for nociceptive neurons, and CD271 expression, the low-affinity receptor for neurotrophin nerve growth factor (NGF), were determined using immunohistochemistry (IHC) and analysed using QuPath. Snap-frozen samples were used for RT-qPCR analysis of inflammatory genes (*CCL2*, *VEGFa, IL8, NGF, CD68, CD86,* and *CD163*). Statistical analysis was performed using R.

RESULTS: CGRP and CD271 immunopositive neurons were detected in both OA and control DRGs (Figure 1). The cross-sectional area of CGRP-positive neurons (948 ± 250 µm²) was significantly smaller than that of CGRP-negative neurons (1960 ± 605 µm²; *paired t-test*, $p < 0.01$). No significant differences or interactions in gene expression across treatments or spinal levels were detected by linear-mixed models or Principal component analysis. RT-qPCR analysis showed significantly lower expression of *NGF* in OA vs healthy control group ($p = 0.046$).

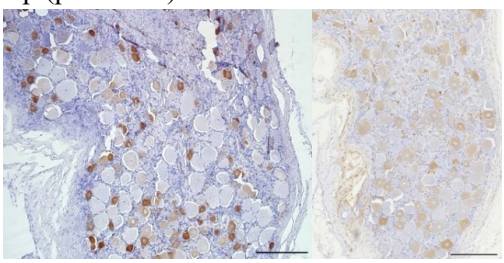

Figure 1: CGRP (left) and CD271 (right) expression in the same L6 OA DRG. Scale bar = 1000 µm.

DISCUSSION: CGRP and CD271 show a similar staining profile to that reported in human and rat DRG pain studies [2]. The absence of significant differences between OA and normal DRGs could be explained by the mild degree of OA created by the modified groove model [1] not being severe or chronic enough to elicit detectable structural and molecular changes at the DRG level. Additional limitations were the small number of samples of each spinal level, several notable outliers in RT-qPCR results, and challenging data analysis and conclusions. While the analysis could not identify the DRG levels involved in knee OA, we proposed that the responsible DRG levels are L5 to L7, based on the anatomical sensory innervation.

ACKNOWLEDGEMENT: This study is part of the Ombion Centre for Animal-free Biomedical Translation (CPBT) programme in the Netherlands that is financed by a National Growth Fund (NGFCPBT241).

REFERENCES:

1. 10.3390/biomedicines13040913
2. 10.1523/JNEUROSCI.0899-17.2017

INTERPLAY BETWEEN CANONICAL WNT SIGNALING AND A5B1 INTEGRINS MODULATES MECHANORESPONSE IN HUMAN ARTICULAR CARTILAGE

Nuria Viudes-Sarrion1,2 · Rocío Castro-Viñuelas2 · Nele Vaes3, Emma Blain4,5, Silvia Monteagudo1, Rik Lories6,1, Ilse Jonkers2

1 Skeletal Biology and Engineering Research Center, KU Leuven, Leuven, Belgium

2 Human Movement Biomechanics Research Group, KU Leuven, Leuven, Belgium

3 Biomechanics Section, Department of Mechanical Engineering, KU Leuven, Leuven, Belgium

4 Biomedicine Division, School of Biosciences, Cardiff University, Cardiff, UK.

5 Biomechanics and Bioengineering Centre Versus Arthritis, School of Biosciences, Cardiff University, Cardiff, UK.

6 Development & Regeneration, KU Leuven, Leuven, Belgium

Introduction: Mechanical cues are essential for maintaining cartilage function, yet how they integrate with molecular pathways dysregulated in osteoarthritis (OA) remains poorly defined in human tissue. Canonical Wnt signalling influences cartilage biology and cell–matrix interactions, but its role in integrin-dependent mechanoregulation in human cartilage is not fully understood. This study aimed to determine how Wnt activation affects chondrocyte responses to physiological mechanical loading, with a focus on α5β1integrin and cytoskeletal organisation.

Methods: Human cartilage explants from non-OA and OA donors were subjected to short-term physiological cyclic compression. Canonical Wnt signalling was activated with CHIR99021, and integrin-mediated adhesion was modulated using the α5β1 blocking peptide ATN-161 during loading. Chondrocyte responses were assessed by analysing mechanoresponsive and matrix-related gene expression, α5β1 complex formation via proximity ligation assay and actin cytoskeletal organisation by confocal microscopy.

Results: OA chondrocytes exhibited a distinct integrin profile, characterised by increased *ITGA5* and *ITGB1* but reduced *ITGA10* expression. In non-OA cartilage, canonical Wnt activation increased *ITGB1* expression and α5β1 integrin complex formation, while mechanical loading further enhanced *ITGA5* and *ITGB1* transcription under Wnt-activated conditions. Under control conditions, loading induced mechanoresponsive and anabolic gene expression in non-OA cartilage; these responses were attenuated following Wnt-activation and partially restored by α5β1 blockade. Mechanical loading induced F-actin reorganization toward a more cortical distribution across cartilage zones, irrespective of disease status or treatment. Wnt activation did not result in distinct cytoskeletal phenotypes under load, and load-induced actin remodelling was comparable between groups.

Discussion & Conclusion: These findings identify 1integrin as a key mediator linking canonical Wnt signalling to altered chondrocyte mechanoresponsiveness in human cartilage. While mechanical loading consistently induced cortical F-actin reorganization, Wnt-associated changes in load responsiveness arose primarily from integrin-dependent mechanisms rather than major alterations in actin organization**.** This study highlights the complexity of cartilage mechanoregulation and identifies integrin-mediated signaling as important contributors to canonical Wnt-driven alterations in load responsiveness relevant to OA.

Native extracellular vesicles derived from notochordal cell matrix contribute to a healthy nucleus pulposus cell state

Chantal Voskamp[1], Noa Rijneveld[1], Daniele Corraini[1], Marca H. M. Wauben[2], Marianna A. Tryfonidou[1]

[1]Department of Clinical Sciences, Faculty of Veterinary Medicine, Utrecht University, Utrecht, the Netherlands, [2]Department of Biomolecular Health Sciences, Faculty of Veterinary Medicine, Utrecht University, Utrecht, the Netherlands

INTRODUCTION: Notochordal cells (NC) exert regenerative effects on the smaller non-vacuolated nucleus pulposus cells (NPCs) and have been shown to partly mediate this via extracellular vesicles (EVs). Extraction of NC-EVs from conditioned medium requires *ex vivo* culturing of NC-rich NP tissue. However, *ex vivo* culturing of unconfined healthy NP tissue results in tissue swelling, an increased inflammatory response and glycosaminoglycan (GAG) release. The function of NC-EVs collected from native tissue is not yet studied. The aim of this study is to determine how native NC-EVs can influence the functional state of NPCs.

METHODS: NC-EVs were isolated from frozen NC-rich matrix of 3-months-old porcine spines, using enzymatic digestion with hyaluronidase (HYase) and sequential centrifugation for purification (N=3). To assess EV-specific effects two different isolation methods were used: NC-EVs were either further purified using an OptiPrep™ density gradient (ODG) in combination with size exclusion chromatography (SEC) or SEC alone. NC-EVs were analyzed by Nanoparticle Tracking Analysis (NTA) to determine particle size and concentration. To assess the regenerative potential, NC-EVs and their respective NC-EV-depleted control were tested on dog NPC pellets (derived from mild degenerated NP tissue, N=3) for 13 days and analyzed using histological and biochemical assays.

RESULTS: HYase treatment increased the efficiency of NC-EV isolation from the NC matrix by 8.7-fold, indicating that native NC-EVs interact with the hyaluronic acid-rich extracellular matrix of the NP tissue. The number of particles derived per gram NP tissue detected in the SEC samples was on average 10.2-fold higher compared to the ODG+SEC samples, determined with NTA. Conversely, the SEC isolation method co-isolated 86.6-fold more glycosaminoglycans (GAG) compared to the ODG+SEC method, which could mask EV-specific signals in downstream analysis. Based on the reduced GAG co-isolation, ODG+SEC was selected for all subsequent functional analysis to determine EV-specific effects on NPCs. NC-EVs increased total GAG production 4.2-fold in NPC pellets compared to EV-depleted controls (**Figure 1**). This effect was primarily driven by an increase in GAG release from NPC pellets. Interestingly, NC-EV treated NPCs showed a slight increase (13%) in the number of TIE2 positive cells (marker for progenitor cells) and reduction (10%) of CAV1 (NC/NPC marker) expression compared to EV-depleted controls, while TBXT (NC/NPC marker) expression remained unchanged.

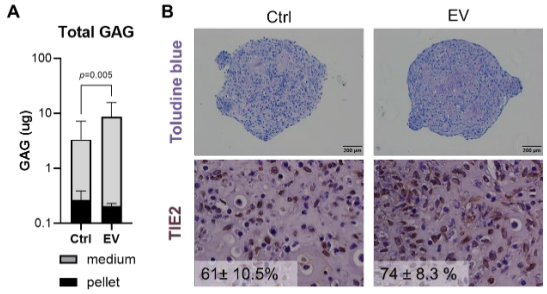

Figure 1: Total GAG production (A) and (immuno)histological for GAGs (Toludine Blue) or TIE2 of dog NPCs after 13 days of ODG+SEC isolated EVs (N=3) and their respective EV-depleted control (Ctrl).

DISCUSSION & CONCLUSIONS: This study highlight that native NC-EVs are present in NC-matrix and contribute to an increase in GAG production. Moreover, TIE2 and CAV1 showed divergent expression patterns after stimulation with NC-EVs. Considering that with increasing degeneration NPC show reduced TIE2 and elevated CAV1 levels (1), it is tempting to hypothesize that native NC-EVs support healthy NPC function. Current studies focus expanding the set of cellular markers, studying the role of native NC-EVs during inflammation, and aim to decode their protein composition.

ACKNOWLEDGEMENTS: NC-CHOICE project (file number 19251). Dutch Technology Foundation STW - Netherlands Organization for Scientific Research (NWO).

REFERENCES: (1) Bach FC, et al. Arthritis Res Ther. 2016 Mar 3;18:59. doi: 10.1186/s13075-016-0960-y.

Notochordal cell-derived extracellular vesicles : a functional protein corona affecting regenerative signaling pathways

Chantal Voskamp[1†], Josette C. van Maanen[1†], Frank M. Riemers[1], Harmjan R. Vos[2], Anouk Eversdijk[1], Marije Kleinjan[3], Martijn J. C. van Herwijnen[3], Frances C. Bach[1], Tim J.M. Welting[4,5], Christine L. Le Maitre[6], Guus G.H. van den Akker[4], Marca H.M. Wauben[3], M.A. Tryfonidou[1]

[1]Department of Clinical Sciences, Faculty of Veterinary Medicine, Utrecht University, Utrecht, the Netherlands, [2]Center for Molecular Medicine, University Medical Center Utrecht, Utrecht University, Oncode Institute, Utrecht, The Netherlands, [3]Department of Biomolecular Health Sciences, Faculty of Veterinary Medicine, Utrecht University, Utrecht, the Netherlands, [4]Laboratory for Experimental Orthopedics, Department of Orthopedic Surgery, Maastricht University, Maastricht, the Netherland [5]Division of Clinical Medicine, Faculty of Health, University of Sheffield, Sheffield, United Kingdom, [†]Equally contributed to this study

INTRODUCTION: Extracellular vesicles (EVs) have emerged as a promising cell-free regenerative therapy for intervertebral disc degeneration because they can modulate inflammation and matrix production. Especially EVs derived from notochordal cells (NC-EVs) are increasingly recognized for their regenerative capacity. The aim of this study is to study the modulatory role of the NC-EV associated proteome in the context of intervertebral disc regeneration.

METHODS: NC-EVs were isolated from conditioned medium from porcine NC-rich tissue (N=7) using differential centrifugation, size exclusion chromatography and sucrose density gradients. To decode the full protein spectrum, the EV fraction was subjected to mass spectrometry (LC-MS/MS). To test bioactivity of selected signaling nodes, functional analysis was done using a chondrocyte-like reporter cell line with transcriptional binding elements for SMAD (SBE), TCF/LEF and NF-κB, driving luciferase reporter gene expression. To functionally assess the protein corona on the EV surface, NC-EVs were purified using an OptiPrep™ density gradient and hyaluronidase was used to further strip away part of the glycosaminoglycan-rich biomolecular corona.

RESULTS: Functional proteomic analysis on NC-EVs identified >4,000 unique proteins associated with NC-EVs, a large number of matrisome proteins and proteins around critical nodes in multiple signaling pathways. The NC-EV cargo affected specific signaling cascades involved in intervertebral disc regeneration, including TGFβ, WNT and IL1β signaling. These three signaling pathways were functionally analyzed with chondrocyte-like reporter cells using transcription factor response elements (SBE for TGFβ/SMAD signaling, TCF/LEF for WNT activity and NF-κB for IL1β activity). These reporters showed respectively that NC-EVs activate SBE with 2-fold, had no effect on TCF/LEF activity, and inactivate NF-κB with 50% upon IL1β stimulation. The effects of the NC-EVs were comparable to NC-EV depleted controls, indicating that the soluble proteins contributing to the biomolecular corona of the NC-EVs play a profound role in modulating signaling. This was further supported by the fact that treatment of NC-EVs with hyaluronidase resulted in a significant functional difference between NC-EVs and NC-EV depleted controls for both SBE (p<0.0001) and NF-κB (p=0.0315; **Figure 1**). These results show that NC-EVs outperformed their EV-depleted controls in NF-κB pathway reduction, while EV-depleted controls outperformed NC-EVs for the SBE activation, the latter indicating SMAD3/4 binding to SBE, commonly mediating TGFβ signaling.

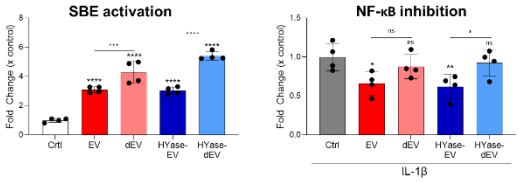

Figure 1. Reporter activity of SW1353 cell lines upon NC-EVs isolated with OptiPrep™ density gradient, size exclusion chromatography and hyaluronidase (HYase).

DISCUSSION & CONCLUSIONS: This study reports the first NC-EV functional proteomics with downstream validation. Targeted reporter assays demonstrate EV-mediated regenerative effects at the level of TGF and NF-κB signaling, and illustrates that the adsorbed proteins on the NC-EV surface contribute to their functionality in NF-κB inhibition and SMAD3/4 activation.

ACKNOWLEDGEMENTS: This work was supported by Nederlandse Organisatie voor Wetenschappelijk Onderzoek, 19251 and the Horizon 2020 Framework Programme, 825925.

Large-scale proteomic / metabolomic analyses reveal new pathophysiological insights between Sleep behaviours and Osteoarthritis risk

Jiajun Wang[1], Qiang Tong[1], Rui Shao[1], Hengfeng Yuan[1]

[1]*1Institute of Microsurgery on Extremities, Department of Orthopedic Surgery, Shanghai Sixth People's Hospital Affliated with Shanghai Jiao Tong University School of Medicine, Shanghai, China.*

INTRODUCTION: Osteoarthritis (OA) is a leading cause of global disability, affecting over 500 million adults and imposing a substantial health burden through chronic pain and reduced quality of life. Sleep disturbances can trigger oxidative stress and pro-inflammatory activation—key processes in OA pathogenesis. This study aims to identify the core molecular mediators linking sleep disturbances to incident OA, offering new pathophysiological insights and a foundation for early risk stratification and precision prevention.

METHODS: Using data from the UK Biobank, this study integrated epidemiological, proteomic, and metabolomic analyses to investigate sleep behaviors and incident osteoarthritis (OA) of the knee, hip, and hand. After exclusion, 389,494 individuals were included in the primary analysis, with sub-cohorts for proteomics (~50,000) and metabolomic (~470,000) profiling. Sleep behaviors were quantified using a risk score (0-6). Multivariable Cox regression, restricted cubic spline (RCS) analyses, and a two-step mediation framework were applied to assess associations and identify molecular mediators. Finally, gradient boosting models (LightGBM) evaluated the predictive utility of these mediators for OA over 5- and 10-year intervals.

RESULTS: Among 389,494 UK Biobank participants (mean age: 57.8 years; 55.21% female) followed for a median of 13–14 years, 25,038 knee OA, 16,409 hip, and 4,026 hand OA cases were documented. Adverse sleep behaviors were associated with site-specific OA risk in a linear dose-response manner ($P<0.001$). Integrative multi-omics analyses revealed that adverse sleep promotes OA pathogenesis through immune-inflammatory activation and metabolic dysregulation, with CRTAC1 and COL9A1 mediating sleep-OA associations. Machine learning models incorporating proteomic biomarkers enabled effective 5- and 10-year OA prediction.

DISCUSSION & CONCLUSIONS: Our findings reveal site-specific effects of unhealthy sleep behaviors on osteoarthritis (OA), with sleep apnea (SA), sleeplessness, short sleep, and difficulty waking as stable risk factors for knee, hip, and hand OA. A "chronotype paradox" emerged: morningness predicted incident OA despite showing a "healthy" molecular profile, suggesting non-proteomic/metabolic pathways are involved. Shared biomarkers like LEP, FABP4 and M-HDL-PL-pct highlight core sleep-joint nodes. Knee and hip OA shared molecular features distinct from hand OA. Mediating proteins (e.g., CRTAC1, COL9A1, AMBP) outperformed metabolites in explaining behavioral links and improved predictive models, underscoring their translational value.

Oxysterol undersulfation promotes osteoarthritis by fueling chondrocyte lipid accumulation

Huanbo Wang[1], Bowei Ni[1], Liu Yang[1], Chao Zheng[1]

[1]*Institute of Orthopedic Surgery, Xijing Hospital, Fourth Military Medical University, Xi'an, China.*

INTRODUCTION: Metabolic abnormalities of chondrocytes are strongly linked to osteoarthritis (OA) by recent studies [1-3]. However, the predominant focus has been on metabolism-regulatory genes and proteins, leaving regulatory metabolites themselves largely unexplored. We investigated sulfation, a largely unexplored chemical modification of lipid metabolites [4], in driving pathogenic lipid synthesis in OA chondrocytes.

METHODS: Genetic models and sulfotransferase screening were employed to identify sulfation's regulatory role and key substrates. Transcriptomics, molecular docking, and peptide-centric local stability assays were performed to elucidate mechanisms. Directionally concordant findings were validated in human using GWAS summary and single-cell RNA sequencing datasets and clinical samples.

RESULTS: Halting sulfation via genetic ablation of the sulfate transporter SLC26A2 induced chondrocyte lipid accumulation and cartilage damage. Under global sulfation deficiency, 25-hydroxycholesterol (25HC) emerged as the critical substrate: ablating its sulfotransferase SULT2B1 recapitulated, while supplying its sulfated derivative (25HC3S) ameliorated, the cartilage damage of Slc26a2 knockout mice. Transcriptomics revealed 25HC and 25HC3S oppositely regulated key genes in fatty acid and steroid biosynthesis, and approximately half of 25HC-upregulated genes were transcriptional targets of Liver X Receptor (LXR). Mechanistically, 25HC activated LXR ligand-dependently to potentiate lipid synthesis, while 25HC3S deactivated LXR by altering its nuclear localization and promoting nucleolar sequestration, thus mitigating chondrocyte lipid accumulation and cartilage damage. Moreover, human studies linked genetic variants in 25HC sulfation pathways to OA risk, with concomitantly reduced SLC26A2 expression and increased lipid accumulation in OA cartilage.

DISCUSSION & CONCLUSIONS: These findings support an "oxysterol undersulfation" model wherein OA disrupts oxysterol sulfation, unleashing nuclear oxysterol receptor activation to drive pathogenic chondrocyte lipid synthesis, and highlight the therapeutic potential of 25HC3S against OA.

REFERENCES:

[1] Bliddal H, Bays H, Czernichow S, Uddén Hemmingsson J, Hjelmesæth J et al: Once-Weekly Semaglutide in Persons with Obesity and Knee Osteoarthritis. N Engl J Med 2024, 391(17):1573-1583.

[2] Collins DH, Ghadially FN, Meachim G: INTRA-CELLULAR LIPIDS OF CARTILAGE. Ann Rheum Dis 1965, 24(2):123-135.

[3] Park S, Baek IJ, Ryu JH, Chun CH, Jin EJ: PPARα-ACOT12 axis is responsible for maintaining cartilage homeostasis through modulating de novo lipogenesis. Nat Commun 2022, 13(1):3.

[4] Mueller JW, Gilligan LC, Idkowiak J, Arlt W, Foster PA: The Regulation of Steroid Action by Sulfation and Desulfation. Endocr Rev 2015, 36(5):526-563.

Immediate-early dynamics of lineage-commitment, mechanotransductive and circadian gene expression in human MSCs in response to a single mechanical loading event

Katrin S. Wendrich[1], Laura Mecchi[1], Qing-Jun Meng[2], Martin J. Stoddart[1]

[1]Regenerative Orthopaedics, AO Research Institute Davos, Clavadelerstrasse 8, 7270 Davos Platz, Switzerland. [2]Division of Cell Matrix Biology and Regenerative Medicine, School of Biological Sciences, Faculty of Biology, Medicine and Health, University of Manchester, UK.

INTRODUCTION: Osteoarthritis (OA) affects millions globally and currently lacks curative treatment. Microfracture surgery (MF) can be used to treat localised cartilage defects due to OA. MF relies on the recruitment of mesenchymal stem cells (MSCs) to regenerate cartilage. However, the resulting repair tissue often lacks native functionality. Mechanical loading during postoperative rehabilitation is a critical but insufficiently understood regulator of MSC fate. Loading can mechanically activate latent TGFβ, initiate downstream signalling through the TGFβ pathway and thus induce MSC chondrogenesis. At the same time, it serves as a zeitgeber for the cartilage clock. Yet, the immediate-early responses of naïve MSCs to physiologically relevant loading remain unclear. This study aimed to define how a single mechanical stimulus of different durations primes hMSCs toward chondrogenesis and modulates cell fate-determining, mechanotransductive, TGFβ-signalling and circadian gene expression over time.

METHODS: Primary hMSCs were encapsulated in 3D GelMA hydrogels and exposed to no load or a single multiaxial loading event (10% static + 10% dynamic compression and shear) for either 1h or 2h. Time point 0h was defined as load cessation. Samples were collected at 0, 1, 2, 4, and 6h post-load and analysed for lineage-related, mechanoresponsive, TGFβ-pathway and circadian clock gene expression using RT-qPCR. Unloaded free-swelling controls and TGFβ-treated positive controls were included.

RESULTS: Mechanical loading induced rapid and load duration-dependent transcriptional responses. **Lineage determinants:** After 2h of load, SOX9, RUNX2 and PPARG were transiently upregulated within 1h post-load, whereas 1h of load produced weaker and no significant changes. **Cartilage matrix markers:** Functional genes COL6A1, COMP and PRG4 showed delayed but stronger induction following 2h versus 1h of loading, with PRG4 elevated from 1-6 h post-load. Contrasting, ACAN was 3.5-fold induced 4h post-load after only 1h of loading. **Fibrotic/hypertrophic markers:** Only 2h of loading induced early, transient upregulation of MMP13 and COL1A1, whereas 1h of load did not increase detrimental markers. **Mechanoresponsive genes:** PIEZO1, TRPV4, and TAK1 were differentially regulated by load duration, with peaks at 1-2 h post-2h-load and return to baseline by 6h, and TAK1 upregulation 4h post-1h-load. **TGFβ-pathway modulation:** Load altered receptor expression and ratios, particularly ACVRL1/TGFBR2 and TGFBR1/TGFBR2, with effects dependent on load duration and resolving by 6h. **Circadian clock genes:** Multiple core clock genes (CRY1/2, BMAL1, NPAS2, DBP) were load-responsive, displaying distinct timing and load-duration dependence, indicating that a single mechanical event can act as a zeitgeber for hMSCs.

DISCUSSION & CONCLUSIONS: Mechanical loading elicited rapid and transient transcriptional changes across lineage-associated, mechanotransductive, TGFβ-related, and circadian pathways in naïve hMSCs. These responses were influenced by load duration, with 2h of loading generally producing more pronounced and coordinated gene regulation than 1h. While longer loading activated chondrogenic and mechanosensitive markers more robustly, it also induced short-lived increases in hypertrophic or fibrotic genes, suggesting that extended load may carry both beneficial and undesirable stimuli. The identification of distinct temporal expression peaks, especially within the first 1-4 h post-load, highlights the importance of precise sampling windows in mechanobiology studies. Load-responsive modulation of TGFβ-receptor ratios and circadian components indicates that mechanical cues may transiently alter hMSC sensitivity to growth-factor and timekeeping pathways. Overall, these findings suggest that a single mechanical stimulus can prime early hMSC fate decisions, but that the magnitude and specificity of these effects depend on load duration. Fine-tuning loading parameters may thus help optimise mechanically driven cartilage repair strategies.

Differences between histochemical glycosaminoglycan staining methods for cartilage tissues

R.V. Wolff[1], N. Kops[1], E. Salzer[1], R. Narcisi[1], M.S.B. Rathnayake[2], K.S. Stok[2], G.J.V.M. van Osch[1]

[1] Department of Orthopaedics & Sports Medicine, Erasmus MC, Rotterdam, the Netherlands.

[2] Department of Biomedical Engineering, The University of Melbourne, Parkville, Australia.

INTRODUCTION: Matrix composition is closely linked to cartilage function in health and disease. Therefore, glycosaminoglycans (GAG) are a key component of the extracellular matrix (ECM) to assess during histological evaluation. Currently, there is no gold standard for GAG staining. This study provides a comparative analysis of the three commonly used histological staining methods on native and degraded cartilage, aiming to enhance understanding of their utility in cartilage research.

METHODS: Native articular, auricular and nasal septum cartilage explants were obtained from calves aged 8 months or less. Additionally, articular cartilage explants were treated with hyaluronidase to remove GAG (200 and 2,000 U/ml) and cultured for one week. Consecutive sections (6 µm) were stained with alcian blue (AB) (1% w/v in 3% acetic acid, pH 2.5) [1], Safranin O (SO) (0.1% w/v) [2], or thionine (TH) (0.04% w/v in sodium acetate) [3], for 10, 12 and 5 minutes, respectively. Sections stained with AB were counterstained with nuclear fast red (1 minute), SO with light green (0.1% w/v for 8 minutes) and TH were not counterstained.

RESULTS: The three staining methods resulted in three different staining patterns (Fig 1). Native (untreated) articular cartilage showed increasing GAG content towards the subchondral bone for SO and TH, but not AB (Fig 1). Auricular cartilage stained with SO or TH showed most intense staining in the centre, and AB at the edges of the cartilage (not shown). Nasal cartilage stained with SO or TH showed a homogeneous GAG distribution throughout the ECM, whereas AB-stained samples showed intense staining only near the perichondrium (not shown). These differences for articular cartilage were further exaggerated after enzymatic degradation of the ECM. With SO, most GAG loss was localized in the superficial to middle zones, while AB and TH indicated only partial loss of GAG (Fig 1). Further degradation of the ECM (2,000 U/ml) showed faint staining throughout the ECM for AB and TH, but SO only stained GAG pericellular (not shown).

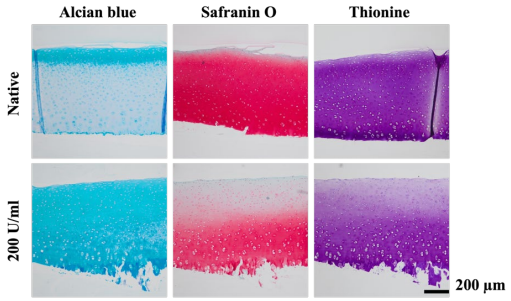

Fig. 1: Representative images of stained bovine articular cartilage samples (native and treated).

DISCUSSION & CONCLUSIONS: Observed differences between three commonly used GAG staining methods are, to the best of our knowledge, not previously reported in a systematic way. All dyes are cationic and electrostatically driven towards the negatively charged GAG molecules. Since the molecular weight of AB is ~1,300 g/mol vs. ~350 g/mol for SO and ~265 g/mol for TH, we hypothesize that this difference in size plays an important role in the staining observed. This is possibly due to differences in molecular transport and binding dynamics/mechanisms. The staining pattern of AB in native cartilage does not correctly reflect localization of GAG based on literature, and SO seems to lack sensitivity when GAG content is low. The staining pattern of TH balances these aspects, compared to AB and SO, reflecting GAG localisation in native cartilage and providing sensitivity when GAG content is low. These findings highlight the need for caution when assessing cartilage, native or tissue engineered, using AB or SO as a staining method, as it may lead to misinterpretations.

ACKNOWLEDGEMENTS: Flagship Healthy Joints-Convergence Health and Technology and the LoaD project (# NWA1389.20.009) of the Dutch Research Council (NWO).

REFERENCES: 1. Arunachalam, et al., *Springer Protocols Handbooks,* (2025). 2. Mankin, et al., *J Bone Joint Surg Am,* (1971). 3. Bulstra, et al., *Biotech Histochem,* (1993).

Inflammatory cytokines alter the response to physiological loading in osteochondral explants

R.V. Wolff[1], E. Salzer[1], N. Kops[1], R. Narcisi[1], G.J.V.M. van Osch[1]
[1] Dept. of Orthopaedics & Sports Medicine, Erasmus MC, Rotterdam, the Netherlands.

INTRODUCTION: The importance of physiological mechanical stimulation for maintaining cartilage health is well known. Inflammation is a key contributor to the onset and progression of osteoarthritis (OA). However, the effects of inflammation on the response of cartilage to mechanical cues remain poorly understood. In this study, we investigate whether pro-inflammatory cytokines modify the chondrocytes' response to simulated physiological loading.

METHODS: Bovine osteochondral explants were harvested from the proximal metacarpophalangeal joint. The explants were cultured for 48 hours, during which they were exposed to a combination of cytokines (IFNγ, TNF and IL1β) at 10, 1 and 0.1 ng/ml, respectively, or a 10x higher dose for all cytokines. Cytokines were dissolved in ITS-supplemented medium, and medium was renewed after 24 hours. Explants were loaded daily with simulated physiological intermittent loading: 15% compression at 1 Hz, 3 cycles of 30 min on/off. The experiment was repeated 3 times (n=3 per experiment).

RESULTS: Simulated physiological loading showed reductions in gene expression of *ACAN* (aggrecan, Fig. 1), *ADAMTS5* (aggrecanase, Fig. 1), and *MMP13* (collagenase, not shown) in healthy control explants. In an inflamed environment, however, expression of *ACAN* and *ADAMTS5* were no longer influenced by mechanical loading (Fig. 1). Conversely, *NOS2* expression in healthy control explants was not influenced by loading (Fig. 1) and significantly increased when explants were loaded in an inflamed environment. Showing an additional effect on top of the dose-response to cytokines alone (Fig. 1).

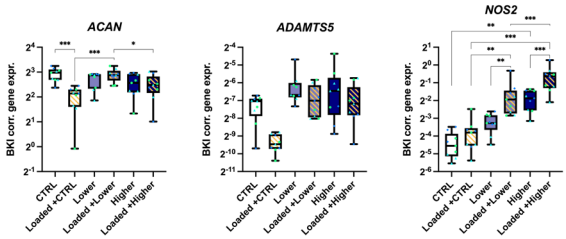

*Fig. 1: Response to loading for ACAN, ADAMTS5, and NOS2 was altered in an inflammatory environment. Linear Mixed Model with Bonferroni correction: * $p < 0.05$, ** $p < 0.01$, *** $p < 0.001$.*

DISCUSSION & CONCLUSIONS: The effect of simulated physiological compression on osteochondral explants changes in the presence of pro-inflammatory cytokines. The observed response of healthy cartilage to loading is a reduction of expression levels of anabolic and catabolic matrix related genes. Interestingly, this response disappears in inflammatory conditions. The upregulation of *NOS2*, induced by cytokines, is even increased by loading, suggesting that loading might further stimulate the catabolic response in an inflamed environment. The altered mechano-inflammatory response could arise from changes in sensitivity of the regular mechanotransduction pathways, and/or interference with the inflammatory pathways (and downstream effectors). This study used one loading regime on healthy cartilage. Ongoing work within our group includes the effect of combinations of compression and shear, and the influence of cartilage degeneration status to gain more insight in the effect of loading on cartilage in a joint with inflammation.

ACKNOWLEDGEMENTS: Flagship Healthy Joints-Convergence Health and Technology and the LoaD project (# NWA1389.20.009) of the Dutch Research Council (NWO).

Decellularized Extracellular Matrix Particle-Based Biomimetic Hydrogel Preserves Cartilage Matrix Components and Attenuates Inflammation in a Human Osteochondral Explant Osteoarthritis Model

Jiangyao Xu [1, 2], Matteo D'Este [1], Mauro Alini [1], Sibylle Grad [1], Jeroen Geurts [2], Zhen Li [1 *]

[1] *AO Research Institute Davos, Davos Platz, Switzerland.* [2] *Lausanne University Hospital, Lausanne, Switzerland.*

Introduction: This study aimed to investigate the reparative and regulatory effects of a biomimetic hydrogel incorporating decellularized extracellular matrix (dECM) particles in a human osteochondral explant model of osteoarthritis (OA).

Methods: dECM particles were prepared from bovine cartilage using a detergent-free protocol. Human osteochondral explants (8 mm diameter, 5 mm height) were harvested with general consent from patients undergoing total hip arthroplasty. An OA model was established by stimulation with inflammatory cytokines (1 ng/mL IL1β+TNFα) for 7 days. Chondral defects (5 mm diameter, 2 mm height) were made, a tyramine-modified hyaluronan (THA) hydrogel loaded with P3 human chondrocytes and dECM particles was implanted, and the osteochondral explants cultured under free-swelling conditions for 7 days. In the third week, mechanical loading (dynamic axial compression at 0.1-0.2 mm, and ball oscillation at ±25°, 0.5 Hz for 1 hour/day) was applied for 7 days. Four experimental groups were designed: (1) THA hydrogel group; (2) THA-dECM composite hydrogel group; (3) OA-THA group; and (4) OA-THA-dECM group. N=3-5 donors, n=5-9 explants.

Results: In comparison with the control group, IL-6 and IL-8 protein release into conditioned medium were markedly increased in the OA group, indicating that stimulation with IL-1β and TNF-α successfully induced an inflammatory response. ELISA results further indicated that under inflammatory OA condition, the THA-dECM group significantly reduced IL-6 release in the conditioned medium compared with the THA group.
On day 21 in the OA model, compared with the THA group, the THA-dECM group exhibited significantly upregulated expression of COL2, PRG4, and Procr (chondroprogenitor marker), along with downregulated expression of IL-8 in implanted human chondrocytes. Furthermore, under OA conditions at day 21, THA-dECM hydrogels significantly suppressed MMP-3 expression in the surrounding cartilage tissue compared with the THA group.
Biochemical analyses demonstrated that under inflammatory OA conditions, dECM particles retained abundant glycosaminoglycans (GAGs) and collagen (COL) within the chondral defect. Safranin O staining demonstrated preserved proteoglycan (PG) retention in the dECM group under inflammatory conditions. Immuno-histochemical staining further indicated that the dECM group exhibited higher COL2 expression in both the hydrogel and the adjacent cartilage tissue compared with the THA group. In contrast, COL1 expression showed no increase (Fig. 1).

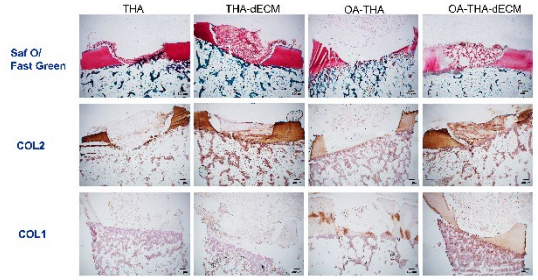

Figure 1. *Safranin O/Fast Green and IHC staining of hydrogel-chondrocytes construct implanted human osteochondral explant after 21 days of culture under multi-axis mechanical stimulation, bar=500μm.*

Metabolic labelling assays showed that at day 21, compared with the THA group, the THA-dECM group significantly enhanced GAG synthesis by chondrocytes within the hydrogel under both control and OA conditions.

Conclusion: This study is the first to apply a dECM-based hydrogel in a human osteochondral explant model of osteoarthritis. The results demonstrate that the hydrogel preserves cartilage matrix components under osteoarthritic conditions and exhibits anti-inflammatory potential, highlighting a promising strategy for cartilage regeneration.

Functional Complementation of Neonatal and Adult Intervertebral Disc ECM: An A&NIVD-dECM Scaffold for Enhanced Intervertebral Disc Degeneration Repair

Feifei Yuan[1,2,3], Chengjun Li[1,2,3], Tao Zhang[1,2,3], Jiefu Zhou[1,2,3], Jianzhong Hu[1,2,3], Hongbin Lyu[1,2,3]

[1]Department of Sports Medicine, Xiangya Hospital, Central South University, Changsha, China, 2Key Laboratory of Organ Injury, Aging and Regenerative Medicine of Hunan Province, Changsha, China, 3National Clinical Research Center for Geriatric Disorders, Xiangya Hospital, Central South University, Changsha, China

INTRODUCTION: Decellularized extracellular matrix (dECM) is a natural scaffold that preserves the native 3D structure, fiber composition, and bioactivity of tissues while removing cellular components. It is widely used in preclinical and clinical research and better mimics native tissue ECM than traditional bioactive polymer hydrogels. Neonatal ECM generally shows stronger regenerative potential than adult ECM, but the effects of neonatal intervertebral disc dECM (NIVD-dECM) remain unclear. In this study, early-stage intervertebral discs were found rich in ECM proteins related to immune regulation, cell proliferation, migration, and differentiation. Adult IVD-derived dECM (AIVD-dECM) tended to drive nucleus pulposus cells toward an annulus fibrosus-like phenotype. SPON2 in NIVD-dECM and CCN2 in AIVD-dECM were identified as key regulators. We therefore developed a functionally complementary composite scaffold (A&NIVD-dECM) by combining neonatal and adult dECM to improve intervertebral disc degeneration (IVDD) repair.

METHODS: We prepared decellularized hydrogels from neonatal and adult rat intervertebral discs. In vitro and in vivo experiments showed that neonatal disc-derived dECM with high SPON2 levels regulated the immune microenvironment and maintained nucleus pulposus cell homeostasis and stemness, while adult disc-derived dECM with high CCN2 promoted chondrogenic differentiation. We then fabricated a composite A&NIVD-dECM Gel by mixing the two decellularized disc materials for transplantation, achieving effective repair of intervertebral disc degeneration.

RESULTS: We compared NIVD-dECM and AIVD-dECM and found that NIVD-dECM rebuilds a regenerative microenvironment for IVDD, whereas AIVD-dECM promotes chondrogenic differentiation of nucleus pulposus cells. We constructed the A&NIVD-dECM composite scaffold, which integrates the functions of both age-stage ECMs, offering a promising strategy for adult IVDD repair.

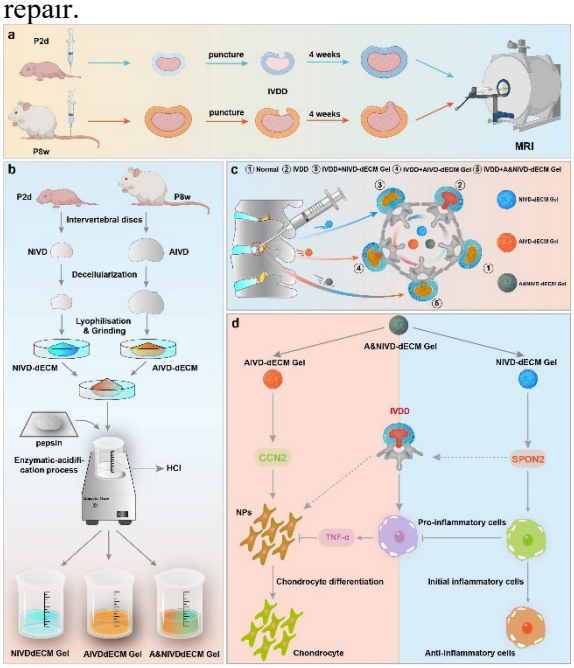

Figure 1 Preparation of A&NIVD-dECM and its application in IVDD.

DISCUSSION & CONCLUSIONS: Neonatal tissue ECM is known to support regeneration across organs. Proteomic and functional analyses revealed major compositional and bioactive differences between NIVD-dECM and AIVD-dECM: NIVD-dECM is enriched in immune-regulatory proteins (especially SPON2) that sustain homeostasis, while AIVD-dECM rich in CCN2 enhances chondrogenesis. The complementary A&NIVD-dECM scaffold combines these advantages for IVDD repair. Physical properties such as fiber diameter, pore size, and modulus influence therapeutic effects, and future work will optimize mixing ratios for different disc lesions. Overall, composite neonatal-adult dECM scaffolds represent a promising biomaterial approach for treating IVDD.

REFERENCES:

1 Bronfort G, et al. Spinal Manipulation and Clinician-Supported Biopsychosocial Self-Management for Acute Back Pain: The PACBACK Randomized Clinical Trial. JAMA. 2026;335:497-510.

Redox Responses to Mechanical Loading are Heterogeneous in Human Cartilage

Chenhao Yu[1], Corinne R. Henak[1,2,3]

Departments of [1]Mechanical Engineering, [2]Biomedical Engineering, [3]Orthopedics and Rehabilitation, University of Wisconsin-Madison, USA.

INTRODUCTION: Diagnostic approaches for osteoarthritis (OA) focus on cartilage structural health. However, biological health is both relevant to the disease stage and a potential mediator for the efficacy of biological interventions. Therefore, the development of a stimulus-response framework for diagnosing cartilage biological health has potential to improve patient outcomes. Our approach is to use optical redox imaging (ORI) to evaluate cartilage health. ORI has been used previously in porcine cartilage (e.g., [1]), but not in human cartilage. In this study, our objectives were to (1) validate ORI in human cartilage, and (2) explore heterogeneity in stimulus-response outcomes in human cartilage.

METHODS: Articular cartilage was collected from total knee replacement surgical discard (IRB 2021-0522). Cartilage strips were cultured 12-48 hours in chemically defined media at 37°C in 5% O_2 and 5% CO_2 prior to subsequent steps.

ORI was conducted using an inverted epifluorescent microscope. NADPH and NADH were imaged in channel 1 (361-389 excitation, 435-485 emission, 0.5 s exposure) and FAD was imaged in channel 2 (470-490 nm excitation, 500-525 emission, 2 s exposure) (Figure 1A,B).

Chemical inhibition was used to validate ORI in human cartilage samples from 7 subjects (1 man, 6 women, 55-77 years old). Samples were treated with 0.33 mg/ml diphenyleneiodonium (DPI, N = 8) or 1 mg/ml rotenone (N = 7). Treatment and cartilage zone effects were evaluated using a two-way ANOVA in Matlab (v2024b), after data were checked for normality.

Mechanical stimuli were used in 8 samples from 7 subjects (4 men, 3 women, 44-72 years old). One subject had cartilage regions that were visually healthy and regions that were visually degraded (Pt6-1 and Pt6-2, respectively). Samples were loaded at 1.5 mm·s^{-1} to either 0.50 mm or 0.25 mm displacement using a 1 mm diameter cylindrical indenter (Figure 1C). Post-loading ORI was normalized to pre-loading ORI.

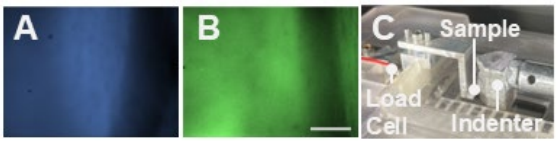

Figure 1. Representative images from channel 1 (A) and 2 (B) (bar = 100 µm). (C) Loading device.

RESULTS: Samples treated with DPI had lower channel 1 and 2 than control samples. Rotenone caused no significant effect on ORI channels.

The response to mechanical stimulus varied by sample, channel, and displacement (Figure 2).

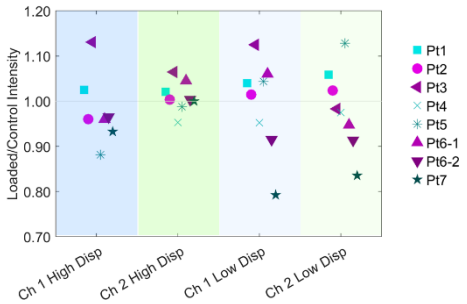

Figure 2. Responses to mechanical loading for high (0.50 mm) and low (0.25 mm) displacement for each sample (cyan are male, pink are female). Values above one indicate an increase in the corresponding channel following loading.

DISCUSSION & CONCLUSIONS: This study presents a first report of ORI in human cartilage, including validation of ORI metrics using DPI and data on mechanoresponse heterogeneity.

Cartilage responded as expected to DPI, but not to rotenone. While this validates ORI in human cartilage, it contrasts with prior research using ORI on adolescent pig cartilage [1]. This can be attributed to a muted response to chemical inhibition in damaged cartilage, coupled with the dense extracellular matrix in mature cartilage.

Variant stimulus responses are consistent with prior literature. Chondrocyte phenotype is heterogeneous as a function of cartilage zone, anatomical region, and degeneration [2]. Heterogeneous responses to matched stimuli as a function of disease state have been reported [3], and recent evidence suggests that OA chondrocytes have increased mechanosensitivity [4]. It is this variation in mechanosensitivity that can form the basis of stimulus-response methods for diagnosing cartilage health. Ongoing research is required to confirm cartilage health using structural and biological measures.

FUNDING: NIH R01 AR083413.

REFERENCES: [1] Walsh+, *Osteoarth Cartil*, 2019; [2] Zheng+, *Ageing Res Rev*, 2021; [3] Wu+, *Mechanobiol in Med*, 2025; [4] Castro-Viñuelas+, *Osteoarth Cartil*, 2025.

COMBINING EXPERIMENTAL DATA AND MATHEMATICAL MODELING TO INTERPRET GLUCOSE TRANSPORT AND METABOLIC GRADIENTS IN A JOINT TISSUE CO-CULTURE MODEL

Jovana Zvicer[1], Fatemeh Safari[2], Jasmina Stojkovska[1], Predrag Petrovic[3], Sibylle Grad[2], Martin J. Stoddart[2], Zhen Li[2], Bojana Obradovic[1]

[1]University of Belgrade, Faculty of Technology and Metallurgy, Belgrade, Serbia, [2]AO Research Institute Davos, Davos Platz, Switzerland, [3]Innovation Center of the Faculty of Technology and Metallurgy, Belgrade, Serbia

INTRODUCTION: Osteochondral–synovial *ex vivo* co-culture models represent an advanced platform for studying joint biology, as they preserve critical tissue interactions such as cartilage–bone crosstalk and synovial regulation. However, their broader application is limited by the lack of consensus on optimal culture conditions, particularly glucose concentration and oxygen availability. This study aimed to evaluate the effects of glucose levels on tissue viability and to apply a mathematical model of axial and/or radial diffusion to interpret cell viability.

METHODS: Bovine osteochondral explants and synovial tissue were harvested from the stifle joint and maintained in a static co-culture system for 7 days. Cultures were established in low-glucose (LG, 1 g/L) or high-glucose (HG, 4.5 g/L) DMEM under hyperoxic conditions (21% O_2). Cell viability was assessed after the culture time. Glucose consumption was quantified for each tissue separately over 24 h by measuring residual glucose concentrations in the medium using a Megazyme D-glucose assay kit, adapted for 96-well plates, and normalized to wet weight (mg/g tissue/24 h). Additionally, a mathematical model incorporating diffusion and tissue-specific glucose consumption rates was developed to predict the spatial distribution of glucose within cartilage.

RESULTS: Cell viability was significantly affected by medium glucose concentration. HG medium significantly improved tissue viability compared to LG, despite LG being closer to physiological glucose levels. In LG, increased cell death was observed in the deep cartilage zone and subchondral bone (41 dead cells/area), compared to HG (8 dead cells/area). Synovial cell viability was high and unaffected by glucose levels (88% in LG and 87% in HG).
Measured glucose consumption exhibited clear tissue-specific differences. Under LG conditions, cartilage showed the highest metabolic demand (9.24 ± 1.66 mg/g/24 h), followed by synovium (4.75 ± 1.70 mg/g/24 h), and bone (1.71 ± 0.54 mg/g/24 h). In HG medium, glucose consumption increased by approximately 80% across all tissues: cartilage (15.06 ± 3.67 mg/g/24 h), synovium (8.62 ± 2.64 mg/g/24 h), and bone (3.17 ± 1.57 mg/g/24 h). Mathematical modeling successfully predicted glucose gradients within cartilage, indicating spatial limitations in nutrient transport that correlate with reduced viability in deeper regions.

DISCUSSION & CONCLUSIONS: This study demonstrates that HG conditions, although supraphysiological, better support tissue viability and metabolic stability in osteochondral–synovial co-culture systems. The difference between physiological glucose levels and optimal *in vitro* conditions highlights the importance of transport limitations in dense tissues such as cartilage.
The integration of experimental data with mathematical modeling provides insights into spatial nutrient distribution and its impact on tissue viability. These findings establish a framework for optimizing culture conditions in complex joint models and improving their physiological relevance and translational applicability.